

Sheffield Hallam University

The fate of organotin biocides in marine antifouling elastomers.

BAILEY, Stephen.

Available from the Sheffield Hallam University Research Archive (SHURA) at:

<http://shura.shu.ac.uk/19301/>

A Sheffield Hallam University thesis

This thesis is protected by copyright which belongs to the author.

The content must not be changed in any way or sold commercially in any format or medium without the formal permission of the author.

When referring to this work, full bibliographic details including the author, title, awarding institution and date of the thesis must be given.

Please visit <http://shura.shu.ac.uk/19301/> and <http://shura.shu.ac.uk/information.html> for further details about copyright and re-use permissions.

POLYTECHNIC LIBRARY 7025
POND STREET
SHEFFIELD S1 1WB

101 184 701 9

TELEPEN



Sheffield City Polytechnic Library

REFERENCE ONLY

~~10/11/94
18.08~~
~~15/11
18.09~~
~~19/10 20.55~~
25/10. 18.30.
850. 9/11/95

ProQuest Number: 10694182

All rights reserved

INFORMATION TO ALL USERS

The quality of this reproduction is dependent upon the quality of the copy submitted.

In the unlikely event that the author did not send a complete manuscript and there are missing pages, these will be noted. Also, if material had to be removed, a note will indicate the deletion.



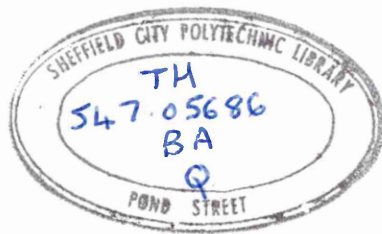
ProQuest 10694182

Published by ProQuest LLC (2017). Copyright of the Dissertation is held by the Author.

All rights reserved.

This work is protected against unauthorized copying under Title 17, United States Code
Microform Edition © ProQuest LLC.

ProQuest LLC.
789 East Eisenhower Parkway
P.O. Box 1346
Ann Arbor, MI 48106 – 1346



ABSTRACT

The Fate of Organotin Biocides in Marine Antifouling Elastomers

by

Stephen Bailey

The technique of tin-119m Mössbauer spectroscopy has been used to study the chemical and structural changes undergone by a series of triorganotin biocides when dispersed in neoprene-based marine antifouling elastomers. Chemical speciation using tin-119 nuclear magnetic resonance spectroscopy and gas chromatography, indicate that the majority of the tri-n-butyltin (TBT) biocides are converted to TBT-chloride, TBT-stearate and di-n-butyltin distearate during the polymer processing and curing conditions. Similar studies of triphenyltin (TPT)-containing elastomers demonstrate the extensive chemical degradation suffered by these compounds upon incorporation into the elastomer matrix.

Spectroscopic and chromatographic analyses of a marine-exposed elastomer, originally containing bis(TBT)oxide (TBTO), revealed the presence of monobutyl- and dibutyltin compounds as degradation products. A "backscatter" Mössbauer technique showed that the ultimate degradation product, distributed in the near surface regions of the sample, was stannic oxide.

The possible binding of organotin biocides with components of the coating formulation was investigated by variable temperature Mössbauer measurements on TBT-chloride systems. At temperatures below 60K, the organotin was shown to exist as a polymeric compound in which the tin atom is penta-coordinate. Application of the Debye model of solids yielded a value of the recoilless fraction at 80K, $f(80K)$, of 0.30 and the vibrational freedom of the tin atom was isotropic. This associated structure was observed to break down upon dispersion into uncured neoprene. The Mössbauer parameters and $f(80K) = 0.17$ were consistent with the presence of discrete, tetra-coordinate molecules. In the authentic coating matrix, the Mössbauer parameters indicated a tetra-coordinate geometry for the biocide. However, the large $f(80K) = 0.34$ is more typical of the penta-coordinate structure exhibited by pure TBT-chloride.

The presence of TBT and TPT additives on the curing behaviour of the basic coating formulation was investigated and it was found that TBTO effectively delayed the onset of curing in this system. This effect was attributed to interfering reactions between the organotin and the accelerated zinc oxide cure system, and to the existence of a competing crosslinking reaction directly involving TBTO. The TPT biocides were seen to promote the onset of curing and this was attributed to the formation of tin-based Lewis acid catalysts during the chemical breakdown of the original biocide.

CHAPTER ONE : ORGANOTIN-BASED MARINE ANTIFOULINGCOATINGS

	1
1.1 Introduction	2
1.2 The Problem of Marine Fouling	2
1.3 Antifouling Systems	4
1.4 Triorganotin Compounds as Biocides	5
1.5 Controlled-Release Elastomers	7
1.6 Structural Studies of Organotin-based Coatings	10
1.7 Objectives of Present Study	11
1.8 References	18

CHAPTER TWO : THE MÖSSBAUER EFFECT, HYPERFINEINTERACTIONS AND EXPERIMENTALMETHODS

	22
2.1 The Mössbauer Effect	23
2.1.1 Resonance Fluorescence	23
2.2 The Hyperfine Interactions	31
2.2.1 The Isomer Shift	31
2.2.2 Quadrupole Splitting	35
2.2.3 Magnetic Hyperfine Interaction	38
2.3 Applications to Organotin Chemistry	40
2.3.1 Isomer Shifts	41
2.3.2 The Quadrupole Splitting Parameter	45
2.4 Experimental Details	50
2.4.1 Suitable Mössbauer Isotopes	50
2.4.2 The Mössbauer Source	52
2.4.3 Mössbauer Absorbers	54

	<u>Page</u>
2.5 Instrumentation	57
2.5.1 Mössbauer Drive System and Multichannel Analyser	57
2.5.2 Detectors	61
2.5.3 Cryogenics	61
2.6 Data Handling	67
2.6.1 Data Transfer	68
2.6.2 The Folding Program	69
2.6.3 The Fitting Program	70
2.7 Calibration	71
2.8 References	73

CHAPTER THREE : INITIAL STUDIES OF MARINE

<u>ANTIFOULING ELASTOMERS</u>	76
3.1 Introduction	77
3.2 Tributyltin-containing Elastomers	80
3.2.1 Tin-119m Mössbauer Studies	80
3.2.2 Results and Discussion of the Tributyltin Systems	82
3.2.3 Studies of the Fate of Tributyltin Biocides Dispersed in Neoprene	92
3.2.4 An Investigation into the Effects of Carbon-Black on the Mössbauer Parameters of Organotins	95
3.3 Triphenyltin-containing Elastomers	104
3.3.1 Results and Discussion of the Triphenyltin Systems	104
3.3.2 A Mössbauer Investigation of the Thermal Stability of some Phenyltin Compounds	111

	Fate of Triphenyltin Biocides Dispersed in Neoprene	119
3.4	Conclusions	124
3.5	References	128
<u>CHAPTER FOUR : SPECTROSCOPIC AND CHEMICAL</u>		
<u>ANALYSIS OF A MARINE-</u>		
<u>EXPOSED ELASTOMER</u>		
		131
4.1	Introduction	132
4.2	Results and Discussion	132
4.3	An Attempt at Surface Analysis using Conversion Electron Mössbauer Spectroscopy (CEMS)	138
	4.3.1 Introduction	138
	4.3.2 CEMS, Principles and Detection System	138
	4.3.2.1 Detection System	140
4.4	Discussion and Conclusions	142
4.5	References	154
<u>CHAPTER FIVE : VARIABLE TEMPERATURE</u>		
<u>MÖSSBAUER STUDIES OF</u>		
<u>TRI-N-BUTYL TIN CHLORIDE IN</u>		
<u>THE PURE STATE AND IN</u>		
<u>ELASTOMERIC MEDIA</u>		
		156
5.1	Introduction	157
5.2	Theory	158
5.3	Experimental and Results	160
5.4	Discussion	165
5.5	Conclusions	171
5.6	References	179

<u>CHAPTER SIX : THE EFFECTS OF ORGANOTIN TOXICANTS ON THE CURING OF NEOPRENE-BASED ANTIFOULING ELASTOMERS</u>	180
6.1 Introduction	181
6.2 Experimental	184
6.2.1 Torque Rheometry	184
6.2.2 Results	186
6.3 Discussion and Conclusions	192
6.4 References	204
<u>CHAPTER SEVEN : GENERAL CONCLUSIONS</u>	206
ACKNOWLEDGEMENTS	214
COURSES AND CONFERENCES ATTENDED	215
PUBLISHED PAPERS	216

CHAPTER 1 : ORGANOTIN-BASED MARINE ANTIFOULING COATINGS

1.1 Introduction

1.2 The Problem of Marine Fouling

1.3 Antifouling Systems

1.4 Triorganotin Compounds as Biocides

1.5 Controlled-Release Elastomers

1.6 Structural Studies of Organotin-based Coatings

1.7 Objectives of Present Study

1.8 References

1.1 Introduction

Any non-toxic surface that is exposed to a marine or fresh-water environment, will rapidly become colonized by a variety of animal and plant species. It has been estimated [1] that one cubic centimetre of sea-water contains between one and ten thousand living cells, many of which constitute slime-forming bacteria. These establish themselves on a surface in the form of primary fouling which then acts as a source of nutrition for secondary fouling organisms such as; algae (Enteromorpha, Ectocarpus, Ulva, Laminaris and Polysiphonia species), hydrozoa, bryozoa (Bugulae sp., watersipora sp. and Cryptosula sp.), tubeworms (Hydroides norvegica), shipworms (teredo), barnacles and molluscs. [2]

1.2 The Problem of Marine Fouling

The onset of marine fouling poses a number of serious economic and technological problems. Fouling accumulation adds to the weight of the immersed object and this can be a particularly undesirable problem with navigation buoys which will gradually sink as fouling builds up. Attachment of material to a ship's hull leads to significant drag effects which, along with the increased mass, means that the vessel must burn considerably more fuel in order to maintain speed.

One estimate [3] suggests that if friction at the hull/water interface increases at a rate of 0.25% per day, after a six month period the vessel must consume 35-50% more fuel to maintain speed and, furthermore, the maximum attainable speed will be reduced by 1 to 2 knots. Another estimate [4] states that of the Royal Navy fuel bill of twenty million pounds per annum, about four million pounds is spent on overcoming the effects of marine fouling.

As well as the economic consequences of fouling accumulation, there are also a variety of technical problems associated with the phenomenon. Certain types of fouling greatly accelerate corrosion. A growing barnacle shell, for example, is able to lift a protective coating thereby exposing the substrate to salt water. Excessive fouling will also inhibit the performance of delicate underwater equipment. Sonar apparatus suffer loss of range, signal distortion and increased background noise levels due to the presence of hard-shelled organisms on the equipment housings.

The severity of the fouling problem is influenced by the type of environment (seawater or freshwater, temperate or tropical), the type of vessel and its sailing pattern. Small vessels (pleasure craft, certain fishing boats) are relatively easy to clean during periods when their services are not required. However, the dry-docking of large ocean-going vessels represents considerable

expense in terms of associated docking fees and loss of revenue during the docking period. The overall annual cost (c.a. 1970) to the UK shipping industry was put at fifty million pounds [2]. From a naval standpoint, economic considerations and also a change in the strategic role of surface vessels are demanding greater in-service periods between dry docking. Submarines often spend months at underwater duty stations during which time they could suffer badly from the effects of marine fouling. Other fouling targets include sea walls, pilings, oil drilling rigs, cables and pipes.

1.3 Antifouling Systems

There are basically two methods of controlling marine fouling. One approach is to remove the fouling organism as it attaches which is not very practical. The other, more effective, method is to periodically apply a protective coating that destroys or repels the organisms before they establish themselves on the surface. Such coatings function by releasing chemicals (biocides) to the coating/water interface where they then exert a toxic effect on the aquatic organisms.

Three approaches have been adopted in the development of antifouling coatings. In the first approach, a biocide is dispersed in a paint matrix and efficacious surface concentrations are maintained via a leaching mechanism. The second approach is to disperse the biocide into an elastomer matrix which, via a diffusion-

dissolution process, affords the controlled release of biocide to the surface. The third approach involves appending a toxicant moiety to a polymer backbone. The biocide release mechanism involves hydrolytic cleavage of the toxic entity from the polymer chain.

1.4 Triorganotin Compounds as Biocides

Biocides suitable for antifouling use must satisfy a number of criteria. Firstly, they must show a high degree of toxicity towards a wide spectrum of fouling organisms. The compounds should possess low mammalian toxicity and preferably be biodegradable. The biocide should be released at a rate which is compatible with its toxic properties and must be an economically viable proposition in terms of practical coating production.

Over the years, a number of compound types have been shown to possess biocidal activity towards a variety of fouling organisms. Organomercurials, cyanides, arsenic salts and oxides have all been evaluated but their high mammalian toxicity and environmental persistence has prevented widespread application of such materials. Several organolead compounds have shown promising potential as antifoulants, namely, triphenyllead -sulphide, -chloride, -2-ethylhexanoate, -laurate, -imidazole and -benzyl sulphide [3]. However, the long-term environmental hazard of lead compounds has also prevented their use as antifoulants.

During the 1930's to the 1950's, cuprous oxide (Cu_2O) became the dominant choice of toxicant for incorporation into paint systems. Although this material satisfied the important biocidal criteria (when properly formulated) and offered reasonable foul-free lifetimes (six months in tropical waters, eighteen months in temperate waters), it does suffer a number of serious drawbacks. The first problem concerns the biocide release mechanism for paints which, in turn, determines the effective toxicant loading. A leaching mechanism relies upon the continual growth of a pore structure so that water can penetrate the film and contact fresh copper. System dynamics, therefore, require very high toxicant loadings - typically 85-92%, of Cu_2O (dry weight) for effective leaching and thence fouling control. Such high toxicant loadings lead to detrimental effects on the physical properties of the paint matrix such as tensile strength, peel and abrasion resistance. These loadings also mean that Cu_2O -based paints are necessarily a red-brown colour and no other choice is available. Another serious problem arises from the fact that copper ions readily form a galvanic couple with iron, thereby accelerating the corrosion of steel substrates. Hence, it is necessary to apply a copper-impermeable paint between the substrate and the anti-fouling coating.

In 1961, antifouling paints incorporating triorganotin (R_3SnX) biocides entered the market having as their principal advantages, higher biocidal activity, a non-corrosive nature and the ability to pigment with bright colours. The main disadvantages in the use of organotins stem from their inherent mammalian toxicity and the resultant hazards in coating application. They are more costly than Cu_2O and offer shorter foul-free lifetimes (3-4 months) than the better Cu_2O compositions [3]. The most effective and widely used organotin biocide is bis(tri-n-butyltin)oxide - TBTO [®]. Other organotins that have been incorporated into paints include tributyltin carboxyethylmercaptals [5], trialkyltin oxymercuric alkyls [6], bis(tributyltin) tetrachlorophthalate [7], tributyltin sulphide [8] and tributyltin fluoride [9].

1.5 Controlled Release Elastomers

The need to provide longer periods of protection for naval vessels and giant tankers, in particular, has led to the development of organotin/elastomeric systems. In this type of coating, the biocide is compounded into the base polymer along with a variety of essential additives such as curatives, curing accelerators, protective agents (antioxidants) and reinforcing pigments. These materials are mixed together in a rubber mill and the whole mass is then heated (typically to $150^{\circ}C$) to effect cross-linking of the polymer chains and thereby produce a coating with useful physical properties.

The biocide release mechanism in these coatings is based on a diffusion-dissolution process which requires the toxic agent to possess a high level of solubility in the elastomer and relatively low solubility in water. Under these conditions as biocide molecules on or near the surface are lost due to dissolution and passage to the surrounding environment, internal toxicant molecules migrate towards the depleted area under solution pressure. The process is continuous with either internal diffusion or surface dissolution being rate controlling.

The solution properties of a variety of tri-n-butyltin compounds render them amenable to this kind of dynamic system. The effectiveness of TBTO, tri-n-butyltin fluoride (TBTF) and tri-n-butyltin acetate (TBTAc) in natural rubber, nitrile rubber and neoprene (polychloroprene) was investigated at the Australian Defence Standards Laboratories in 1972 [10]. In this study, it was concluded that TBTO and TBTAc were slightly soluble (> 5%) in nitrile rubber and neoprene, whilst TBTF is essentially insoluble in all three elastomers. As a result of this observation, it was clear that TBTF could not migrate through the bulk of the coating as required by the diffusion-dissolution model. Since TBTF had demonstrated superior antifouling protection over TBTO and TBTAc in each of the elastomer systems, the concept of water absorption followed by leaching had to be considered. This alternative biocide

release mechanism was then demonstrated when each organotin was dispersed in a butyl rubber formulation which exhibited only very slight water absorption (0.7-1.0%) compared with 7.0-8.4% for neoprene). In this experiment the TBTF-based coating, after three months marine exposure, was the most extensively fouled system.

The overall conclusion drawn from these experiments was that the choice of toxicant for a particular matrix should be based on the solubility of the toxicant in the elastomer, its solubility in sea water and the water absorption properties of the elastomer. Other factors that will influence biocide release rates are the carbon-black content and vulcanisation time and temperature of the elastomer matrix.

Since the development of the first antifouling elastomers in 1964 by scientists of the BF Goodrich Company, numerous patents and publications have appeared describing the use of various organotins in different elastomer matrices. One of the most successful general purpose coatings is that based on neoprene incorporating TBTO or TBTF as the biocide [10,11]. Navigation buoys covered with these types of coating and immersed in tropical waters were essentially free of fouling after 7½ years' immersion [12]. In another application, a neoprene sheet containing TBTO was applied to the hull of a pleasure boat [13]. After 9½ years, the hull was virtually free of all fouling and adhesion of the rubber to the steel substrate was reported as "excellent".

1.6 Structural Studies of Organotin-based Coatings

Although the formulation of new coatings containing organotin biocides, used alone or with a co-toxicant (eg triazine herbicides), has been the subject of much active research, the determination of the chemical form of the toxicant in the bulk and on the surface of the coatings has received less attention.

One of the first attempts to investigate the fate of TBTO and tri-n-butyltin chloride (TBTC1) in neoprene was undertaken by Kanakkanatt et al [14]. Using torque rheometry, they were able to demonstrate the participation of TBTO in the polymer curing reaction under standard conditions. As a result of this interaction, it was concluded that in a neoprene/TBTO formulation the toxicant that actually reaches the water is probably TBTC1 - or at least a mixture of TBTC1 and TBTO. Woodford has examined the parameters controlling the release of TBTO, TBTF and TBTAc of various elastomers [10]. This work, extended by de Forest et al [15], involved standard formulation procedures (compounding followed by curing at 150°C) and it was suggested that each organotin may be converted during vulcanisation into a single organotin compound such as TBTC1.

Since these experiments, very little work has been reported in the literature regarding the fate of organotin biocides in elastomer matrices. Some structural

studies have been made on tributyltin-based paint systems. Hoffman et al [16] using infrared spectroscopy, demonstrated the conversion of TBTO to what was almost certainly a tributyltin carboxylate. Likewise, O'Brien et al [17] used tin-119 Mössbauer spectroscopy to indicate the structural changes undergone by TBTO when dispersed into a commercial paint matrix.

1.7 Objectives of the Present Study

It is clear from the foregoing discussion on controlled-release elastomers, that there exist a number of areas that are worthy of detailed investigation. These include:

- (i) A study of the fate of typical antifouling biocides when incorporated into an elastomer formulation and cured under standard conditions.
- (ii) Determining the nature and identify of the most likely products formed in organotin-matrix interactions, and thence to assess the usefulness of the original organotin in these types of coatings.
- (iii) An examination of the long-term degradation of the toxicants and the environmental implications of using organotin-based elastomers.
- (iv) A study of the role of one particular organotin, TBTO, in the curing of neoprene.

Many of the studies involving the characterisation of organotins have relied upon chemical separation techniques (usually solvent extraction or leaching) to remove the compound(s) from the rest of the matrix, followed by some form of selective detection method. For example, Sherman employed a complexometric method on hexane extracted residues to monitor the controlled release of TBTF from a polythene-based molluscicide [18]. Monaghan et al [19] have employed solvent extraction (chloroform) on aqueous solutions followed by thin-layer chromatography (TLC) and infrared spectroscopy to identify various triphenyl- and tributyltin derivatives in a study of the environmental fate of organotin antifoulants. Organotin degradation was also of interest to Barug and Vonk [20] who utilised carbon-14 labelled TBTO and a radiocounting technique to demonstrate the degradation of this compound in different soil types. Solvent extraction followed by TLC established the presence of dibutyltin derivatives as degradation products. Gas-chromatography (GC) with flame-photometric detection has been successfully applied to the analysis of Canadian waters for n-butyltin derivatives [21]. In this procedure, the organotins were converted to the volatile n-pentyl derivatives prior to injection into the GC apparatus. The problem of identifying organotin degradation products and assessment of their role as environmental pollutants has also been addressed by Guard et al [22]. They used tin-119 nuclear

magnetic resonance (NMR) spectroscopy to characterize the organotin compounds recovered from sediments and sea-water solutions of TBTO, TBTAc and TBTC1.

Tributyltin compounds (mainly TBTO) have also found wide and satisfactory use as fungicides in wood preservative formulations [23]. In an attempt to evaluate the performance of TBTO as a fungicide and to monitor its breakdown in wood, Hill et al [24] employed TLC followed by atomic absorption spectroscopy with electrothermal atomization for the quantitative determination of TBTO breakdown products in sawdust samples. Degradation of the preservative was attributed to a combination of biological (coniothecium puteana, Chaetomium globosum and Aureobasidium pullulans organisms), chemical and physical factors (atmospheric exposure, temperature effects on surface layers). The use of atomic absorption as a means of environmental analysis, coupled with a chromatographic separation procedure has recently been reviewed by Harrison et al [25].

Finally, in an experiment to establish the occurrence and extent of biomethylation processes in sediment environments, Craig and Rapsomanikis [26] used GC with mass spectroscopic detection to conclude that the major route to the methylation of tin in the environment (> 95%) is chemical rather than biological in origin.

A major drawback with each of the methods discussed above is the need to remove the tin species from its working environment (water, paint, polymer, wood etc.) prior to characterisation of the various moieties. This necessarily implies that any information regarding the nature and distribution of organotins within a particular matrix is either lost completely or limited by the subjective interpretation of data from extracted residues. In order to achieve the objectives outlined earlier for organotins in elastomers, a method capable of probing the chemical environment of the biocide in situ on a non-destructive basis is required. By analysing the intact matrix, it should then be possible to study biocide-coating interactions (either with the base polymer or the compounding ingredients) and to examine the distribution of organotins on the surface and throughout the bulk of the matrix.

Mössbauer spectroscopy (nuclear gamma fluorescence spectroscopy) has been successfully applied to the study of organotins in a variety of matrices. The useful parameters that are derived from Mössbauer spectra of organotins in non-magnetic systems are the Isomer Shift (δ) and the Quadrupole Splitting (ΔE_Q). These concepts will be discussed more fully in Chapter 2. The main advantage that the technique offers over more widely used analytical methods are:

- (i) it provides structural information on amorphous as well as crystalline systems,
- (ii) the isomer shift offers unambiguous distinction between the oxidation states of tin (in most cases [26]),
- (iii) the quadrupole splitting parameter is sensitive to the tin atom stereochemistry,
- (iv) the technique is non-destructive,
- (v) the technique is free of the spectral interference problems common to most atomic spectroscopic methods.

These properties have been exploited by many workers in the structural analysis of a variety of industrially important organotin-based systems. For example, cellulosic materials such as cotton textiles or wood can be protected from the effects of fungal attack if they are impregnated with a solution of TBTO. Smith et al [28] using tin-119 Mössbauer spectroscopy, have demonstrated the structural changes undergone by TBTO when dispersed in these media. With supporting infrared data, they proposed the in situ conversion of TBTO to the corresponding carbonate (TBTCO) via reaction with adsorbed carbon dioxide.

Dialkyltin dimercaptides are widely used for the thermal stabilisation of PVC and several workers have employed the Mössbauer effect to elucidate their mode of action, migration and degradation within the polymer matrix. Allen et al [29] studied the thermal degradation of PVC containing dibutyltinbis(isooctylthioglycollate) and dibutyltinbis(isooctylmaleate) stabilisers. A comparison between the ΔE_Q values for the PVC systems and neat organotin compounds indicated that, in each case, the stabiliser had been converted into the dialkyltin monochloroester only and not into the dialkyltin dichloride as was previously suggested [30]. The bis(maleate) is reported to be an excellent stabiliser towards the UV degradation of PVC whereas the bithioglycollate has only limited efficiency in this capacity [31].

Brooks et al [32] used tin-119 Mössbauer spectroscopy to show that after exposing PVC sheets, stabilised with these materials, to artificial sunlight the maleate stabiliser remains chemically unchanged, whereas the thioglycollate rapidly converts to the monochloroester and subsequently degrades to inorganic tin compounds. The same workers have reported an interesting "dilution effect" on ΔE_Q for dibutyltin dichloride when dispersed in PVC at 1.2% by weight [33]. They observed a decrease in ΔE_Q for this compound upon dispersion and attributed the effect to the breakdown of an associated six coordinate structure and the progressive formation of dimeric units involving five coordinate tin.

Further work involving organotin PVC stabilisers has included a Mössbauer study of the changes undergone by these materials when exposed to gamma radiation [34]. The three stabilisers studied, dioctyltinbis(isooctylthioglycollate), dibutyltinbis(isooctylthioglycollate) and dibutyltin(isooctylmaleate) were all shown to degrade to stannic chloride when exposed to radiation levels typically employed in packaged food sterilisation. The maleate stabiliser was shown to be the most stable of the three with respect to degradation, but the thioglycollate stabiliser was shown to degrade via the formation of the monochloro ester and dibutyltin dichloride.

The suitability of the Mössbauer technique for the structural analysis of amorphous materials containing low levels of tin has, therefore, been amply demonstrated in the previous studies. As a means of achieving the objectives stated earlier concerning antifouling elastomers, Mössbauer spectroscopy is, then, the choice of principal analytical technique for this work. The basic principles of the method will be outlined in the next chapter.

1.8 References

1. C. J. Evans and R. Hill, Reviews on Silicon, Germanium, Tin and Lead Compounds, 1983, 7(1), pp 57-125.
2. D. R. Houghton, Underwater Science and Technology Journal, June 1970, pp 100-104.
3. N. Cardarelli, "Controlled Release Pesticides Formulations", 1976, CRC Press Incorporated.
4. D. Brown, "Fouling and Economic Ship Performance", Proc. 5th Inter-naval Corrosion Conference (1976), Paper 7.
5. I. Hechenbleickner and P. F. Thompson, US Patent 3 463 644, 1969 CA: 71:100813
6. Mitsui Shipbuilding and Engineering Co. British Patent 1 211 768, 1970.
7. H. O. Wirth, H. H. Friedrich and V. Mias, German Patent, 1 937 307, 1971.
8. J. R. Leebrick, A. Ross and R. J. Zedler, US Patent 3 234 032, 1966.
9. S. H. Morgan, Ger Offen. 1 941 849, 1970.
10. J. M. D. Woodford, Australian Defence Scientific Service, Defence Standards Laboratories, Report No 496, 1972.

11. N. F. Cardarelli and H. F. Neff, US Patent
3.639.583, 1972.
12. E. H. Bollinger, Report No 19, Proc. Controlled
Release Pesticides Symposium, Univ. Akron, Akron,
Ohio, 1974.
13. G. A. Janes and R. L. Senderling, Proc. 6th
International Symposium on the Controlled Release
of Bioactive Materials, New Orleans, LA, USA (1979)
p II-3.
14. S.V. Kanakkanatt, P. P. Patnode and N. F. Cardarelli,
Int. Congr. Pure and Appl. Chem.: Macromol Reprint,
1, pp 614-619 (1971).
15. A de Forest, R. W. Pettis and A. T. Phillip,
Department of Supply, Australian Defence Scientific
Service, Defence Standards Laboratories, Report
No 589, 1974.
16. J. F. Hoffman, K. C. Kappel, L. M. Frenzel and
M. L. Good, "Organometallic Polymers",
C. E. Carraher Jr, J. E. Sheats and C. U. Pittman Jr
(eds), Academic Press, London (1978), p 195.
17. E. J. O'Brien, C. P. Monaghan and M. L. Good,
ibid, p 207.
18. L. R. Sherman, J. Appl. Polym. Sci., 28,
pp 2823-2829 (1983).

19. C. P. Monaghan, V. I. Kulkarni, M. Ozcan and M. L. Good, US Govt. Report, Office of Naval Research, Technical Report No 2, AD-A087374, 1980.
20. D. Barug and J. W. Vonk, Pestic. Sci., 11 (1980), pp 77-82.
21. R. J. Maguire, K. Chau, A. Bengert, E. J. Hale, P. T. S. Wong and O. Kramar, Environ. Sci. Technol., 16 (1982), 698.
22. H. E. Guard, W. M. Coleman and A. B. Cobet, Am. Chem. Soc., Reprints of Papers, Div. Environ. Chem. 22(1), 180-183 (1982).
23. C. J. Evans and R. Hill, J. Oil Colour Chemists Assocn., 64, pp 215-223 (1981).
24. R. Hill, A. H. Chapman, A. Samuel, K. Manners and G. Morton, Int. Biodeter., 21(2), pp 113-121 (1985).
25. R. M. Harrison, C. N. Hewitt and S. J. de Mora, Trends in Anal. Chem., 4(1), pp 8-11 (1985).
26. P. J. Craig and S. Rapsomanikis, Environ. Tech. Lett., 5, pp 407-416 (1984).
27. A. B. Cornwell and P. G. Harrison, J. Chem. Soc. (Dalton), 1975, pp 1486-1490.
28. P. J. Smith, A. J. Crowe, J. S. Brooks, D. W. Allen and R. Formstone, Chem and Ind (London), pp 874-875 (1977).

29. D. W. Allen, J. S. Brooks, R. W. Clarkson,
T. J. Mellor and A. G. Williamson, J. Organomet.
Chem., 199, pp 299-310 (1980).
30. P. G. Harrison, T. J. King and M. A. Healy,
J. Organomet. Chem., 182, p 17 (1979).
31. H. O. Wirth and H. Andreas, Pure and Appl. Chem.,
49, p 627 (1977).
32. J. S. Brooks, R. W. Clarkson and D. W. Allen,
Polym. Degradn. and Stability, 4, pp 359-363 (1982).
33. J. S. Brooks, R. W. Clarkson and D. W. Allen,
J. Organomet. Chem., 243, pp 411-415 (1983).
34. J. S. Brooks, D. W. Allen and J. Unwin,
Polym. Degradn and Stability, 10, pp 79-94 (1985).

CHAPTER TWO : THE MÖSSBAUER EFFECT, HYPERFINE INTERACTIONS

AND EXPERIMENTAL METHODS

2.1 THE MÖSSBAUER EFFECT

2.1.1 Resonance Fluorescence

2.2 THE HYPERFINE INTERACTIONS

2.2.1 The Isomer Shift

2.2.2 Quadrupole Splitting

2.2.3 Magnetic Hyperfine Interaction

2.3 APPLICATIONS TO ORGANOTIN CHEMISTRY

2.3.1 Isomer Shifts

2.3.2 The Quadrupole Splitting Parameter

2.4 EXPERIMENTAL DETAILS

2.4.1 Suitable Mössbauer Isotopes

2.4.2 The Mössbauer Source

2.4.3 Mössbauer Absorbers

2.5 INSTRUMENTATION

2.5.1 Mössbauer Drive System and Multichannel Analyser

2.5.2 Detectors

2.5.3 Cryogenics

2.6 DATA HANDLING

2.6.1 Data Transfer

2.6.2 The Folding Program

2.6.3 The Fitting Program

2.7 CALIBRATION

2.8 REFERENCES

2.1 THE MÖSSBAUER EFFECT

The Mössbauer effect, or the recoilless emission and resonant absorption by the nucleus of a γ -photon, was first observed by R L Mössbauer in 1957 [1] using the iridium-191 nucleus. However, the concept of nuclear resonant absorption was predicted as long ago as 1929 by Kuhn, and actually observed in 1951 by P B Moon [2]. In Moon's experiment, however, nuclear recoil energy loss was compensated for by Doppler broadening, rather than eliminated as in Mössbauer's experiments. Mössbauer was thus able to produce monochromatic electromagnetic radiation with a very narrowly defined energy spectrum so that it became possible to resolve minute energy differences.

Since the pioneering work of Mössbauer (for which he was awarded the 1961 Nobel Prize in Physics), recoilless resonance fluorescence (Mössbauer spectroscopy) has been used to study structural and electronic effects in many chemical, metallurgical and other solid state systems. The direct application of the technique to chemistry arises from its ability to detect slight variations in the energy of interaction between the nucleus and the extra-nuclear electrons.

2.1.1 Resonance Fluorescence

Gamma emission occurs when a nucleus drops from an excited state to one of lower energy. If these γ -photons fall upon another ground state nucleus of the same isotope, they

may, under certain conditions, undergo resonant absorption and thereby excite this second nucleus. The fundamental condition is that the energy of the γ -photon exactly matches the nuclear excitation energy of the ground state nucleus.

Unless precautions are taken, however, these energies will not be the same since both emitting and absorbing nuclei will undergo recoil and therefore reduce the γ -photon energy by an amount equal to the recoil energy.

Consider the emission of radiation of energy E_γ from a free nucleus with an excited state energy E_0 above the ground state.



The momentum of the γ -photon $p_\gamma = \frac{E_\gamma}{c} = \frac{h}{\lambda_\gamma}$

Since momentum must be conserved, $p_\gamma = p_{\text{nucleus}}$.

Assuming non-relativistic mechanics, the velocity, v , imparted to the nucleus during recoil gives it momentum:

$$p_{\text{nucleus}} = Mv, \text{ and recoil energy;}$$

$$E_R = \frac{Mv^2}{2}$$

$$\text{Therefore, } E_R = \frac{p_{\text{nucleus}}^2}{2M} = \frac{E_\gamma^2}{2Mc^2}$$

The recoil energy for a free nucleus of mass number A is approximated by:

$$E_R(\text{eV}) \approx \frac{5.37 \times 10^{-4} E_0^2(\text{keV})}{A}$$

Thus, for the 23.8 keV γ -photon arising from the $I = \frac{3}{2}$ to $I = \frac{1}{2}$ energy transition of the excited tin-119 nucleus, $E_R \approx 2.56 \times 10^{-3}$ eV. Since $E_R \ll E_0$, it is valid to assume that $E_0 \approx E_\gamma$ and hence the recoil energy can be estimated from the nuclear transition energy thus;

$$E_R = \frac{E_0^2}{2Mc^2} \quad (1)$$

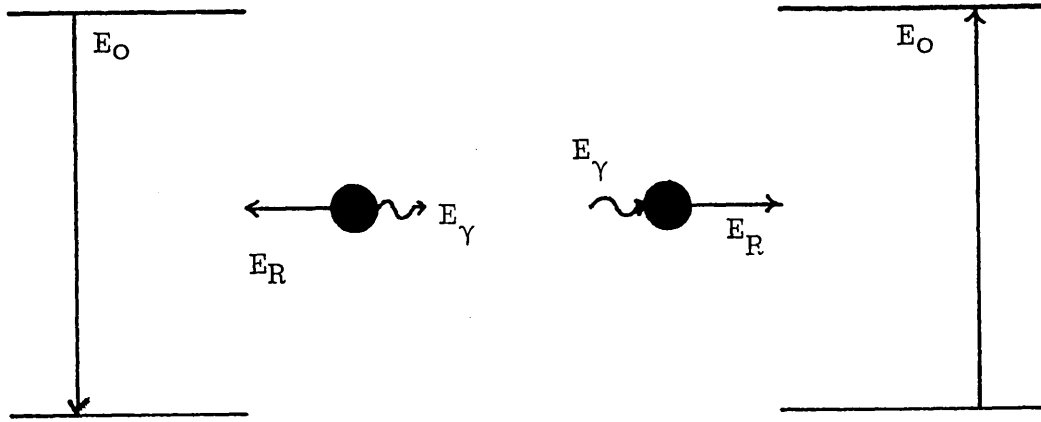
In absorption, the recoil momentum is in the opposite direction so that the absorbed energy is less than E_0 by twice the recoil energy, ie:

$$E_R = \frac{E_0^2}{Mc^2} \quad (2)$$

The net effect of nuclear recoil on the emission and absorption profiles of natural line width Γ is shown in Figure 2.1.

Emitter (source)

Absorber



Emission

Absorption

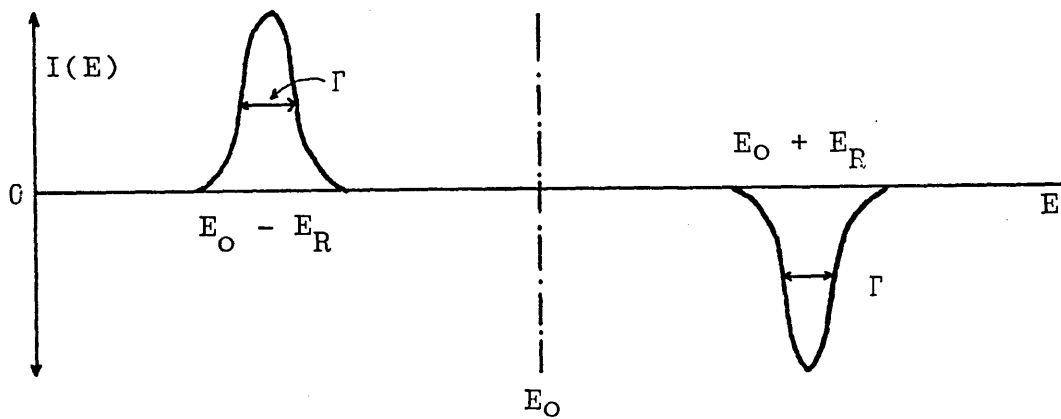


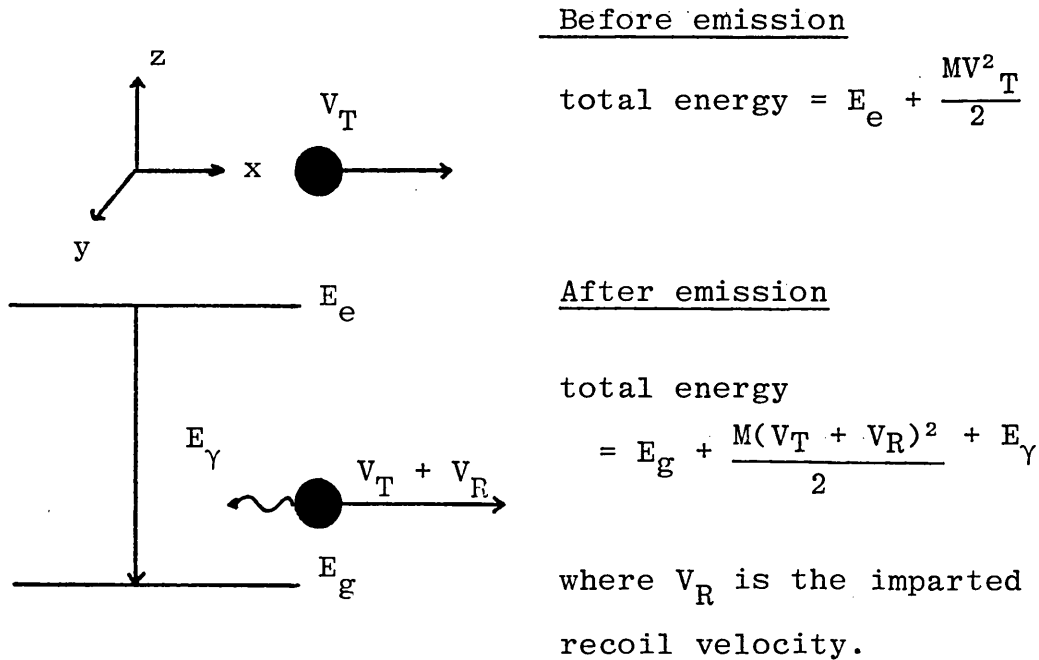
Figure 2.1 : The Mössbauer transitions and corresponding spectra

The above treatment of recoil energy assumes that emitting and absorbing nuclei are initially at rest. In general, however, this will not be the case since at a given temperature, T , the nuclei will possess appreciable random thermal velocities, V_T . In the gaseous state, the mean kinetic energy, E_k , of the nuclei, resulting from this random thermal motion, can be estimated from classical considerations, thus;

$$E_k = \frac{MV^2}{2} = \frac{3kT}{2} \quad (3)$$

where M is the mass of a particular nucleus and k is the Boltzmann constant.

Such velocities will lead to Doppler broadening of the emission and absorption profiles. This effect, combined with the concept of nuclear recoil, can be demonstrated for an excited state free nucleus moving with random thermal velocity, V_T , in one dimension. Recoil arises from the transition from the excited state E_e to the ground state E_g ;



Since energy must be conserved:

$$E_e + \frac{MV^2_T}{2} = E_g + \frac{M(V_T + V_R)^2}{2} + E_\gamma$$

If E_0 is the actual transition energy, then

$E_0 = E_e - E_g$. Thus:

$$E_0 - E_\gamma = \frac{M(V_T + V_R)^2}{2} - \frac{MV_T^2}{2}$$

$$\therefore E_0 - E_\gamma = \frac{MV_R^2}{2} + MV_T V_R \quad (4)$$

It can be appreciated from equation (4) that the difference between the γ -photon energy and the nuclear transition energy depends upon a recoil energy term ($E_R = \frac{1}{2} MV_R^2$), which is itself independent of the random thermal velocity, and a Doppler effect term ($E_D = MV_T V_R$) which depends upon both the magnitude and sign of V_T .

Using non-relativistic mechanics (permissible since V_T and $V_R \ll c$), it can be shown that the Doppler term E_D is related to absolute temperature, T , by the expression:

$$E_D = \sqrt{2E_R kT} \quad (5)$$

Equation (5) indicates that the extent of Doppler broadening will increase as the recoil and average thermal energy of the nucleus increases. This, in turn, increases the energy separation between the actual nuclear transition energy, E_0 , and the γ -photon energy, E_γ , as described by equation (4).

The inter-relationship between E_0 , E_R and E_D on the emission and absorption line profiles is indicated in

Figure 2.2.

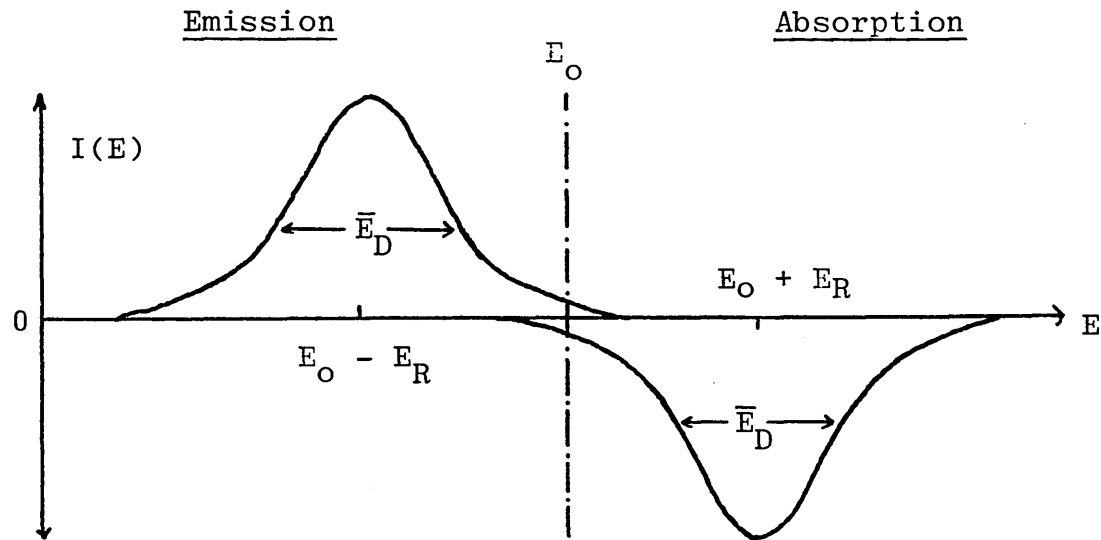


Figure 2.2 : Mössbauer emission and absorption profiles showing resonance due to Doppler broadening

It is clear from the above treatment that the relationship between the natural line width, Γ , the recoil energy and Doppler broadening will dictate whether or not nuclear fluorescence will be observed. The line width, Γ , is given by the Heisenberg relationship:

$$\Gamma = \frac{h}{2\pi\tau}$$

where h = Planck's constant (6.626×10^{-34} Js) and τ is the mean lifetime of the excited state in seconds.

In general for γ -emission, $E_D \gg \Gamma$ and $E_D \approx E_R$ so at least two possible methods of observing nuclear fluorescence are evident. The energy separation, $2E_R$, may be directly supplied by (i) utilising the Doppler effect [2], or (ii) increasing thermal broadening by heating the source and absorber, so that E_D increases and some overlap

of the lines occurs, Figure 2.2.

Both methods, however, result in only a small degree of overlap and hence a small resonance effect, and they also produce very broad lines leading to poor resolution.

In 1957, Mössbauer observed the unexpected increase in γ -absorption by iridium-191 with decreasing temperature. An explanation of this effect requires consideration of the quantised nature of the lattice. The so-called Einstein model of the solid considers the lattice to be a quantum-mechanical system in which transitions occur through phonon interactions. The lowest energy required to stimulate a phonon interaction is given by E_E , the Einstein energy. If $E_R \gg E_E$ interactions involving many phonons occur and the emitted photon suffers recoil energy loss and Doppler broadening. However, when $E_R \ll E_E$, that particular decay corresponds to a zero-phonon interaction and the γ -photon is emitted without recoil, and is not Doppler broadened. Under these conditions, the emitting nucleus has effectively been 'frozen' into the lattice and the recoil momentum is taken up by the infinite recoil mass of the whole crystal.

The basis of Mössbauer's observation involved the elimination of nuclear recoil by lowering the experimental temperature such that the condition $E_R \ll E_E$ was satisfied. The need to eliminate recoil means that Mössbauer spectroscopy is restricted to measurements on solids.

Therefore, studies on organotin (many of which are liquids at room temperature) and amorphous materials such as elastomers, can only be performed at low temperatures - usually liquid nitrogen temperature (77K).

2.2 THE HYPERFINE INTERACTIONS

The hyperfine interactions are the small interactions that occur between a nucleus and its electronic environment. They arise because a nucleus is not a structureless point charge, but a cluster of moving charges, distributed over a finite volume.

The hyperfine interactions give rise to three effects:

1. The Isomer Shift (δ)
2. The Quadrupole Splitting (ΔE_Q)
3. The Magnetic (Zeeman) Splitting.

2.2.1 The Isomer Shift

The term Isomer Shift refers to the extent by which the maximum of absorption is shifted from a suitable calibration point and arises from an electrostatic interaction between the nuclear charge and the electron density which penetrates it, ie s-electron density.

It is generally assumed that the electron contribution from the inner shells of the Mössbauer isotope is constant and that changes in isomer shift reflect changes in the population of the valence-shell s-orbital. Changes in the population of the valence p and d-orbitals will also affect the electron density at the nucleus by shielding effects.

The electrostatic shift, δE , of a nuclear energy level with respect to a hypothetical point nucleus, is given by:

$$\delta E = \frac{2\pi}{5} Ze^2 R^2 |\psi(0)|^2 \quad (6)$$

Z is the atomic number, e is the electronic charge, $|\psi(0)|^2$ represents the electron density within the nuclear volume and R is the nuclear radius, assuming it to be a uniform sphere. In general, the nuclear radius in the ground and excited states will differ. Therefore, the electrostatic interaction energies will also differ according to the value of R in equation (6).

The effect of the isomer shift on a hypothetical isolated nucleus is illustrated in Figure 2.3.

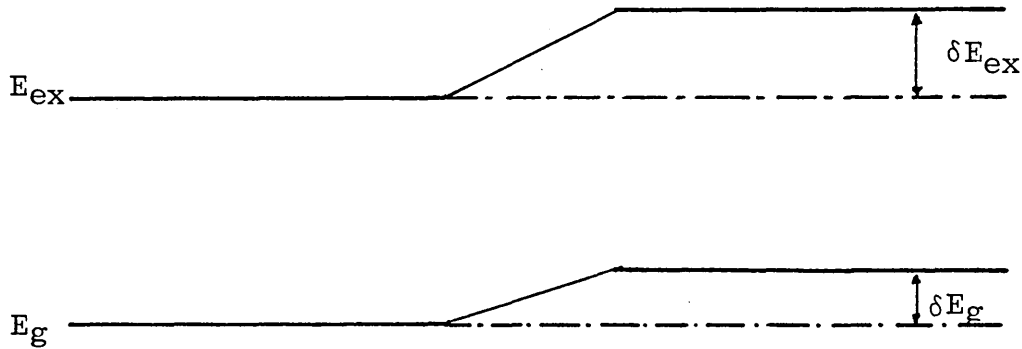


Figure 2.3 : The effect of the isomer shift on the ground and first excited states of a hypothetical point nucleus

Observation is normally made of transitions between excited (ex) and ground (g) states. The change in energy of the γ -transition is, therefore, due to the difference of two terms given by equation (6) involving the excited (R_{ex}) and ground state (R_g) nuclear radii:

$$\delta E_{\text{ex}} - \delta E_{\text{g}} = \frac{2\pi}{5} Ze^2 |\psi(0)|^2 (R_{\text{ex}}^2 - R_{\text{g}}^2) \quad (7)$$

It is possible to compare magnitudes of the electrostatic interaction energy by means of a suitable reference material. In general, isomer shifts are measured relative to a 'standard' source nucleus; in the case of tin-119 experiments, stannic oxide (SnO_2) and barium stannate (BaSnO_3) are widely used as source matrices. The isomer shifts for these materials are identical within experimental error and all data given in the following sections are referred to a BaSnO_3 standard absorber.

The effect of the isomer shift on a source and absorber existing in different chemical environments is shown in Figure 2.4.

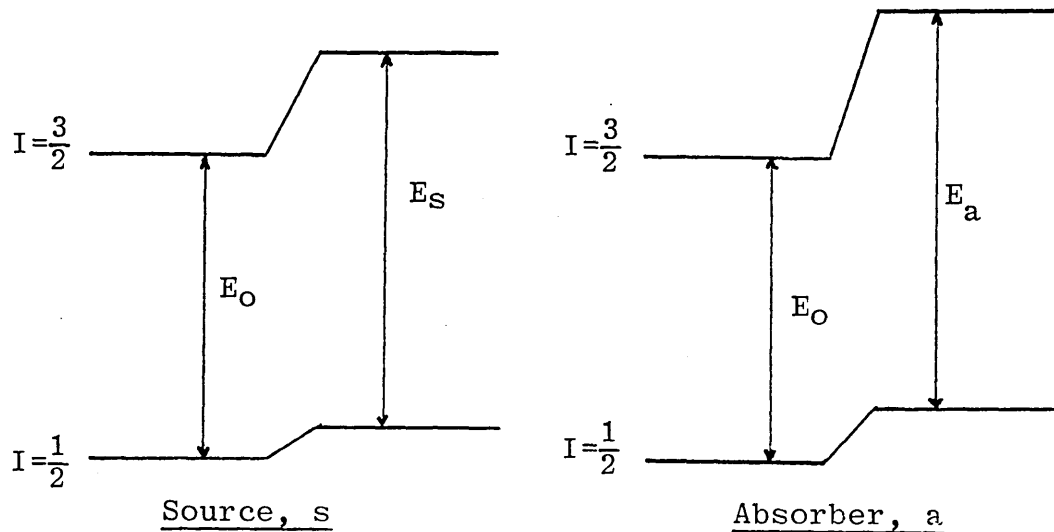


Figure 2.4 : The effect of the isomer shift on source and absorber nuclear energy levels

Since the source and absorber exist in different chemical environments, $|\psi(o)|^2$ will differ in each case. However, they both contain the same isotope and, therefore, possess the same excited and ground state nuclear radii. The source transition energy, E_s , and absorber transition energy, E_a , may now be combined to yield an expression for the isomer shift, δ :

$$E_s = E_o + \frac{2\pi}{5} Ze^2 |\psi(o)|_s^2 (R_{ex}^2 - R_g^2)$$

$$E_a = E_o + \frac{2\pi}{5} Ze^2 |\psi(o)|_a^2 (R_{ex}^2 - R_g^2)$$

ISOMER SHIFT, $\delta = E_a - E_s$

$$\therefore \delta = \frac{2\pi}{5} Ze^2 (|\psi(o)|_a^2 - |\psi(o)|_s^2) (R_{ex}^2 - R_g^2) \quad (8)$$

The change in nuclear radius is very small (typically about 0.1%) so that its square can be neglected. The isomer shift may then be expressed in terms of the normalized radius difference, $\delta R/R$, thus:

$$\delta = \frac{4\pi}{5} Ze^2 R^2 \left(\frac{\delta R}{R} \right) (|\psi(o)|_a^2 - |\psi(o)|_s^2) \quad (8a)$$

In tin systems, δR is positive which means that increases in s-electron density at the absorber nucleus result in positive isomer shifts. The opposite is true in iron systems for which $\delta R < 0$.

2.2.2 Quadrupole Splitting

The expression for the isomer shift equation (8) assumes that the nucleus is spherical and has uniform charge density. These conditions, however, only apply to nuclei in spin states $I = 0$ or $I = \frac{1}{2}$. When $I > \frac{1}{2}$, a deviation from spherical symmetry occurs, the magnitude of which is reflected by the Nuclear Quadrupole Moment, Q . If the distribution of charge about the nucleus has less than cubic symmetry, an electric field gradient (efg) will be generated which is capable of interacting with the nuclear quadrupole moment. The presence of a quadrupole interaction splits the $(2I + 1)$ - fold degenerate energy levels into a set of sublevels whose energies are characterized by the magnetic spin quantum number m_I :

$$E_Q = \frac{e^2 q Q}{4I(2I-1)} \left[3m_I^2 - I(I+1) \right] \left(1 + \frac{1}{3}\eta^2 \right)^{\frac{1}{2}} \quad (9)$$

where Q = nuclear quadrupole moment

eq = maximum value of the efg

η = an asymmetry parameter

m_I = magnetic spin quantum number

e = electronic charge

For example, for tin-119, $I_{\text{ex}} = \frac{3}{2}$ and $I_{\text{g}} = \frac{1}{2}$, Figure 2.5.

The $I = \frac{3}{2}$ level splits into two ($m_I = \pm \frac{3}{2}, \pm \frac{1}{2}$) sublevels whilst the $I = \frac{1}{2}$ remains degenerate. Transitions from the ground state to both excited levels are allowed

according to the selection rule $\Delta m_I = 0, \pm 1$, and a characteristic two line spectrum is obtained.

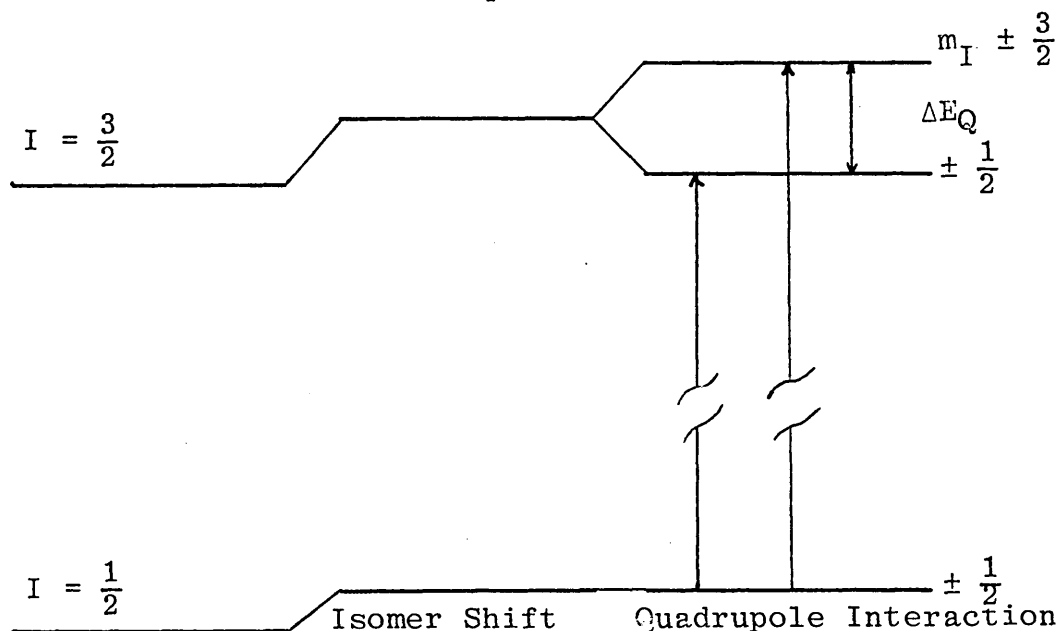


Figure 2.5 : Absorber energy levels: excited $I = \frac{3}{2}$ split into two sub-levels by the quadrupole interaction

The peak separation, ΔE_Q , defines the quadrupole splitting parameter. For the $I = \frac{3}{2}$ case (eg Sn-119) the quadrupole splitting, $\Delta E_Q = E_Q(\pm \frac{3}{2}) - E_Q(\pm \frac{1}{2})$, can be expressed as:

$$\Delta E_Q = \frac{e^2 q Q}{2} \left(1 + \frac{\eta^2}{3} \right)^{\frac{1}{2}} \quad (10)$$

The origin of the asymmetry parameter, η , can be traced to the original efg tensor derived by applying the gradient operator to the three components of the electric field. The electric field gradient at the nucleus is defined as the second derivative of the electric potential. The result is a 3 x 3 tensor which can be reduced to

three components:

$$\frac{\partial^2 V}{\partial x^2}, \quad \frac{\partial^2 V}{\partial y^2} \quad \text{and} \quad \frac{\partial^2 V}{\partial z^2} \quad \text{written as:}$$

$$V_{xx}, \quad V_{yy} \quad \text{and} \quad V_{zz}$$

It is customary to define the co-ordinate system of the resonant nucleus so that $V_{zz} = eq$ is the maximum value of the field gradient. The components of the efg are related by the Laplace equation in a region where the charge density vanishes. Thus;

$$V_{xx} + V_{yy} + V_{zz} = 0 \quad (11)$$

Consequently, only two independent parameters are needed to specify the efg completely, and the two which are normally chosen are V_{zz} (the z-component of the efg) and an asymmetry parameter, η , defined as

$$\eta = \frac{V_{xx} - V_{yy}}{V_{zz}} \quad (12)$$

Using the convention that $|V_{zz}| > |V_{xx}| > |V_{yy}|$ ensures that $0 \leq \eta \leq 1$.

It is possible to evaluate η and the quadrupole coupling constant, e^2qQ , from a Mössbauer spectrum. However, it is much more difficult to rationalise the parameters in terms of the electronic structure which generated them.

Contributions to the efg may be considered to arise from (a) the valence electrons of the Mössbauer atom and of the bonds between it and the ligands, q_{val} , (b) charges

on the atoms directly bonded to the Mössbauer atom, and (c) charges on neighbouring molecules and ions in the lattice. Both (b) and (c) constitute q_{lat} but as the efg decreases with the third power of distance, contribution (c) is often neglected.

2.2.3 Magnetic Hyperfine Interaction

So far, it has been assumed that the nucleus is not exposed to a magnetic field, either internal or applied and this is generally the case for organotins in non-magnetic matrices. There are, however, many systems which have a magnetic hyperfine field capable of interacting with the nuclear dipole moment, μ_N . This interaction completely removes the degeneracy of the nuclear state with spin I into its $2I + 1$ component Zeeman states.

According to the selection rule, $\Delta m_I = 0, \pm 1$, six transitions are allowed which for a random powder or unmagnetized foil where $V_{zz} = 0$, produces a six-line spectrum with intensity ratios given by 3:2:1:1:2:3.

The magnetically split spectrum of iron-57 is used for spectrometer calibration as discussed in Section 2.7.

A summary of each hyperfine interaction and the form of the resulting Mössbauer spectra are shown diagrammatically in Figure 2.6.

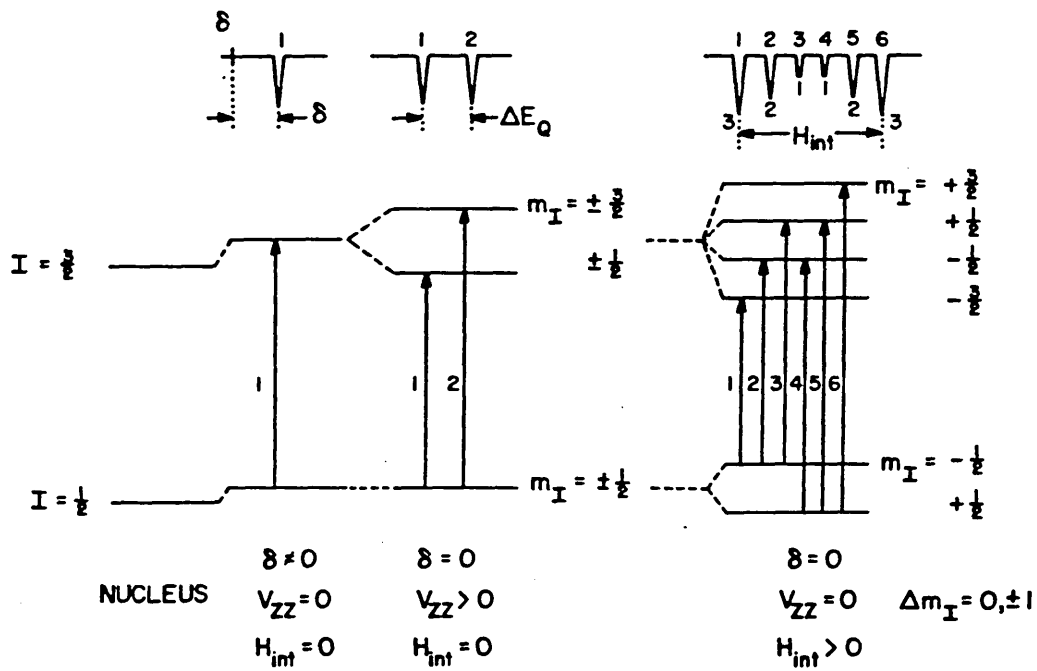


Figure 2.6 : Schematic diagram of the nuclear energy level shift and splitting as a function of chemical environment, electric field gradient, and internal magnetic hyperfine field

It is clear from the foregone discussion that the energy shifts resulting from the hyperfine interactions, will only be observed if the source energy can be modified in a precise manner that will facilitate scanning of the absorption spectrum over the required energy distribution. The resonance condition, $E_\gamma = E_{\text{absorber}}$, can be restored, and the spectrum scanned, by applying a variable velocity, V_D , to the source. The energy, E_γ , then perceived by the absorber, depends upon the energy of the γ -photons emitted by the source, E_s , and the magnitude of V_D

according to equation (13).

$$E_{\gamma} = E_S (1 + V_D/c) \quad (13)$$

where c is the velocity of light.

The energy changes involved in the hyperfine interactions are such that Doppler velocities of only a few millimetres per second are required to restore the resonance condition. A Mössbauer spectrum, therefore, consists of a plot of accumulated γ -ray counts versus Doppler velocity in mm s^{-1} . For the 23.8 keV transition in tin-119, a source velocity of 1.00 mm s^{-1} corresponds to an energy shift of $7.94 \times 10^{-8} \text{ eV}$ and this represents an energy resolution, $\Delta E/E_S$, of 3×10^{-12} . The practical details of the Mössbauer experiment and Doppler modulation will be discussed in Section 2.5.

2.3 APPLICATIONS TO ORGANOTIN CHEMISTRY

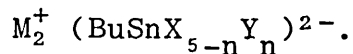
The unique properties of tin-119 which make it such a useful isotope for the spectroscopic elucidation of structure, are the combination of a nuclear ground state of spin $I = \frac{1}{2}$ which makes it amenable to NMR studies, plus an accessible isomeric state of suitable spin ($I = \frac{3}{2}$), lifetime and energy whose γ -decay makes it an ideal Mössbauer nuclide (Section 2.5).

2.3.1 Isomer Shifts

As mentioned in Section 2.2.1, isomer shift (δ) values are largely determined by the s-electron density at the nucleus. For all tin compounds, positive isomer shifts correspond to increased s-electron density at the tin nucleus with respect to the source. The assumption that the inner shell electron contribution to the electrostatic interaction is essentially constant, implies that changes in isomer shift reflect changes in the s-electron density of the valence shell, i.e. in the 5s sub-level for tin. Consequently, δ should vary with the polarity of the tin-ligand bonds and also the number of stereochemical arrangements of bonds.

(i) The Nature of the Tin-Ligand Bond

The tin-ligand bond is expected to become increasingly polarised in the sense $\text{Sn}(\delta+) - \text{X}(\delta-)$, as the electronegativity of ligand X increases. The withdrawal of s-electron density from the tin 5s-orbital would then be expected to result in a decrease in the isomer shift. This trend is observed and is illustrated in Table 2.1 for tin(IV) tetrahalides and a series of anionic monobutylpentahalogeno stannate salts,



Compound	δ (mm s ⁻¹)
SnCl ₄	0.82 ^a
SnBr ₄	1.13 ^a
SnI ₄	1.55 ^a
(Et ₄ N) ₂ (BuSnCl ₅)	1.03 ^b
(Et ₄ N) ₂ (BuSnCl ₄ Br)	1.08 ^b
(Et ₄ N) ₂ (BuSnCl ₃ Br ₂)	1.15 ^b
(Et ₄ N) ₂ (BuSnCl ₂ Br ₃)	1.20 ^b
(Et ₄ N) ₂ (BuSnBr ₅)	1.38 ^b

a Data taken from reference [3] were measured relative to BaSnO₃ at 80K with an associated experimental error of 0.01 mm s⁻¹.

b Data taken from reference [4] were measured relative to BaSnO₃ at 80K with an associated experimental error of 0.05 mm s⁻¹.

Similar trends have been observed in tetraorganotin (R₄Sn) and triorganotin (R₃SnX) systems. In general, for a constant X group in a series of R₃SnX compounds, δ increases as the electron donating power of the organic group increases, Table 2.2.

R	$\delta(R_4Sn)$ (mm s ⁻¹)	$\delta(R_3SnOH)$ (mm s ⁻¹)
CH ₃ -	1.20	1.20
C ₂ H ₅ -	1.30	1.30
C ₃ H ₇ -	1.30	1.34
C ₄ H ₉ -	1.35	1.37
C ₆ H ₅ -	1.15	1.16

Table 2.2 : Variation of δ with R in R₄Sn and R₃SnOH derivatives [5,6]

Isomer shifts are measured relative to BaSnO₃ with an absorber temperature of 80K.

It will be noted from Table 2.2 that the phenyl (C₆H₅-) derivatives give appreciably lower isomer shifts than any of the alkyltins. This reflects the strongly electron withdrawing nature of the phenyl group.

(ii) Co-ordination Number

Organotins assume a wide variety of structural types which encompass four to eight coordination in neutral and charged species. Many compounds associate through inter- and intra-molecular bonding to give bridged dimers and other oligomers with one, two and three dimensional crystal lattices.

Increasing the coordination number from four leads to increased population of the tin 5d-orbitals which must,

in turn, increase shielding of the 5s-electrons from the nucleus. Therefore, it is to be expected that an increase in the coordination of the tin atom will lead to a decrease in isomer shift. This trend is illustrated in a series of halogenotin(IV) species where the isomer shifts for SnX_6^{2-} are 0.2 to 0.3 mm s^{-1} less than for the corresponding SnX_4 compounds, (Table 2.3).

X	SnX_4 ^a	SnX_6^{2-} ^b
Cl	0.82	0.50
Br	1.13	0.84
I	1.55	1.23

Table 2.3 : Isomer Shift Data for 4- and 6-Coordinate Halogenotin(IV) species, mm s^{-1}

a Data from Table 2.1

b Data taken from reference [7] for the Et_4N^+ salts, were measured relative to SnO_2 at 77K. An experimental error of $\pm 0.02 \text{ mm s}^{-1}$ is assumed for these measurements.

In complexes involving neutral ligands, the decrease in δ resulting from increased coordination number may be offset by electron donation from the soft ligand.

(iii) Structure

It has been suggested [8] that the isomer shift in organotin compounds is sensitive towards the stereochemical arrangement of ligands about the tin nucleus.

This is most clearly demonstrated in a comparison of octahedral cis- and trans-diorganotin complexes (Table 2.4).

cis-R ₂ SnX ₄	δ	trans-R ₂ SnX ₄	δ
Me ₂ Sn(oxin) ₂	0.88	Me ₂ Sn(acac) ₂	1.18
Et ₂ Sn(oxin) ₂	0.87	Bu ₂ Sn(NCS) ₂ bipy	1.43
Ph ₂ Sn(acac) ₂	0.74	Bu ₂ Sn(NCS) ₂ phen	1.42
Ph ₂ Sn(NCS) ₂ bipy	0.82	Ph ₂ SnCl ₂ .bipy	1.22

Table 2.4 : Isomer Shift Data for cis- and trans-R₂SnX₄, mm s⁻¹

Data taken from references [5], [9] and [10].

In general, it is found that the cis-complexes have significantly lower isomer shifts than the trans complexes and this is thought to originate from the increased s-character of the Sn-C bonds in the latter [10].

2.3.2 The Quadrupole Splitting Parameter

It was established in Section 2.2.2 that the quadrupole interaction resulted from the establishment of an electric field gradient (efg) in the vicinity of the nucleus. The principal contributions to the efg, q_{val} and q_{lat} , indicate that, if the tin atom has a perfectly cubic charge symmetry ($V_{zz} = 0$), then no quadrupole interaction will exist and only a single line spectrum will be obtained. This is the situation

regarding symmetrical tetraorganotin, fac-octahedral complexes and symmetrical inorganic tin compounds (eg, SnX_4).

Any deviation of the nuclear charge environment from cubic symmetry produces a quadrupole interaction that results in a characteristic two-line spectrum. The magnitude of the quadrupole splitting, ΔE_Q , is estimated from the spectrum as the separation between the two peaks.

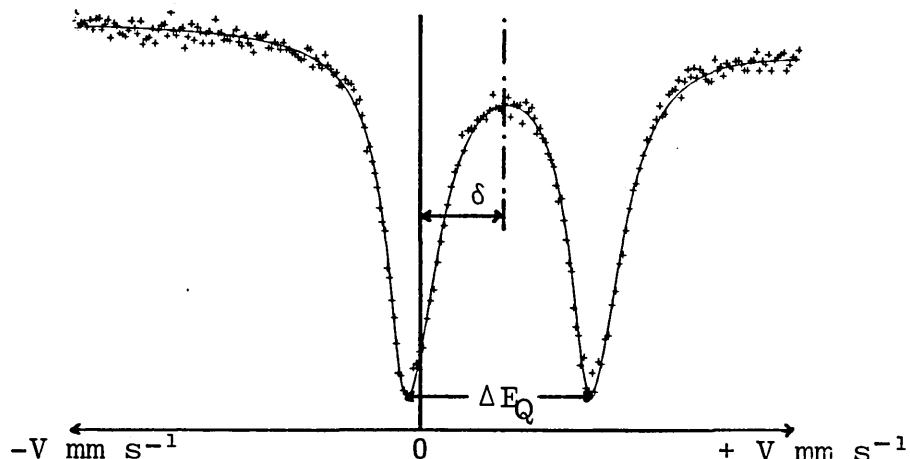


Figure 2.6a: The effect of the quadrupole interaction on the resultant Mössbauer spectrum

The point charge model has been shown to be a useful method of correlating quadrupole splitting with structure in organotin systems [11]. The model assumes that each ligand, L, makes a fixed contribution, [L], to the quadrupole splitting regardless of the structure of the compound and the nature of the other ligands. Thus, within a series of octahedral complexes, RSnX_5^- , $\text{cis-R}_2\text{SnX}_4$ and $\text{trans-R}_2\text{SnX}_4$, the quadrupole splittings are expected to lie in the ratio 1:1:2. Data for some

compounds whose structures have been determined independently, are given in Table 2.5.

R ₅ SnX		cis-R ₂ SnX ₄		trans-R ₂ SnX ₄	
BuSnCl ₅ ²⁻	1.86 ^a	Me ₂ Sn(OX) ₂	2.02	Me ₂ Sn(acac) ₂	4.02 ^d
BuSnCl ₃ .2DMSO	1.73 ^a	Bu ₂ Sn(OX) ₂	2.21 ^c	Me ₂ SnCl ₄ ²⁻	4.32 ^b
BuSnCl ₃ .2Ph ₃ PO	2.32 ^a	Ph ₂ Sn(OX) ₂	1.63 ^c	Bu ₂ Sn(NCS) ₂ bipy	4.04 ^c

Table 2.5 : Quadrupole Splitting Data for Octahedral Organotin Complexes, mm s⁻¹

- a Data, from reference [7], are quoted relative to SnO₂ with the absorber at 77K.
- b Data, from reference [11], are quoted relative to SnO₂ with the absorber at 77K and are associated with error of ± 0.05 mm s⁻¹.
- c Corrected data from reference [13] are quoted relative to BaSnO₃ with an absorber temperature of 80K and associated with an error of ± 0.07 mm s⁻¹.
- d Data obtained from reference [14] are quoted relative to BaSnO₃ with the absorber at 80K and have an associated experimental error of ± 0.02 mm s⁻¹.

Point charge calculations on four coordinate compounds, R₅SnX₃, R₂SnX₂ and R₃SnX indicate that the quadrupole splittings should lie in the ratio 1:1.15:1. Data for related organotins, Table 2.6, show good agreement between the experimentally observed trend and the

predicted behaviour.

R, X	R_2SnX_2	R_3SnX
Me, $C_6F_5^1$	1.51	1.27
Ph, $C_6F_5^2$	1.11	0.90
Ph, C_6Cl_5	1.23	0.84
Ph, Cl	2.82	2.48
Ph, Br	2.54	2.48
Ph, I	2.38	2.09

Table 2.6 : Quadrupole Splitting Data for 4 coordinate Organotin Compounds, $mm\ s^{-1}$

1. $MeSn(C_6F_5)_3$, $\Delta = 1.14\ mm\ s^{-1}$
2. $PhSn(C_6F_5)_3$, $\Delta = 0.92\ mm\ s^{-1}$

Data selected from reference [10] were obtained from absorbers at 80K.

Generally, five-coordinate organotins exhibit intermediate ΔE_Q values with respect to four- and six-coordinate organotins [10].

Experimentally, it is possible to associate a range of ΔE_Q values with particular tin atom stereochemistries. Table 2.7 illustrates this correlation for typical geometries [15].

Stereochemistry		ΔE_Q (mm s ⁻¹)
Tetrahedral	R ₃ SnX	1.00-2.40
	R ₂ SnX ₂	
Trigonal Bipyramidal	trans-R ₃ SnX ₂	3.00-4.00*
	cis-R ₃ SnX ₂	1.70-2.40
	mer-R ₃ SnX ₂	3.50-4.10
Octahedral	fac-R ₃ SnX ₃	0.00
	mer-R ₃ SnX ₃	3.50
	cis-R ₂ SnX ₄	~ 2.00
	trans-R ₂ SnX ₄	~ 4.00

Table 2.7

*When the axial Sn-X bonds are almost equal in length, $\Delta E_Q \approx 3.00$ mm s⁻¹. As the difference between these two bonds increases, ΔE_Q tends towards 4.00 mm s⁻¹.

There is a considerable degree of overlap between the ΔE_Q ranges and certain stereochemical arrangements. This illustrates the limitation of using this type of correlation in structural assignments, and it is clear that ΔE_Q ranges themselves cannot be relied upon to indicate absolute tin site geometries.

2.4 EXPERIMENTAL DETAILS

The Mössbauer experiment is essentially a measurement of the resonant absorption in the sample being studied, as a function of energy. The principal components of a Mössbauer spectrometer are thus:

- (i) a suitable source of γ -photons,
- (ii) an energy modulation system,
- (iii) a detector,
- (iv) a means of storing accumulated counts,
- (v) a cryogenic system.

2.4.1 Suitable Mössbauer Isotopes

The most widely studied isotopes utilising the Mössbauer effect are iron-57 and tin-119, although at least forty other elements show the effect.

The nucleus of an isotope suitable for Mössbauer spectroscopy must have an excited state of moderately low energy (less than about 150 keV) to permit the occurrence of recoilless emission and absorption. The excited state must be accessible, preferably by the spontaneous decay of a parent isotope with a reasonably long half-life ($t_{\frac{1}{2}}$). Also, the spectral line width of the Mössbauer γ -photon must be small enough to permit resolution of the hyperfine interactions, but not so small that the slightest laboratory vibration destroys the resonance condition.

For a given absorber in which absorption saturation effects can be neglected (the "thin" absorber criterion), the magnitude of the Mössbauer effect is proportional to the area, (A), beneath the absorption profile. This is given by:

$$A = \frac{\pi}{2} \cdot f_a \cdot f_s \cdot \sigma_o \cdot n \cdot x \cdot \beta \quad (14)$$

where σ_o is the isotope cross-section, n is the natural isotopic abundance, x is the absorber thickness, β is a splitting ratio equivalent to 1/number of absorption lines, and f_a and f_s are absorber and source Recoilless Fractions respectively. The recoilless fraction, to be discussed later (Section 5.2), gives a measure of the probability that γ -emission or absorption will be a zero-phonon interaction (Section 2.1.1). It is related to the γ -photon energy and the mean square vibrational amplitude, $\langle x^2 \rangle$, of the emitting (or absorbing) nucleus, thus:

$$f = \exp \left(\frac{-4\pi \langle x^2 \rangle}{\lambda^2} \right) \quad (15)$$

where λ is the wavelength of the γ -photon. Thus, f varies from 0 to 1. From equation (14), it is apparent that only those isotopes that have a large natural abundance, large cross-section and large recoil-free fraction will show a significant Mössbauer effect.

2.4.2 The Mössbauer Source

The properties of the two common Mössbauer isotopes, iron-57 and tin-119, are compared in Table 2.8. The parent isotope for tin-119 is the 89.5 keV tin-119m which has a half-life of 245 days and decays directly to the 23.8 keV Mössbauer level, Figure 2.7. The metastable source isotope is conveniently prepared by neutron bombardment of a matrix enriched in tin-118 (natural abundance 23.84%) to increase the specific activity of the resultant metastable nuclide, and to deplete the amount of 119-isotope thereby reducing self-absorption of the γ -photons.

Several source matrices are available (SnO_2 , BaSnO_3 , Mg_2Sn , Pd_3Sn) and the one which has been used in this work is barium stannate (BaSnO_3), the source having initial activity at 15 mCi. This matrix produces a strong ($f_{S,239K} \approx 0.6$ [16]) single resonance with a full experimental line width of 0.8196 mm s^{-1} and an isomer shift of -2.56 mm s^{-1} measured relative to an 0.0125 mm β -tin foil absorber. The experimental line widths quoted in the following work are actually the sum of the natural line widths of the emission and absorption profiles, ie $\Gamma_{\text{exp}} \approx \Gamma_{\text{abs}} + \Gamma_{\text{source}}$.

Tin-119	Iron-57
$E_{\gamma} = 23.871 \text{ keV}$ $t_{\frac{1}{2}} = 17.75 \text{ ns}$ $IA = 8.58\%$ $\alpha = 5.12 \pm 0.10$ $\mu_g = -1.04621(6) \text{ nm}$ $\mu_e = +0.682(8) \text{ nm}$	$E_{\gamma} = 14.413 \text{ keV}$ $t_{\frac{1}{2}} = 97.81 \text{ ns}$ $IA = 2.14\%$ $\alpha = 8.21 \pm 0.12$ $\mu_g = +0.09024(7) \text{ nm}$ $\mu_e = -0.15460(16) \text{ nm}$
$\Gamma = 2.570 \times 10^{-8} \text{ eV}$ $\omega_0 = 0.646(4) \text{ mm s}^{-1}$ $E_R = 2.5703(11) \times 10^{-3} \text{ eV}$	$\Gamma = 4.665(7) \times 10^{-9} \text{ eV}$ $\omega_0 = 0.1940(3) \text{ mm s}^{-1}$ $E_R = 1.956275(25) \times 10^{-3} \text{ eV}$
	Line Positions enriched Fe, RT symmetrical $\pm 5.312(4) \pm 3.076(2)$ $\pm 0.840(2) \text{ mm s}^{-1}$
$1 \text{ mm s}^{-1} \equiv 7.9625(23)$ $\times 10^{-8} \text{ eV}$	$1 \text{ mm s}^{-1} \equiv 4.80766(3)$ $\times 10^{-8} \text{ eV}$

Table 2.8 : Mössbauer Nuclear Parameters and Calibration
Data for Tin-119 and Iron-57

Data taken from references [17] and [18].

KEY

IA = natural isotopic abundance, μ = magnetic moment of ground (g) and excited (e) states, α = internal conversion coefficient of Mössbauer transition and E_R = recoil energy.

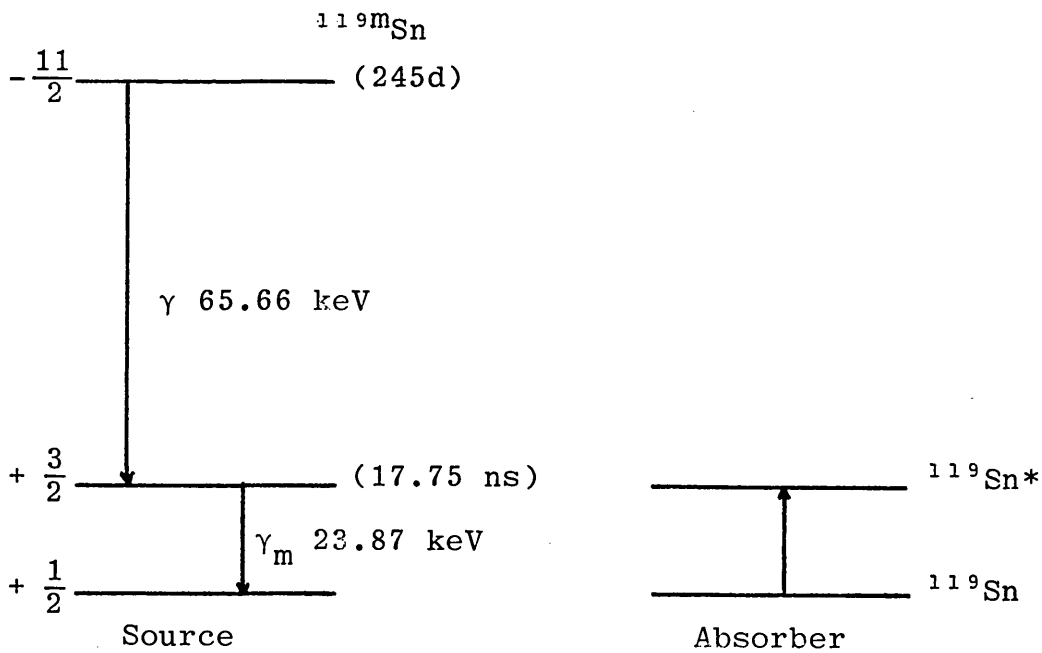


Figure 2.7 : Nuclear Decay Scheme for Tin-119m

2.4.3 Mössbauer Absorbers

It was stated in Section 2.1.1 that the line width, Γ , of the emitted γ -photon is related to the half-life of the excited nuclear state, thus $\Gamma = h/2\pi \tau$, where the mean lifetime, τ , is equal to $t_{1/2}/0.693$. In practice, the experimental line width is influenced by the absorber thickness, t .

This is evaluated from equation 16 [19] in which σ_0 is the peak nuclear cross-section at resonance, f_a is the absorber recoilless fraction, n is the number of resonant nuclei/cm² and β represents the partial strength of the absorption line intensity in hyperfine split spectra. Thus, for a symmetrically split quadrupole doublet, $\beta = 0.5$

$$t = \beta \cdot n \cdot f_a \cdot \sigma_0 \quad (16)$$

For tin-119, $\sigma_0 = 1.40313 \times 10^{-18} \text{ cm}^2$ [20].

As the absorber thickness increases beyond $t \approx 10$ [19], the line shape begins to deviate from purely Lorentzian as saturation effects become evident. In order to minimise line broadening without incurring excessive accumulation times to observe the effect, it is necessary to optimise t for each of the sample types under study. The actual area under the absorption curve for an absorber of thickness t is given by:

$$A(t) = f_s \Gamma_a \pi \frac{t}{2} \exp\left(-\frac{t}{2}\right) \left[I_0\left(\frac{t}{2}\right) + I_1\left(\frac{t}{2}\right) \right] \quad (17)$$

where I_0 and I_1 are the zeroth and first order Bessel functions, f_s is the recoilless fraction of the source and Γ_a is the line width of the absorber [16]. The small t expansion of equation (17) leads to:

$$A(t) \propto f_s t (1 - 0.25t + 0.0625t^2 + \dots) \quad (17a)$$

which holds when $t \ll 5$. For $t \geq 10$, equation (17) must apply.

Typical values for t in authentic antifouling elastomers can be estimated from equation (16) if approximate f_a values are assumed. A typical calculation from AFR 3644 containing 2.5% by weight of TBTC1 is shown below:

Mass of elastomer = 1.8243 g \equiv 0.04561 g TBTC1

Therefore mass of tin-119 in elastomer = 1.43×10^{-3} g

Sample area = 2.27 cm^2 .

So we have : $\frac{1.43 \times 10^{-3} \times N_A}{119 \times 4.91}$ atoms tin-119/cm²

i.e. $n = 1.47 \times 10^{18}$ atoms/cm².

Organotins typically exhibit f-values between 0.06 and 0.4 at 80K. Substituting the maximum value into equation (16) along with n yields:

$$\begin{aligned} t &= 0.5 \times 1.40313 \times 10^{-18}(\text{cm}^2) \times 3.19 \times 10^{18}(\text{cm}^2) \\ &\quad \times 0.4 \\ &= \underline{0.41} \end{aligned}$$

Because $t \ll 5$, the small t expansion of equation (17) may be used to demonstrate that the area beneath the absorption profile is directly proportional to the absorber thickness in this sample:

$$\begin{aligned} A(t) &\propto f_S t - 0.25 f_S t^2 + 0.0625 f_S t^3 + \dots \\ \rightarrow A(t) &\propto 0.41 f_S - 0.042 f_S + 0.00431 f_S + \dots \end{aligned}$$

The non-linear t-terms are considered negligible and the area can be expressed in the form

$$A(t) = \text{const.} \cdot t, \text{ for a given source.}$$

Under these conditions, a good quality spectrum for the elastomers could be obtained in 24 hours. Certain neat organotins required much shorter run times (ca. 2 hours) whilst other organotin systems needed days to reveal fine detail. These will be discussed in the appropriate sections.

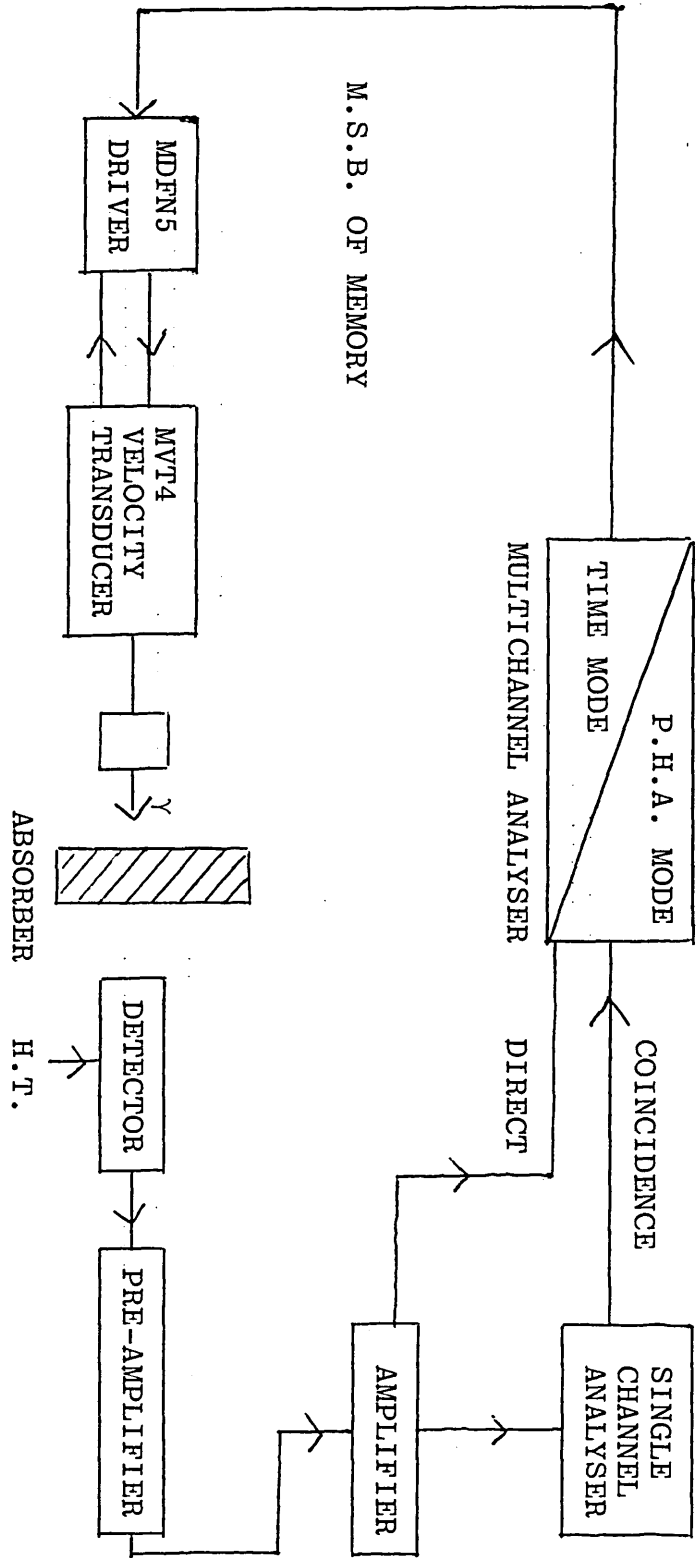
2.5 INSTRUMENTATION

The principal elements of a Mössbauer spectrometer were briefly mentioned in the previous section (2.4). Figure 2.8 gives a schematic diagram of the Mössbauer spectrometer used in this study.

2.5.1 Mössbauer Drive System and Multichannel Analyser

A transmission Mössbauer spectrum consists of a plot of the number of γ -photons transmitted through an absorber as a function of the instantaneous relative velocity of the source with respect to the absorber. In this work, Doppler velocities were imparted to the source by mounting it on the moving rod of an Elscint Linear Velocity Transducer, Model MVT4. This was operated in conjunction with the Elscint Transducer Driving Unit, Model, (i) MDF-N-G or (ii) MFG-N-5. A Multi-Channel Analyser (MCA) (Canberra Industries Series 30) employing 512 channels was used, and from this a square wave having its leading edges at channels 256 and 512 was extracted by the transducer driving unit. The integrated square wave results in a symmetrical triangular wave form that is fed to the velocity transducer. The source is then vibrated under constant acceleration and feedback circuits ensure that the transducer follows the waveform precisely. The amplitude of the triangular wave determines the velocity scan of the transducer and is adjusted using a conventional potentiometer (helipot). For the organotin studies, a velocity range of $\pm 6 \text{ mm s}^{-1}$ provided a convenient scale for the Mössbauer spectra.

Figure 2.8 : Schematic of the Mössbauer System



The MCA operates in two modes:

- (i) Pulse Height Analysis (PHA) mode employs a single channel analyser (SCA) to set an energy window on the appropriate Mössbauer γ -photon, Figure 2.9 (a).

- (ii) Time mode where the analyser operates as a multichannel scaler (MCS). In this mode, the analyser sequentially sweeps through 512 channels (or 1024 or 256 depending on the particular experiment) with typical dwell times per channel of 200 μ s. At the end of one 512 channel sweep, the analyser repeats the cycle at a frequency of about 10 Hz. Clock pulses from the waveform generator enable the MCA to synchronise with the transducer so that each channel corresponds to a specific Doppler velocity. The symmetrical nature of the velocity waveform, Figure 2.9 (b), means that the source moves under a certain velocity twice during one cycle. This results in the accumulation of two spectra, mirror imaged about the central channel (\approx 256). The duplicate spectra can easily be combined using an appropriate computer folding program (Section 2.6) and they provide a means of identifying any lack of linearity in the velocity scan.

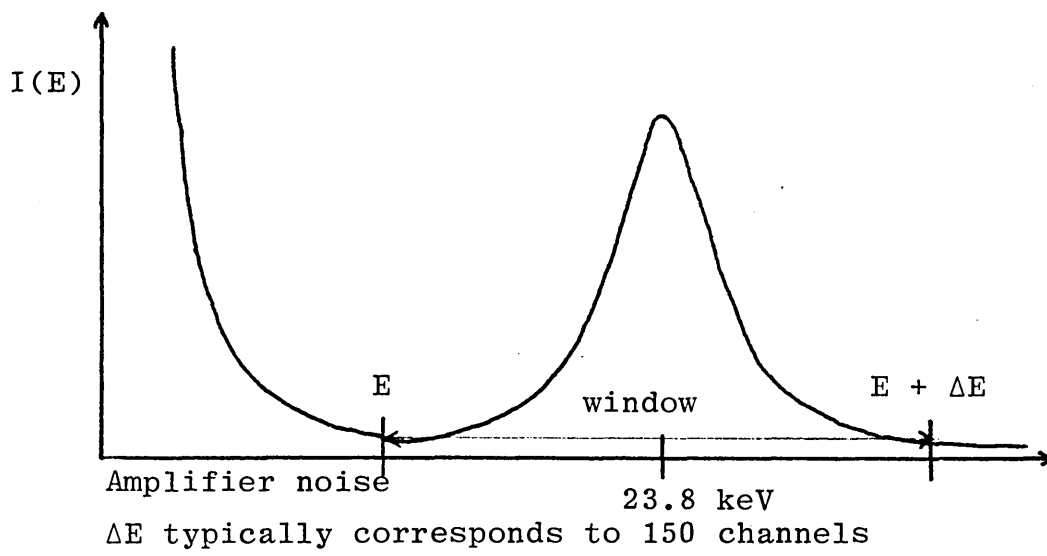


Figure 2.9 (a) PHA spectrum of the 23.8 keV photopeak
 for the $I = \frac{3}{2}$ to $I = \frac{1}{2}$ transition in
Tin-119

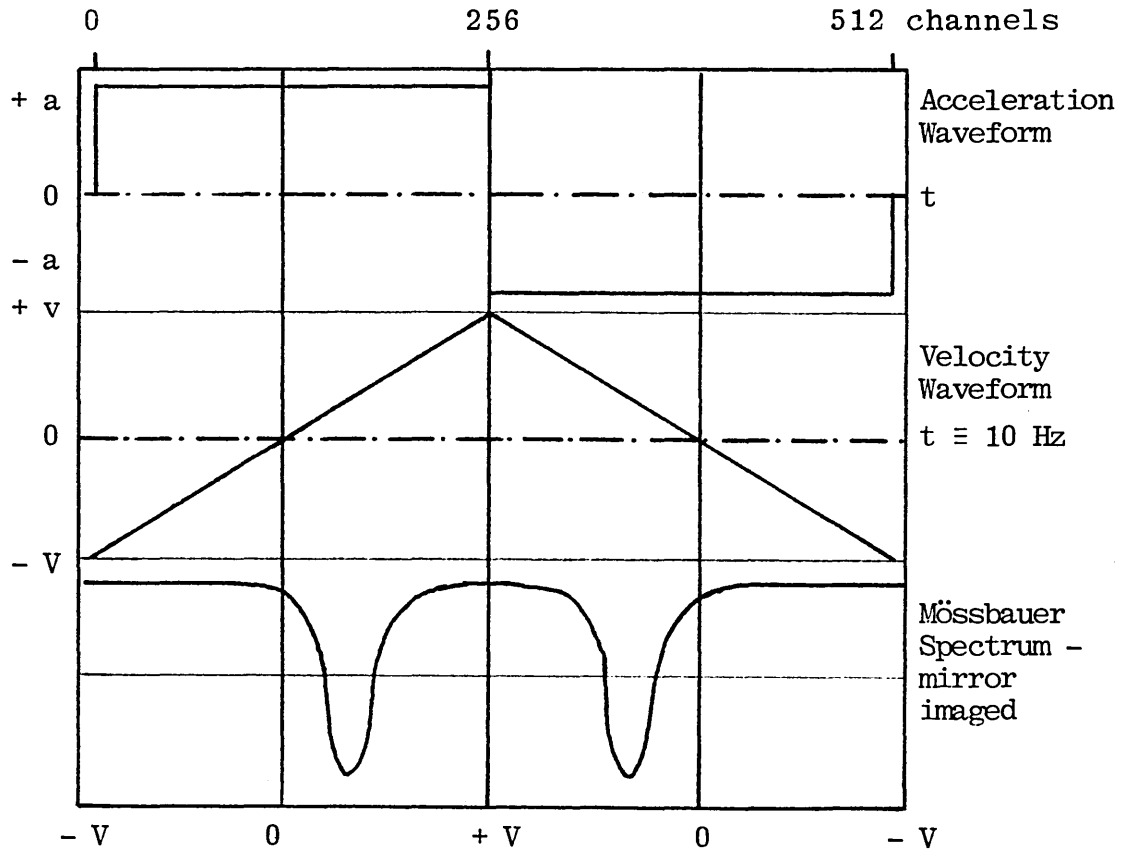


Figure 2.9 (b) Synchronization of MCA and transducer
sweeps

2.5.2 Detectors

The detection system consists of either a scintillation counter or gas-filled proportional counter (depending upon E_γ), together with a pre-amplifier and amplifier. For iron-57 spectroscopy and lower energy γ -photons, the gas proportional counter is preferred because of its high efficiency and good resolution at low energy. Thus, for spectrometer calibration employing the magnetically split spectrum of natural iron (enriched in iron-57) and the 14.4 keV Mössbauer γ -transition, a gas-proportional counter filled with argon (95%) and methane (5% - quench gas) from the Mössbauer Group, AERE, Harwell, was used.

The sodium iodide-thallium activated, NaI(Tl), scintillation counter (crystal thickness 0.5 mm) is the most efficient detector for the 23.8 keV γ -photons measured in the tin-119 experiments. The particular model (DM1-2) used in this work was supplied by Nuclear Enterprises Limited and was operated at 1 kV in all experiments.

2.5.3 Cryogenics

The principal reason for employing low temperatures in this work, was to increase the absorber recoilless fraction in a variety of organotin systems. Two particular cryogenic systems were employed, depending on the temperature range needed for a particular experiment.

(i) The majority of the experiments were carried out isothermally with the absorber at 80K. For this, an Oxford Instruments liquid nitrogen-cooled cryostat (Model DN1726) with variable temperature facility, was used in conjunction with a Model 3120 digital temperature controller from the same manufacturers.

The cryostat operates on the principle of the controlled continuous transfer of liquid nitrogen from a reservoir to a heat exchanger which surrounds the sample space, Figure 2.10(a). A platinum sensor and a heater fitted to the heat exchanger allow the 3120 temperature controller to offset the cooling effect of the circulating nitrogen, and maintain the sample at a preset desired temperature; 80K. The use of nitrogen exchange gas in the sample space affords rapid thermal equilibration.

The sample itself is held in the low temperature region by a sample probe such that the absorber rests in alignment with the aluminised mylar windows through which the γ -photons pass. Two sample probes were used, one of which could be coupled to the temperature controller for more direct heating of the sample, Figure 2.10(b).

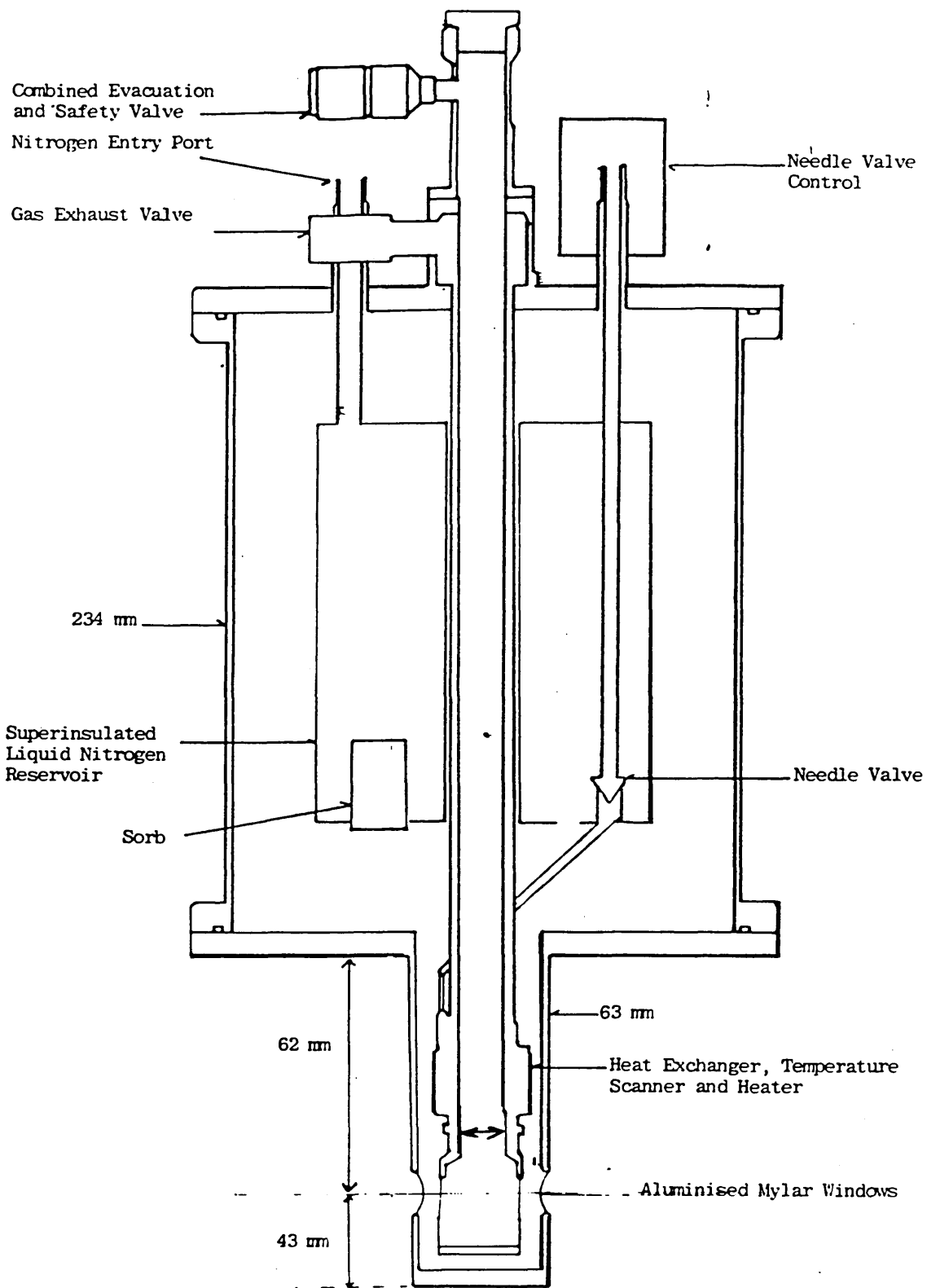


Figure 2.10(a) Vertical Section through DN1726

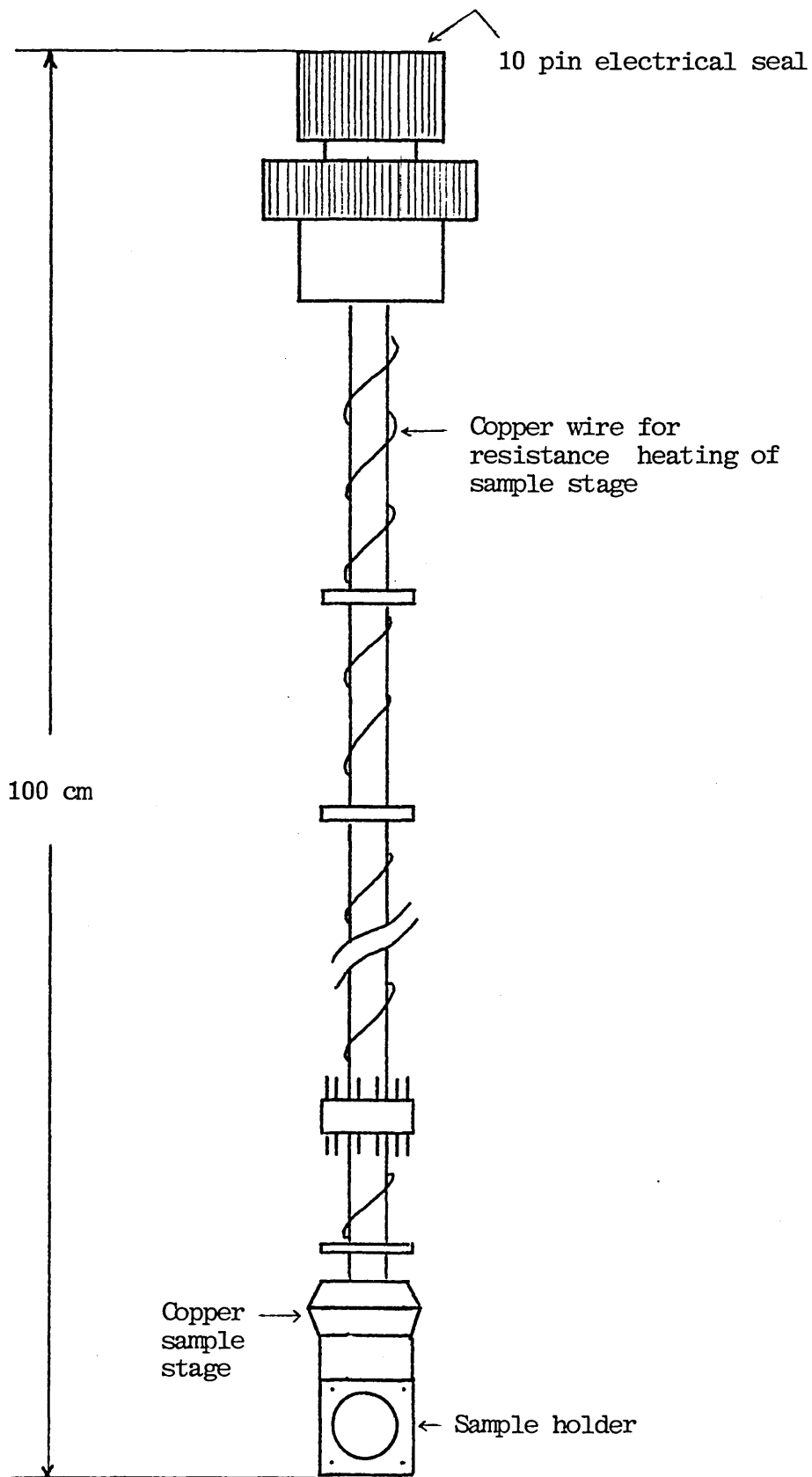


Figure 2.10(b) : Sample probe for use with DN 1726 cryostat

(ii) The variable temperature experiments described in Section 5.3, required much lower absorber temperatures than could be achieved with the DN1726 cryostat. Therefore, a second system using pumped helium gas was used to cool the absorbers down to a base temperature of 12.5K. The system was comprised of four basic components; a helium compressor unit, an expander module and sample stage, a temperature controller and vacuum system shown schematically in Figure 2.11.

This basic arrangement constitutes the "Displex" cryostat and the principal components, supplied by Air Products and Chemicals Inc., were; the expander module (Model DE202), the compressor module (model IRO2W) and the temperature controller (series 3700). The absorbers, held in an appropriate sample holder, were fixed to a "cold-finger". The finger is mechanically isolated from the heat exchanger and is cooled by helium exchange gas. The heat exchanger is cooled by the expansion of high pressure helium gas down from the compressor module. Low pressure helium leaving the expander module is continuously recycled by the compressor for further use as a cryogen. The sample area is held under vacuum ($\approx 10^{-6}$ torr) and the absorbers are cooled by conduction of heat along the cold finger.

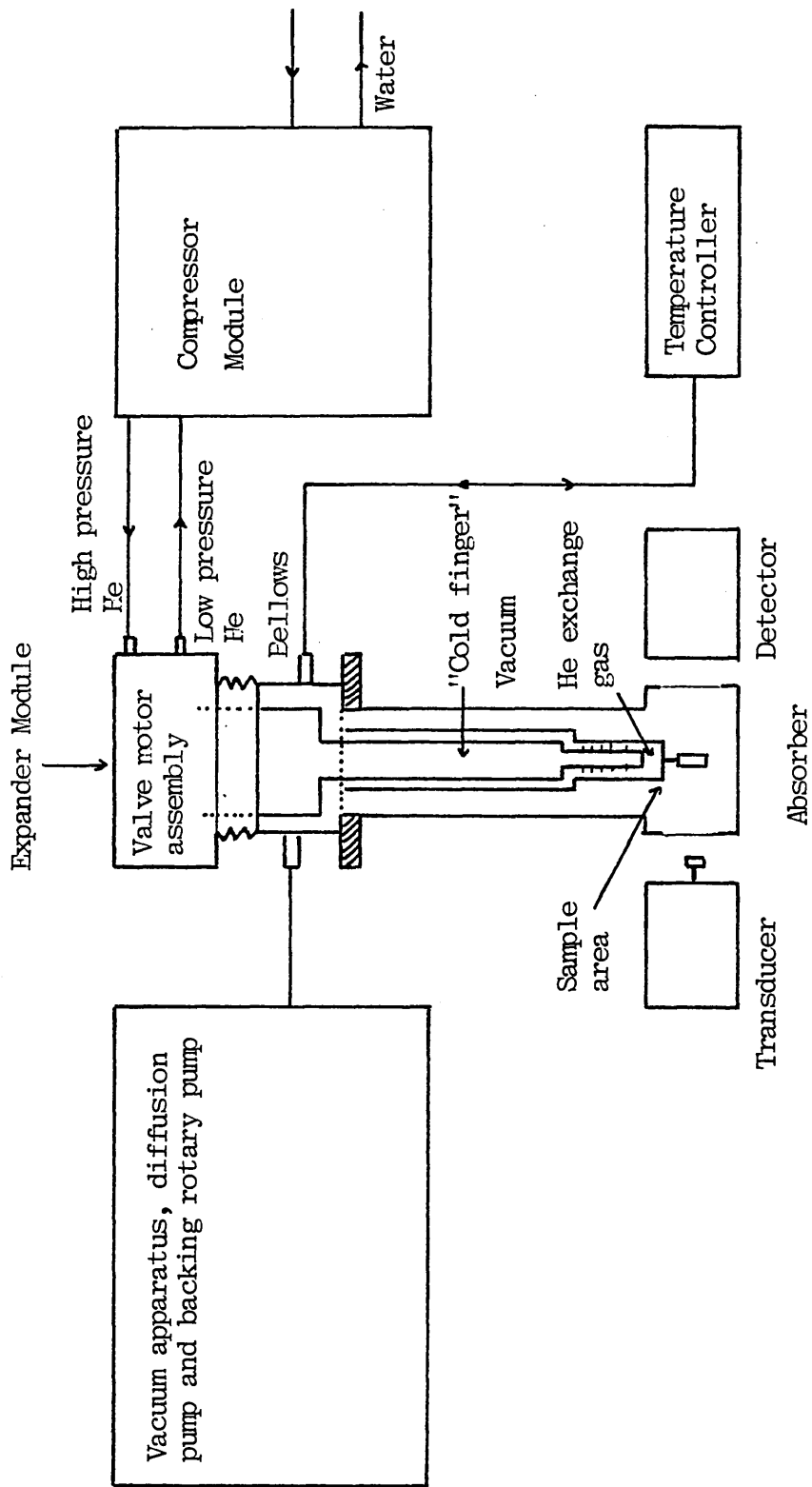


Figure 2.11 : Mössbauer experimental arrangement using the He cooled cryostat-displex system

In order to eliminate vibrations in the sample area which may have destroyed resonance, flexible couplings were used for gas transfer between the vacuum pumps and the compressor module. Vibrations from the valve motor assembly in the expander module were eliminated by mounting this part of the apparatus in a frame that was securely bolted to a concrete pillar in the laboratory. The lower part of the apparatus, containing the sample stage, was similarly supported in a frame that was bolted to the floor of the laboratory. The only physical link between the two portions of the assembly, then, consisted of a set of soft rubber bellows which isolated the vibrations from the expander valve motor.

2.6 DATA HANDLING

Having obtained a mirror imaged Mössbauer spectrum on the MCA (Section 2.5.1), the "raw" data must be combined to produce a single spectrum which may then be interpreted by modelling the data to theoretical Lorentzian line functions. These two operations; folding and fitting, are readily performed by a number of programs running on a laboratory-based Hewlett-Packard HP86 microcomputer and on the Polytechnic mainframe facility, an IBM 4341.

2.6.1 Data Transfer

In the early stages of this project, data transfer between the MCA and the IBM 4341 was accomplished by means of punched paper tape. This involved the rather tedious process of converting the MCA data to paper tape form, followed by the equally tedious process of reading the paper tape data into a file specially allocated in the IBM 4341 memory.

Recently, however, data transfer from the MCA to the mainframe has been greatly simplified (though not hastened!) by the use of two interfacing programs.. The first, "MOSSPLOT 9K", is a BASIC routine running on the HP 86 in the laboratory, and this reads the raw data from the MCA, then stores it on disc in a format suitable for subsequent transfer to the mainframe. This program also allows the plotting of raw folded data on a dedicated HP 7475A plotter.

The second interfacing program, "KERMIT", enables the HP 86 to emulate a mainframe I/O device and facilitates the direct transfer of data from disc storage to the mainframe. The interaction between these data handling elements is illustrated in Figure 2.12.

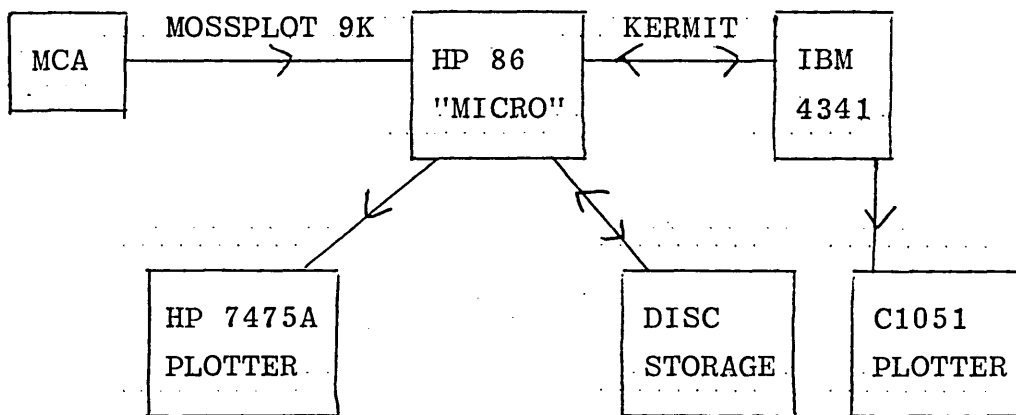


Figure 2.12 : Schematic of the Mössbauer Data Transfer Processes

2.6.2 The Folding Program

On arrival at the mainframe, the raw data for the mirror imaged spectrum must be folded to produce a single spectrum. This is accomplished using the FORTRAN 77 MOSFOLD routine which maps data points from one half of the MCA memory (channels 0-256) to corresponding points in the other half (channels 256-512). A series of folding positions are calculated and the mirror axis is chosen such that the sum $\Sigma(x_{1/2}^2 - x_{2/2}^2)$, where $x_{1/2}$ and $x_{2/2}$ are mirrored data points, is a minimum. This process results in a single Mössbauer spectrum with the zero velocity position located at channel number either 128.5 or 129.0.

2.6.3 The Fitting Program

A FORTRAN program, MOSFIT, developed at UKAEA Harwell [21] is used to model theoretical Lorentzian line functions to the folded data points. Initial guesses are made as to the line positions, widths and relative depths of the computed curve, FIT(I), which best fits the data points, DATA(I). A non-linear least squares regression routine, VA05A, then modifies these parameters until the statistical variation between FIT(I) and DATA(I), denoted by χ^2 is minimum. Thus,

$$\chi^2 = \sum_{i=0}^{255} [\text{FIT}(I) - \text{DATA}(I)]^2 / \sigma_i^2$$

where σ_i^2 is the variance for data in channel i.

The quality of fit depends upon the initial guesses made for the parameters and on the complexity of the spectrum, and the statistical quality of the experimental data.

Finally, a third program, MOSPLOT, is used to produce a graphical output of the computer fit to the experimental data, and these constitute the Mössbauer spectra presented in the following chapters.

2.7 Calibration

The velocity range set by the helipot (Section 2.5.1) is a nominal quantity only and in order to obtain a Mössbauer spectrum with an accurate velocity scale, it is necessary to calibrate the 512 channels of the MCA in terms of mm s^{-1} . This is most readily accomplished by recording the spectra of standard absorbers whose line positions (in mm s^{-1}) have been accurately determined by absolute calibration methods.

Two such absorbers used in this laboratory are iron-57 enriched iron metal, which produces a magnetically split 6-line spectrum, and sodium nitroprusside (SNP) which yields a 2-line quadrupole split spectrum ($\Delta E_Q = 1.705 \text{ mms}^{-1}$). The Mössbauer Effect Reference Data Journal (MERDJ) [22] has published the weighted average values for the enriched iron line positions, and they are:

lines (1,6) occur at $\pm 5.312 \text{ mm s}^{-1}$

lines (2,5) occur at $\pm 3.076 \text{ mm s}^{-1}$

lines (3,4) occur at $\pm 0.840 \text{ mm s}^{-1}$

These lines are used as secondary standards to calibrate the velocity scale of the spectrometer typically over $\pm 6 \text{ mm s}^{-1}$. The single line source used for this purpose was composed of cobalt-57 embedded in a rhodium matrix. Cobalt-57 decays by electron capture to an excited state iron-57 nucleus which then relaxes by emission of the 14.4 keV Mössbauer γ -photon.

The six iron lines are fitted in pairs and an average value for a calibration constant (expressed as $\text{ch.mm}^{-1}.\text{s}$) is evaluated. This quantity is then used in subsequent tin-119 work to convert channels into the corresponding Doppler velocities.

2.8 REFERENCES

1. R. L. Mössbauer, Z. Physik, 151, pp 124-143 (1958).
2. P. B. Moon, Proc. Phys. Rev., 105, p 124 (1951).
3. N. W. G. Debye and M. Linzer, J. Chem. Phys., 61 (11), p 4770 (1974).
4. L. A. Hobbs and P. J. Smith, J. Organomet. Chem., 206, pp 59-67 (1981).
5. P. J. Smith, Organomet Chem Revs (A), 5, p 373 (1970).
6. J. N. R. Ruddick, Reviews in Silicon, Germanium, Tin and Lead Compounds, 2 (2/3), pp 115-222 (1976).
7. A. G. Davies, L. Smith and P. J. Smith, J. Organomet. Chem., 23, pp 135-142 (1970).
8. R. V. Parish and R. H. Platt, Inorg. Chim. Acta., 4, p 589 (1970).
9. A. J. Crowe, R. Hill, P. J. Smith, J. S. Brooks and R. Formstone, J. Organomet. Chem., 204, p 47 (1981).
10. R. V. Parish in "Progress in Inorganic Chemistry", S. J. Lippard, Ed., Wiley Interscience, 15, pp 101-200 (1972).
11. R. V. Parish and R. H. Platt, Inorg. Chim. Acta., 4(1), p 65 (1970).

12. N. W. G. Debye, E. Rosenberg and J. J. Zuckerman, J. Amer. Chem. Soc., 90(2), pp 3235-3236 (1968).
13. M. A. Mullins and C. Curran, Inorg. Chem., 7(12), pp 2584-2588 (1968).
14. G. M. Bancroft and T. K. Sham, Can. J. Chem., 52, pp 1361-1366 (1974).
15. A. G. Davies and P. J. Smith in "Comprehensive Organometallic Chemistry", G. Wilkinson, F. G. A. Stone and E. W. Abel, Eds., Pergamon Press Ltd, pp 525-526 (1982).
16. R. H. Herber in "Chemical Mössbauer Spectroscopy", Plenum Press, New York and London, pp 199-216 (1984).
17. Mössbauer Effect Data Index, J. G. Stevens and V. E. Stevens, Eds, IFI Plenum Data Co., p 23 (1975).
18. J. S. Brooks, J. M. Williams and P. J. Webster, J. Phys. (D) : Appl. Phys., 6, pp 1403-1407 (1973).
19. V. I. Goldanskii and E. F. Makarov in "Chemical Applications of Mössbauer Spectroscopy", V. I. Goldanskii and R. H. Herber, Eds., Academic Press Inc., pp 5-7 (1968).
20. J. M. Williams and J. S. Brooks, Nucl. Instr. and Meth., 128, pp 363-372 (1975).

21. G. Longworth in "Mossbauer Spectroscopy Applied to Inorganic Chemistry", Volume 1, G. J. Long, Ed., Plenum Press, New York and London, pp 43-56 (1984).

22. J. G. Stevens, Mössbauer Effect Reference and Data Journal, J. G. Stevens, V. E. Stevens, R. M. White and J. L. Gibson, Eds, Mössbauer Effect Data Center, North Carolina, 3(4), p 99 (1980).

ELASTOMERS

3.1 INTRODUCTION

3.2 TRIBUTYLTIN-CONTAINING ELASTOMERS

3.2.1 Tin-119m Mössbauer Studies

3.2.2 Results and Discussion of the Tributyltin Systems

3.2.3 Studies of the Fate of Tributyltin Biocides
dispersed in Neoprene

3.2.4 An Investigation into the Effects of Carbon
Black on the Mossbauer Parameters of Organotins

3.3 TRIPHENYLTIN-CONTAINING ELASTOMERS

3.3.1 Results and Discussion of the Triphenyltin Systems

3.3.2 A Mössbauer Investigation of the Thermal Stability
of some Phenyltin Compounds

3.3.3 Tin-119m Mossbauer Studies of the Fate of
Triphenyltin Biocides dispersed in Neoprene

3.4 CONCLUSIONS

3.5 REFERENCES

3.1 Introduction

The production of an elastomeric marine antifouling coating, with useful physical properties, requires the compounding of the base elastomer with several important additives. Two classes of additives are of special importance; curatives that induce further polymerisation of relatively low molecular weight forms into much higher molecular weight materials, and reinforcing fillers that dramatically increase the physical strength of the elastomer. The general additive types are:

(i) Curatives: ("vulcanizing agents"). Materials that chemically combine with the elastomer to effect cross-linking between the molecules and thus increase molecular weight. Most curatives are sulphur containing compounds. However, metal oxides (notably zinc oxide) are generally employed in the curing of neoprenes.

(ii) Accelerators: Compounds used in conjunction with a curative to increase the rate of vulcanization. Such compounds include thiazoles, thiurams and dithiocarbamates.

(iii) Reinforcing Pigments: Materials such as carbon black and certain silicates are added to the elastomer in order to increase post-cure physical strength and resistance to environmental degradation.

(iv) Protective Agents: Elastomers used in marine antifouling applications will be subject to environmental degradation arising mainly from oxidation, hydrolysis and biochemical attack by bacteria and fungi. Thus, certain compounds are added to enhance the service life and durability of the exposed material.

(v) Processing Aids: Materials such as oils, waxes, and fatty acids are used as internal lubricants or dispersants to improve processing qualities. They function by preventing the recombination of polymer fragments during mastication, and by aiding the dispersal of additives such as carbon black and the cure system.

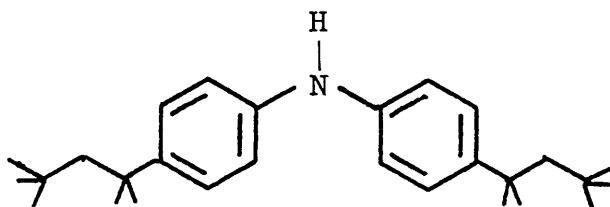
A compounding formulation for a typical antifouling elastomer studied in this work is given in Table 3.1. The ingredients were mixed together using a two-roll rubber mill. During the mixing operation, the elastomeric molecule was broken, through sheer forces, into lower molecular weight fragments and softened. This process is referred to as mastication. Additives were then incorporated into the softened elastomer with the vulcanizing system being added last. During these operations, a significant temperature rise in the mix was noted.

Curing of the elastomer was accomplished by heating the mixed stock in a press for about 30 minutes at 150°C.

Table 3.1 : Typical antifouling elastomer formulation

Additive	%. (wt)	Function
Neoprene, G.W.	53.2	Base elastomer
Phil Black, S.R.	31.9	Carbon black filler - reinforcing pigment
Stearic Acid	0.5	Processing aid
Zinc Oxide	2.7	Curative
Octamine ^a	1.1	Antioxidant
TMTD ^b	0.5	Cure accelerator
Maglite, D	2.1	MgO, cure agent
Circosol 410 ^c	5.3	Processing aid
Organotin	2.7	Biocide

a Octylated diphenylamine:



b Tetramethylthiuram disulphide: $(\text{CH}_3)_2\text{NCSSCN}(\text{CH}_3)_2$



c A light hydrocarbon fraction

The noticeable temperature rise observed during compounding, followed by the elevated temperature curing process, means that the possibility of chemical combination between the biocide and coating ingredients must be considered. The reaction between TBTO and neoprene [poly(2-chloro-1,3-butadiene)] to produce cross-links and a completely different organotin was mentioned earlier (Section 1.6). Also, it is well-known that organotin oxides and hydroxides react readily with carboxylic acids to produce the corresponding stannyl esters [1]. Consequently, the formation of tri-n-butyltin stearate (TBTSt) within the coating must also be considered. There are numerous other potentially reactive systems involving thermal degradation and subsequent chemical combination, and some of these are to be addressed in the following study.

3.2 Tributyltin-containing Elastomers

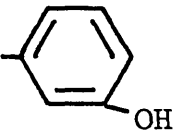
A number of elastomer samples, originally containing different tri-n-butyltin compounds, were received from the Admiralty Research Establishment¹ (A.R.E.) and these are described in Table 3.2.

3.2.1 Tin-119m Mössbauer Studies

Samples for Mössbauer analysis were obtained by cutting discs (17 mm diameter x 3 mm depth) from the original elastomer sheets which were then mounted in the probe

1 Admiralty Research Establishment, Holton Heath, Poole, Dorset, BH16 6JU

Table 3.2 : Authentic tributyltin-containing Antifouling Rubber (AFR) samples obtained from A.R.E.

Sample Code	Biocide	Formula
AFR 3127	TBTO	$\text{Bu}_3\text{SnOSnBu}_3$
AFR 3325	tributyltin stearate	$\text{Bu}_3\text{SnOC}(\text{CH}_2)_{16}\text{CH}_3$ $\begin{array}{c} \parallel \\ \text{O} \end{array}$
AFR 3326	tributyltin carbonate	$\text{Bu}_3\text{SnOCOSnBu}_3$ $\begin{array}{c} \parallel \\ \text{O} \end{array}$
AFR 3426	tributyltin phosphate	$(\text{Bu}_3\text{SnO})_3\text{PO}$
AFR 3428	tributyltin m-hydroxybenzoate	Bu_3SnOC  $\begin{array}{c} \parallel \\ \text{O} \end{array}$ OH
AFR 3466	tributyltin chloride	Bu_3SnCl
AFR 3642	tributyltin fluoride	Bu_3SnF

Note, all of the elastomers were based on the formulation given in Table 3.1.

described in Section 2.5.3. Spectra were recorded in constant acceleration mode at 80K and run times were typically 24 hours in each case. The Mössbauer parameters given in Tables 3.3 and 3.5 have associated errors of $\pm 0.02 \text{ mm s}^{-1}$ (for pure compounds) and ± 0.05 (for the elastomers). These figures take into account errors associated with the measured values of isomer shift (δ), quadrupole splitting (ΔE_Q) and full width at half-height (Γ). They originate from non-linearities, calibration errors, zero-velocity determination and computer fitting errors.

3.2.2 Results and Discussion of the Tributyltin Systems

Table 3.3 lists the Mössbauer parameters obtained for each elastomer sample and the corresponding pure organotin compounds. The following key has been adopted for convenience:

<u>Abbreviation</u>	<u>Organotin</u>
TBTO	bis(tributyltin)oxide
TBTC1	tributyltin chloride
TBTCO	tributyltin carbonate
TBTSt	tributyltin stearate
TBTPO	tributyltin phosphate
TBTPh(OH)	tributyltin m-hydroxybenzoate
TBTF	tributyltin fluoride

Representative Mössbauer spectra are shown in Figures 3.1(a) and (b).

Table 3.3 : ^{119}Sn Mössbauer data for tributyltin

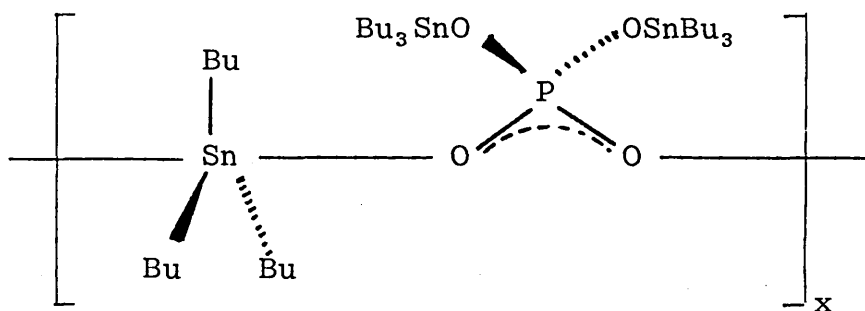
compounds in antifouling elastomers at 80K

Toxicant	δ^a (mm s $^{-1}$)	ΔE_Q (mm s $^{-1}$)	Γ (mm s $^{-1}$)
(i) In elastomers: ~ 2.7% wt.			
TBTO	1.40	2.82	1.09
TBTC1	1.41	2.78	1.05
TBTCO	1.43	2.84	0.97
TBTSt	1.44	2.82	0.99
TBTPO	1.39	2.82	1.08
TBTPh(OH)	1.39	2.72	0.99
TBTF	1.40	2.83	1.04
(ii) Pure materials:			
TBTO	1.25	1.53	1.11
TBTC1	1.52	3.42	1.06
TBTCO ^b	(1.38 1.43)	2.70 3.79	1.08) 0.88)
TBTSt	1.45	3.65	0.95
TBTPO ^c	(1.31 1.33)	2.40 3.53	1.04) 1.04)
TBTPh(OH)	1.43	3.18	1.12
TBTF	1.40	3.82	1.05

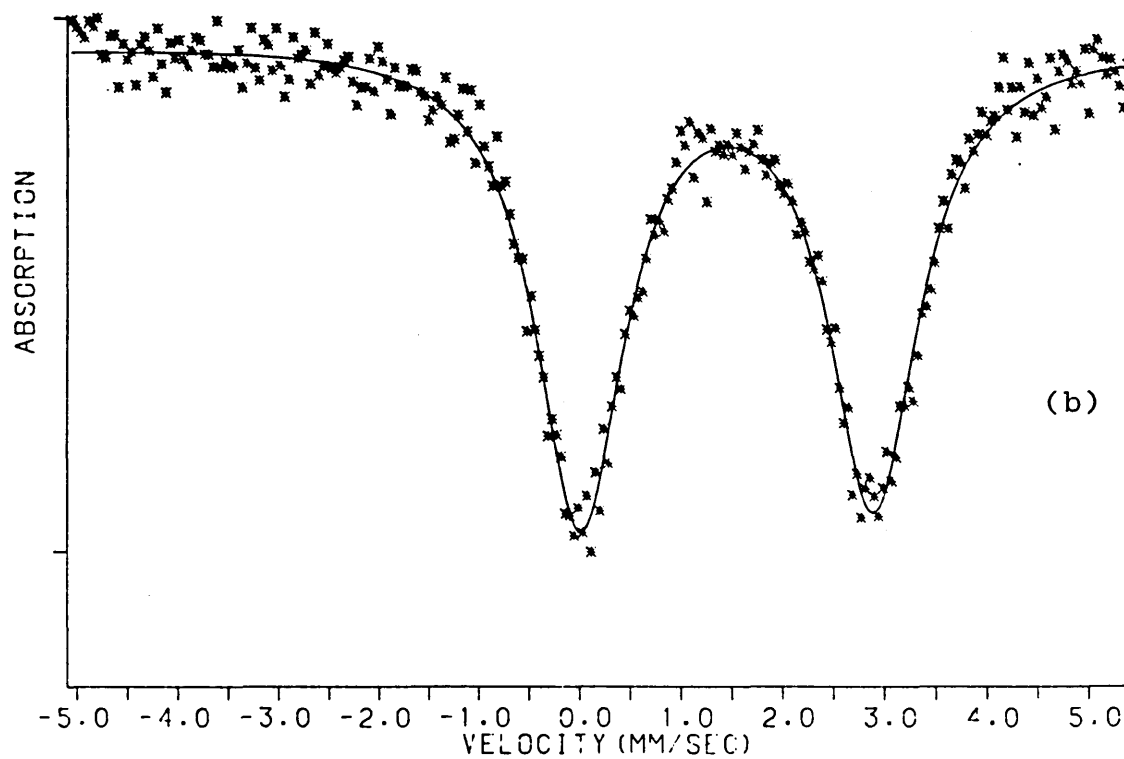
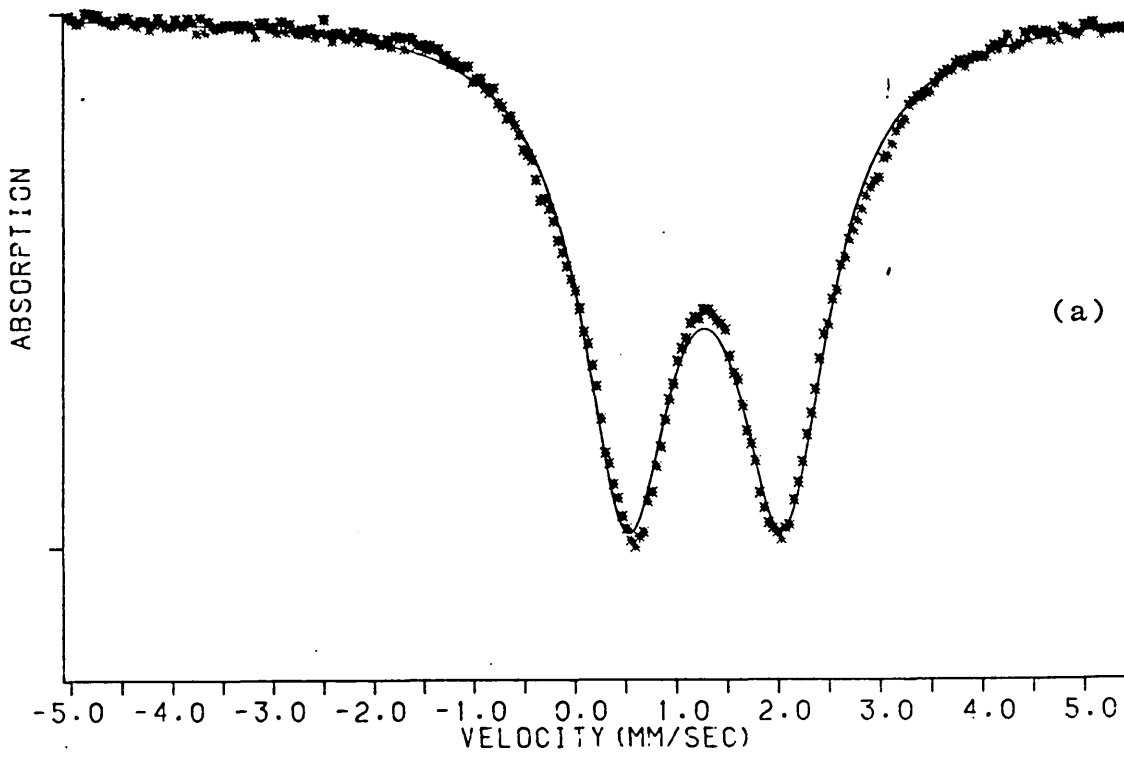
Errors; ± 0.02 mm s $^{-1}$ for neat compounds, ± 0.05 mm s $^{-1}$
for the elastomer samples

Notes on Table 3.3:

- a Isomer shifts were measured relative to BaSnO_3 .
- b Data were computer modelled as 2-unresolved doublets consistent with the presence of both 4- and 5-coordinate tin sites in this molecule [2].
- c Data fitted as 2-unresolved doublets in accordance with the findings of Blunden et al [3] who suggest an auto-associated structure of the type:



It is clear from the results in Table 3.3 that all seven tributyltins have suffered extensive structural modification upon incorporation into the coating matrix. The similarity of results for the elastomer samples, further suggests that each organotin has been converted to the same species during the compounding/curing processes.



Figures 3.1(a) and (b) : Mössbauer absorption spectra
of (a) neat TBTO and (b) TBTO (2.6 % w/w) in an
elastomeric coating matrix.

The identity of this common by-product was established by the ^{119}Sn nuclear magnetic resonance (NMR) spectroscopic analysis of residues extracted from each elastomer sample. The samples (5 - 7g) were subjected to Soxhlet extraction with dichloromethane (b.pt 40°C) for a period of two days. After evaporation of the extracts, the residues were re-dissolved in deuteriochloroform (CDCl_3) and the ^{119}Sn NMR spectra recorded. Chemical shift data ($\delta^{119}\text{Sn}$) relative to tetramethyltin (Me_4Sn) are given in Table 3.4 and a typical, fully decoupled, ^{119}Sn NMR spectrum for a TBTO containing elastomer residue, is shown in Figure 3.2.

The major resonance in most of the spectra was observed at about + 155 ppm and is associated with the extraction of tributyltin chloride ($\delta = + 155.7$ ppm) from the elastomers. There are, however, at least two other tin species in the residues extracted from all but two of the elastomer samples (AFR's 3426 and 3428). On the basis of the pure compound data given in Table 3.4, the peak at ca 98 ppm in the elastomer residues was attributed to the presence of TBTSt formed by the combination of tributyltin moieties with the stearic acid processing aid (Table 3.1). The remaining high-field peak at - 164.2 to - 165.2 ppm was initially thought to originate from the presence of stannic chloride ($\delta(^{119}\text{Sn})$, - 149 ppm [4]) formed by the degradation of the original triorganotin during the

Table 3.4 : ^{119}Sn NMR spectroscopic data for tributyltins
 extracted from marine antifouling rubbers^a

Toxicant	$\delta(^{119}\text{Sn})$ in elastomer (± 0.1 ppm)	$\delta(^{119}\text{Sn})$ pure compound (± 0.1 ppm)
TBTO	- 165.2 97.7 154.7	92.8
TBTCl	- 164.2 98.1 155.4	155.7
TBTO	- 164.6 98.4 154.9	104.9
TBTSt	- 164.6 97.1 154.6	102.7
TBTPO ^b	154.9	-270.4 100.6
TBTPh(OH)	154.9	119.2
TBTF ^c	- 164.2 97.9 155.2	-

a Data obtained using an 80.13 MHz Bruker WP80SY FT NMR
 and a 100.6 MHz Bruker WH400 FT NMR spectrometer.

b Two resonances correspond to the 4-(100.6 ppm) and
 5-coordinate tin sites (- 270.4 ppm).

c This polymeric material was insufficiently soluble
 in any common organic solvent to yield a useful NMR
 spectrum.

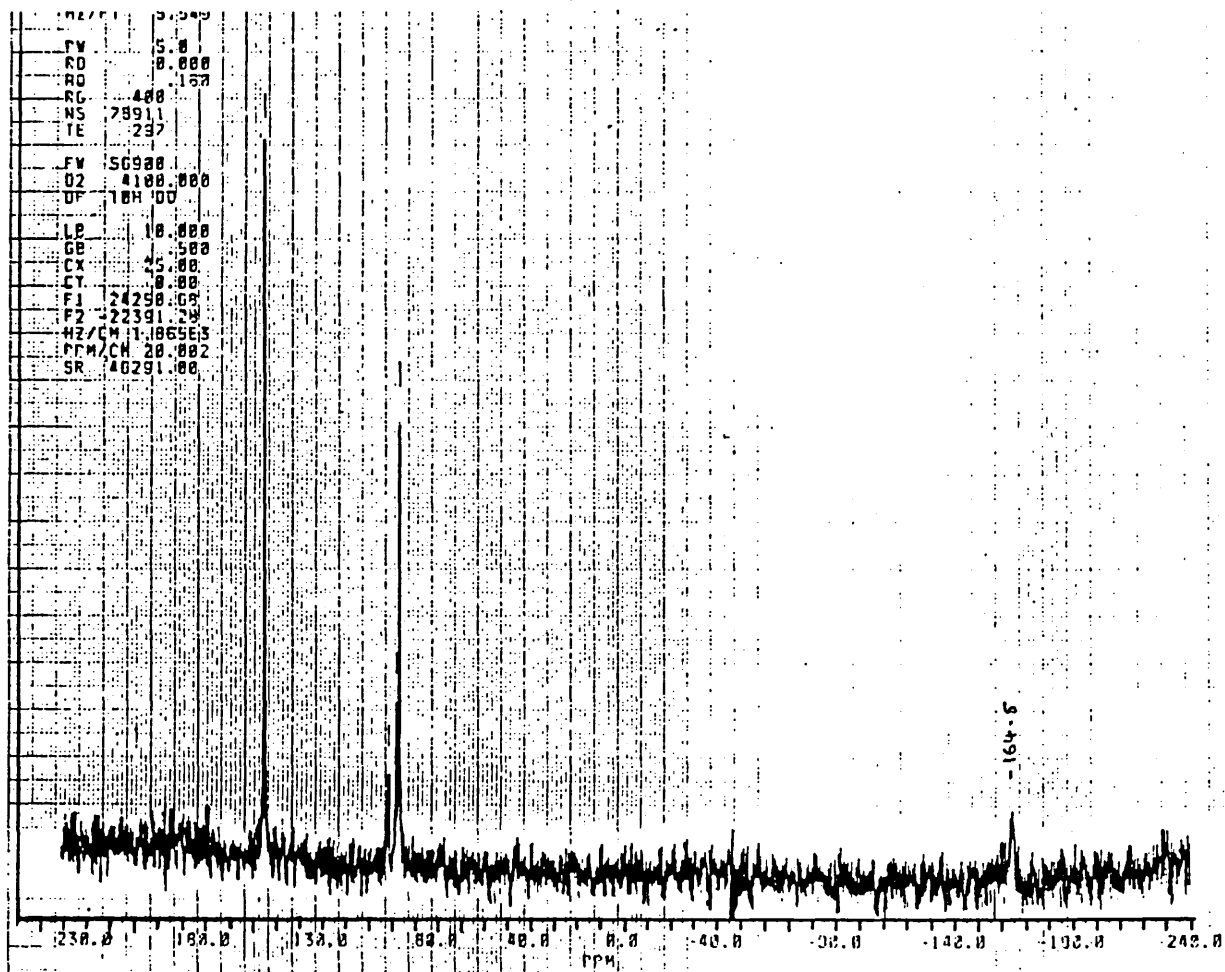
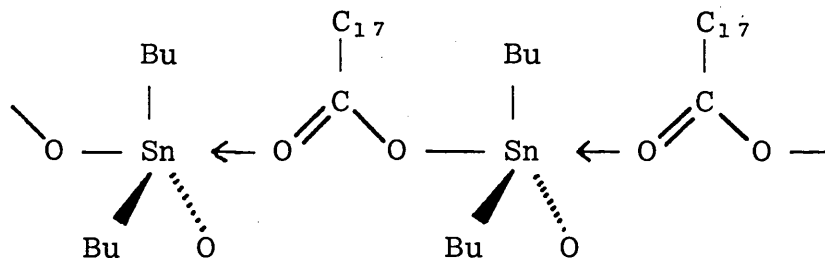


Figure 3.2 : ^{119}Sn NMR spectrum of residue obtained from TBTO containing elastomer

elastomer compounding/curing processes. However, gas-chromatographic analysis of the Soxhlet-extracts, after treatment with n-propyl magnesium chloride, revealed the presence of small quantities of dibutyltin species as the only dealkylation products in the elastomers. Typical of the organotins that resonate in this region of the ^{119}Sn NMR spectrum are the dibutyltin alkoxides [5], 1,3-disubstituted distannoxanes $[(\text{XBu}_2\text{Sn})_2\text{O}]$ [6] and diorganotin carboxylates [7]. The formation of dibutyltin alkoxides during the tile fabrication procedures was ruled out in view of the lack of appropriate alkoxy radicals in the elastomer matrix. Similarly, dialkyl-distannoxane derivatives, which are recognised as the first stable products of the hydrolysis of dialkyltin(IV) compounds [8], were also disregarded since the required hydrolytic reaction mechanisms were unlikely to operate under the elastomer compounding and curing processes. Thus, considering the ease with which diorganotin oxides and halides react with carboxylic acids and metal carboxylates (eg zinc stearate) respectively [9], the formation of dibutyltin bis(stearate) within the elastomer was thought to account for the ^{119}Sn NMR peak at -165 ppm in the elastomer extracts. An authentic sample of dibutyltin bis(stearate) was prepared by heating dibutyltin oxide and stearic acid in refluxing toluene with the removal of water in a Dean-Stark trap. The resulting waxy product showed all the spectroscopic characteristics of a five or six

coordinate organotin compound in both the solid state and in solution; $\delta = 1.42 \text{ mm s}^{-1}$, $\Delta E_Q = 3.45 \text{ mm s}^{-1}$ and $\delta(^{119}\text{Sn}) = -148.1 \text{ ppm}$. Also, the presence of antisymmetric and symmetric OCO infrared stretching modes at 1589 cm^{-1} and 1390 cm^{-1} respectively, along with the SnC modes at 598 cm^{-1} (ν_{as}) and 515 cm^{-1} (ν_{s}), indicate that this molecule probably exists as a coordinated polymer in the solid-state in which the SnC_2 moiety is non-planar [10]. The high solubility of this material in a non-polar solvent (hexane, chloroform) and the observed high-field ^{119}Sn NMR resonance, however, indicates that the polymeric structure breaks down in solution to yield bis-chelated dimers [10]. Representative structures for the solid and solution phases are shown in Figure 3.3.

(a) Solid



$$\delta = 1.42 \text{ mm s}^{-1}$$

$$\Delta E_Q = 3.45 \text{ mm s}^{-1}$$

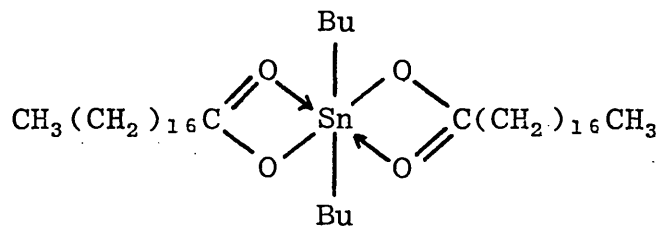
$$\nu_{\text{as}}(\text{OCO}) = 1589 \text{ cm}^{-1}$$

$$\nu_{\text{s}}(\text{OCO}) = 1390 \text{ cm}^{-1}$$

$$\nu_{\text{as}}(\text{SnC}) = 598 \text{ cm}^{-1}$$

$$\nu_{\text{s}}(\text{SnC}) = 515 \text{ cm}^{-1}$$

(b) Solution



$$\delta(^{119}\text{Sn}) = - 148.1 \text{ ppm}$$

The discrepancy of 17 ppm between dibutyltin bis stearate as a pure compound in deuteriochloroform solution and as component of an elastomer extract, may arise from a further coordinative interaction between the di-ester and a co-extracted moiety that results in substantial shielding of the tin nucleus. Other potential ligands in the elastomer matrix include the diphenylated amine antioxidant (Table 3.1), tetramethylthiuram disulphide and its thermal degradation products (eg, tetramethylthiourea), and chloride ions from the thermally induced dehydrochlorination of the base polymer.

It is well-known that a wide variety of organotin derivatives will react with halogen acid (HX) to produce the corresponding organotin halides [11]. In particular, the facile conversion of TBTO to TBTCl was demonstrated in the laboratory by adding the distannoxane to a dilute (ca 2 mol dm⁻³) solution of hydrochloric acid. The evolution of hydrogen chloride within neoprene-based elastomers has been noted by several workers [12-15] and

is thought to arise from two distinct processes: ie thermal dehydrochlorination of the base polymer leading to conjugation within the chloroprene chains, and as a by-product of the cross-linking reaction. Although the formation of tributyltin chloride within the elastomer can be postulated, it is clear from the Mössbauer data presented in Table 3.3 that the simple conversion of one organotin into a predominant by-product has not been observed. There is a discrepancy in the quadrupole splitting of tributyltin chloride in the neat (3.42 mm s^{-1}) and elastomer-dispersed (2.78 mm s^{-1}) states, which can only be interpreted in terms of additional bonding interactions that result in significant modifications of charge symmetry about the tin nucleus. The nature of these additional interactions was investigated further in the following experiments.

3.2.3 Studies into the Fate of Tributyltin Biocides dispersed in Neoprene

A series of neoprene films containing TBTO, TBTCO, TBTC1, TBTSt and bis(tri-n-butyltin) sulphide (TBTS) at 2.5% wt, were prepared by dissolving 4 g of uncured neoprene in 100 cm^3 of dichloromethane and then adding the organotin as a solution in dichloromethane. The mixtures were stirred for approximately two hours after which time they were cast into dishes to yield an elastomeric film by solvent evaporation. Mössbauer analyses of the films were performed at 80K and the

results are shown in Table 3.5.

Table 3.5 ^{119}mSn Mössbauer data for tributyltin compounds dispersed in solvent cast neoprene films at 2.5% wt

Organotin	δ (mm s^{-1})	ΔE_Q (mm s^{-1})	Γ (mm s^{-1})
TBTO	1.46	2.95	1.00
TBTCO	1.40	2.70	1.01
TBTC1	1.44	2.96	1.02
TBTSt	1.40	2.79	0.99
TBTS ^a	1.42	2.51	1.21

a The Mössbauer parameters for neat TBTS are

$$\delta = 1.40 \text{ mm s}^{-1} \text{ and } \Delta E_Q = 1.62 \text{ mm s}^{-1}.$$

The error associated with these measurements is

$$\pm 0.05 \text{ mm s}^{-1}$$

It is clear from the results in Table 3.5 that even under the relatively mild conditions employed in this experiment, structural changes are observed in all of the biocides (see Table 3.3 for pure compound data).

The origin of these structural changes was investigated further by examining the possibility of concentration dependence of the Mössbauer parameters. Brooks et al [16] noted that when dibutyltin dichloride was dispersed in a PVC matrix, the Quadrupole Splitting parameter was reduced from 3.45 mm s^{-1} for the pure compound to 3.09 mm s^{-1} when incorporated in PVC at 1.2% w/w. They attributed this reduction to the breakdown of an associated six coordinate structure and the progressive formation of dimeric units involving five-coordinate tin. Partial quadrupole splitting calculations supported their conclusions.

In this work, a similar study was made of TBTCl dispersed in a non-coordinating solvent (n-hexane) over the concentration range $0.19 - 3.00 \text{ mol dm}^{-3}$ TBTCl. The Mössbauer parameters were found to be insensitive to concentration in this medium and were identical, within the experimental error of $\pm 0.05 \text{ mm s}^{-1}$, to those obtained for neat TBTCl, viz; $\delta 0 1.52 \text{ mm s}^{-1}$, $\Delta E_Q = 3.42 \text{ mm s}^{-1}$. It is apparent, therefore, that at the experimental temperature of 80K the 5-coordinated chlorine bridged structure proposed for this molecule [17] is retained throughout the concentration range studied. This could imply that the Sn----Cl bridging bonds have sufficient energy to resist breaking due to solvation by n-hexane, or, more likely, as each solution was quenched by direct immersion in liquid nitrogen, phase separation between solvent and solute occurred leading to

localised concentration of essentially neat TBTCI. A similar insensitivity of Mössbauer parameters towards concentration was observed in dichloromethane into which TBTCI had been dispersed at 5% by weight. In view of these observations, it is suggested that the observed reduction in quadrupole splitting for TBTCI dispersed in the authentic coating matrix and in the simple neoprene system, is not merely the result of a dilution effect on the organotin, but possibly results from a coordinative interaction with the base polymer. In the authentic coating, other factors have reduced the quadrupole splitting parameter still further.

3.2.4 An Investigation into the Effects of Carbon Black on the Mössbauer Parameters of Organotins

The carbon black, added as a reinforcing pigment to the antifouling coatings, contributes substantially to the mass of these materials (~ 32% wt). It is produced by the partial combustion of oil and coal tar and consists of aggregated spheres (mean particle size; 60 nm) of partly graphitic elemental carbon. The other major constituents are oxygen and hydrogen which are present as chemically bound functional groups (phenolic, ketonic and carboxylic) on the surfaces of individual particles [18].

The surface activity that results from these functional groups is known to affect cure and degradation rates of polymer systems [18,19] and other factors, such as particle size, strongly influence the release rates of organotins

from elastomer matrices [20]. In view of this apparent reactivity, the following experiment was undertaken in order to assess the influence of carbon black on the Mössbauer parameters of several bioactive tri-n-butyl- and triphenyltin derivatives. The organotin compounds were added at 10% by weight to the carbon black (Phil black A[®]) which was suspended in carbon tetrachloride. The materials were then refluxed, under nitrogen, for about thirty minutes after which the solvent was removed by evaporation under reduced pressure. Mössbauer spectra were recorded for each sample at 80K and in some cases the broad experimental line widths and distorted line shapes justified modelling the data as a composite of unresolved quadrupole doublets.

In this procedure, a fitting matrix was constructed which enabled MOSFIT to model several theoretical quadrupole doublets (Lorentzian line functions) to one data set. The fitting matrix required a set of starting parameters (in number of channels) for each proposed doublet in terms of; isomer shift, half-splitting and full width at half-maximum. Each doublet was then fitted independently by varying the starting parameters to achieve the minimum overall χ^2 value.

The result of this fitting process was to produce a composite of theoretical lines which represented an improvement in the quality of computer fit for the complex data obtained in the organotin-Philblack Mössbauer

experiments. In particular, the effect of modelling one, two and three unresolved quadrupole doublets to the raw TBTO-Philblack data can be appreciated from Figures 3.4(a) to (c) in which a reduction of χ^2 is observed as more lines are accommodated. Data which have been processed in this way for the remaining systems yield the Mössbauer parameters which are bracketed together in Table 3.6(a).

All isomer shifts were measured relative to barium stannate with the absorber at 80K. The triphenyltin derivatives that were studied included triphenyltin fluoride (TPTF), triphenyltin chloride (TPTCl), triphenyltin acetate (TPTAc) and triphenyltin hydroxide (TPTOH). The individual experimental line widths, Γ_1 for the low velocity line and Γ_2 for the high velocity line, are given in order to illustrate the appreciable line-shape asymmetry in particular cases.

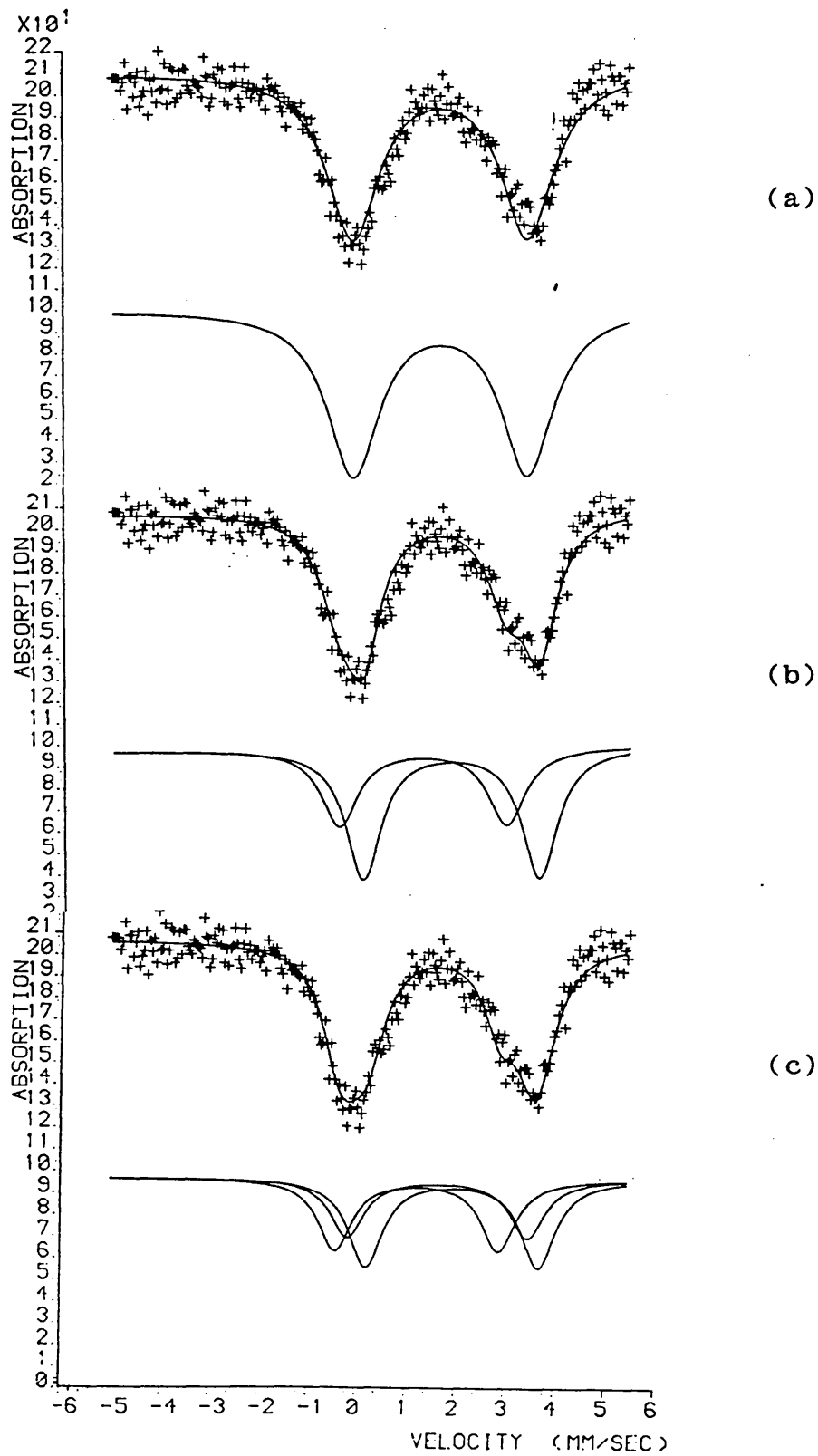


Figure 3.4 : ^{119m}Sn Mössbauer spectra obtained for TBTO dispersed in carbon black (a) 1 doublet, (b) 2 unresolved doublets, (c) 3 unresolved doublets

Table 3.6(a) : ^{119}mSn Mössbauer data for organotin compounds dispersed in carbon black. (Data are modelled as unresolved quadrupole doublets and values in parentheses represent pure compounds) (Error = $\pm 0.05 \text{ mm s}^{-1}$)

Organotin	δ (mm s^{-1})	ΔE_Q (mm s^{-1})	Γ_1 (mm s^{-1})	Γ_2 (mm s^{-1})	χ^2
TBTO ¹	1.61 (1.25)	3.52 (1.53)	1.28 (1.12)	1.30 (1.06)	1111
TBTO ²	[1.24] [1.82]	[3.40] [3.57]	[0.89] [0.86]	[0.89] [0.86]	949
TBTO ³	[1.20] [1.62] [1.92]	[3.32] [3.63] [3.50]	[0.82] [0.82] [0.82]	[0.82] [0.82] [0.82]	936
TBTCO ¹	1.27	3.14	1.00	1.10	1180
TBTCO ²	[1.34 (1.43)] [1.20 (1.39)]	[3.57 (3.79)] [2.68 (2.70)]	[0.76 (0.88)] [0.81 (0.98)]	[0.76 (0.88)] [0.81 (0.98)]	1069
TBTS ¹	1.49 (1.40)	3.50 (1.62)	1.04 (1.06)	1.28 (1.06)	1166
TBTS ²	[0.98] [1.52]	[2.96] [3.53]	[1.06] [0.98]	[1.06] [0.98]	1054
TBTS ³	[0.98] [1.46] [1.48]	[2.96] [3.97] [3.34]	[1.06] [0.84] [0.76]	[1.06] [0.84] [0.76]	1029

Table 3.6(b) : ^{119}mSn Mössbauer data for organotins dispersed in carbon black. Values in parentheses refer to the pure compounds (Error = $\pm 0.05 \text{ mm s}^{-1}$)

Organotin	δ (mm s^{-1})	ΔE_{Q_1} (mm s^{-1})	Γ_1 (mm s^{-1})	Γ_2 (mm s^{-1})
TPBF	1.28 (1.29)	3.83 (3.80)	0.94 (1.08)	0.94 (1.08)
TPBCl	1.49 (1.52)	3.34 (3.42)	0.99 (1.02)	0.98 (1.10)
TPBSt	1.19 (1.45)	2.37 (3.65)	0.90 (0.94)	0.88 (0.96)
TPTF	1.28 (1.29)	3.68 (3.69)	0.92 (1.08)	0.88 (0.90)
TPTC1	1.32 (1.33)	2.57 (2.56)	0.96 (1.02)	0.96 (0.94)
TPTAc	1.29 (1.30)	3.29 (3.35)	0.90 (0.92)	0.84 (0.90)
TPTOH	1.06 (1.18)	1.26 (2.75)	1.02 (1.10)	0.88 (1.08)

Notes on Table 3.6(a)

1. Data fit as a single quadrupole doublet.
2. Data fit as two-unresolved quadrupole doublets.
3. Data fit as three unresolved quadrupole doublets.

The results in Tables 3.6(a) and (b) clearly indicate that dispersion into carbon black has a marked effect on the Mössbauer parameters of most of the organotins studied. Notable exceptions are TBTF and the majority of the triphenyltin derivatives. It is thought that these effects arise from the initial adsorption of the organotin onto the carbon black particles followed by chemical reactions with the surface active groups which have been identified (these also include quinone and free-radical species [19]). Reactions involving TBTO, TBTCO and TBTS, appear to have resulted in the formation of two or more distinct compounds, or the formation of single compounds in which there exist different tin site geometries. The resistance shown by the triphenyltin compounds towards such reactions could imply that steric factors play an important role in the mechanisms involved. The anomalous behaviour exhibited by TPTOH may have resulted from its dehydration during the dispersion process to produce bis(triphenyltin) oxide ($\delta = 1.13 \text{ mm s}^{-1}$, $\Delta E_Q = 1.42 \text{ mm s}^{-1}$).

The possibility of intercalation, in which an organotin moiety is accommodated between the two-dimensional crystalline planes of graphitic carbon, was also considered as an additional interaction mechanism to the surface processes. The photochemically induced intercalation of stannic chloride [21] and trimethyltin chloride [22] has been demonstrated using X-ray diffractometry to monitor the change in interplanar

spacing that occurs between the graphite layers.

Unfortunately, experiments with Philblack A [®] showed this material to be largely amorphous in structure and, therefore, unlikely to produce any meaningful data by X-ray techniques. The diffractogram, obtained over the range $2\theta = 4 - 122^\circ$ and using copper K_α radiation ($\lambda_{\text{mean}} = 1.5418 \text{ \AA}$), was characterized by a broad distribution of reflections centred at $2\theta = 24.5^\circ$, Figure 3.5(a). A similar experiment using synthetically produced graphite (BDH Chemicals Ltd) produced a series of narrow-line reflections; the most intense of which ($2\theta = 26.2^\circ$) was associated with an interlayer spacing of 3.40 \AA , Figure 3.5(b). Simple dispersion of TBTO and TBTC1 at 10% by weight into synthetic graphite, did not result in any modification of the reflected line energies or their relative intensities. Intercalation into graphite under the conditions described in Section 3.2.2 (b), was therefore ruled out as a competing process to the physical and chemisorptive processes already mentioned.

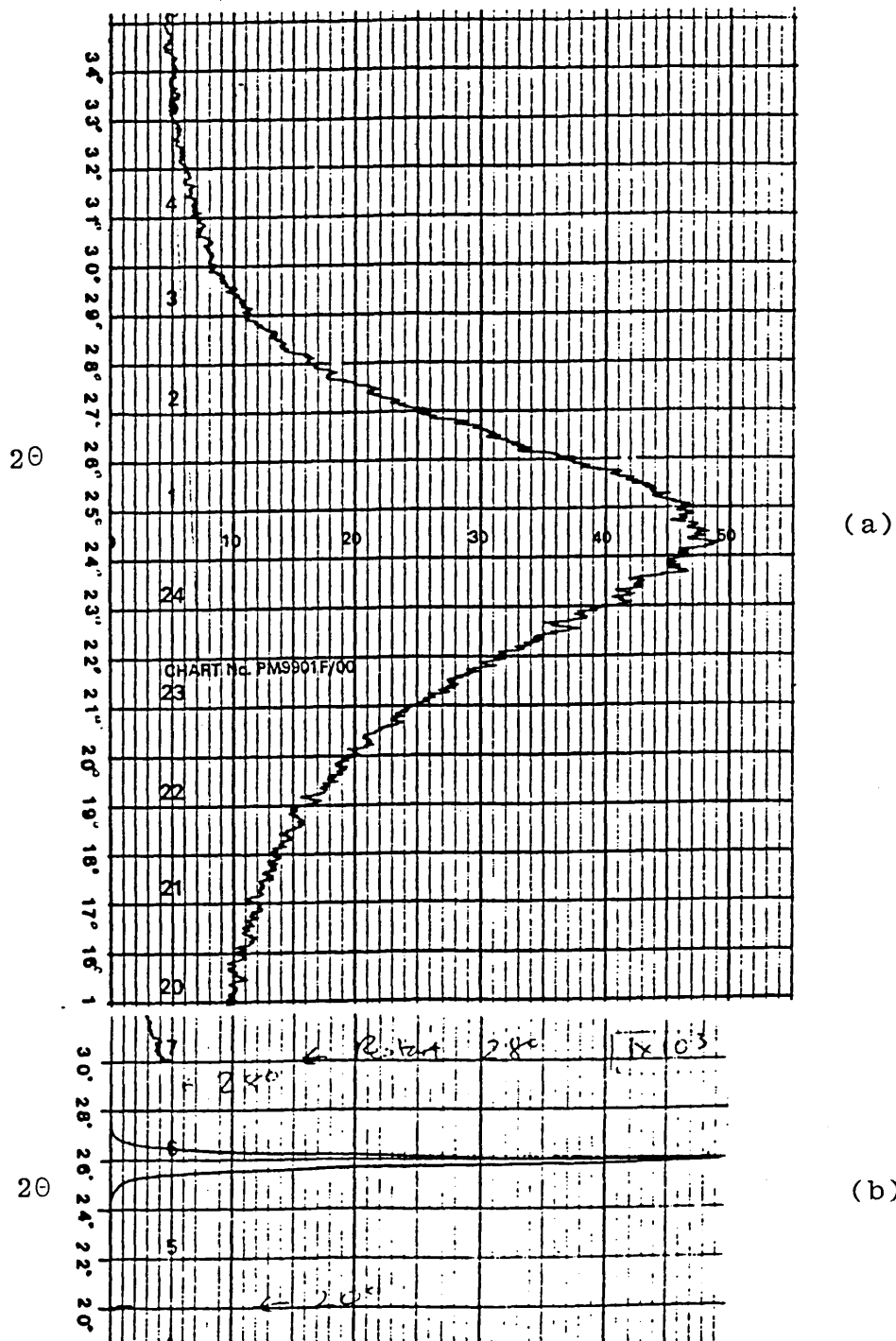


Figure 3.5 : X-ray diffractograms obtained for
(a) Philblack, A[®] and
(b) Synthetic graphite

3.3 Triphenyltin-containing Elastomers

Triphenyltin compounds are highly active fungicides [23] and have been incorporated into antifouling elastomeric coatings [24] where they exhibit comparable biocidal activities to the tri-n-butyl analogues, over the same biological spectrum [11,25]. A number of neoprene-based coatings, containing Ph_3SnX compounds (where X = F, Cl, Ac and OSnPh_3) were supplied by the A.R.E. for studies into the fate of these biocides when incorporated into typical antifouling coating matrices. The coatings were based on the elastomer formulation given in Table 3.1 and contained ca 2.5% by weight of biocide. A description of each sample is given in Table 3.7.

3.3.1 Results and Discussion of the Triphenyltin Systems

The tin-119 Mössbauer spectra for the neat triphenyltin compounds are characterized by well-resolved, symmetrical quadrupole doublets and the measured parameters are given in Table 3.8.

Table 3.7 : Authentic triphenyltin-containing AFR samples obtained from the A.R.E.

Sample Code	Biocide	Abbreviation
3643	triphenyltin acetate	TPTAc
3644	triphenyltin chloride	TPTCl
3645	triphenyltin fluoride	TPTF
3646	<u>bis</u> (triphenyltin)oxide	TPTO

Table 3.8 : ^{119}Sn Mössbauer data for triphenyltin compounds in antifouling elastomers at 80K

Toxicant	δ mm s $^{-1}$	ΔE_Q mm s $^{-1}$	Γ mm s $^{-1}$	Relative Area $\pm 5\%$
(i) Pure compounds ^a				
TPTAc	1.30	3.35	1.01	100
TPPTCl	1.33	2.56	0.97	100
TPTF	1.29	3.69	0.94	100
TPTO	1.13	1.42	0.99	100
(ii) In elastomers ^b				
TPTAc	0.09	0.00	1.42	76
	0.85	2.48	0.98	24
TPPTCl	0.08	0.00	1.50	71
	0.83	2.44	1.04	29
TPTF	0.08	0.00	1.48	81
	0.77	2.38	0.92	19
TPTO	0.08	0.00	1.50	71
	0.83	2.42	1.04	29

^a, error = ± 0.02 mm s $^{-1}$; ^b, error = 0.05 mm s $^{-1}$

The Mössbauer spectra obtained from the elastomers were identical in appearance and a representative example (that obtained from AFR 3646) is shown in Figure 3.6(b). The spectrum of the particular neat organotin (TPTO) is also shown, Figure 3.6(a). Each elastomer spectrum was dominated by an intense broad absorption at ca 0 mm s⁻¹, with a smaller positive velocity contribution at ca 2.25 mm s⁻¹, and clearly illustrated the drastic chemical degradation and structural modifications that were incurred by the original biocides. The major contribution to the zero velocity component of the spectrum was attributed to the presence of a stannic chloride adduct formed by reaction of the ultimate degradation product (SnCl₄) with hydrogen chloride evolved in-situ.

In order to substantiate the proposed formation of stannic chloride, and to help identify the remaining organotin components evident in the elastomer spectra, Figure 3.6(b), the samples AFR 3644 and 3646 were subjected to gas chromatographic analysis following alkylation. The procedure was based upon that employed by Allen et al [26] in their study of the gamma-ray induced degradation of diorganotin(IV) PVC stabilisers. The samples (4 - 5g) were chopped into small pieces and added to a solution of n-propylmagnesium chloride in diethyl ether. The mixture was then heated under reflux in a nitrogen atmosphere for about three hours after which

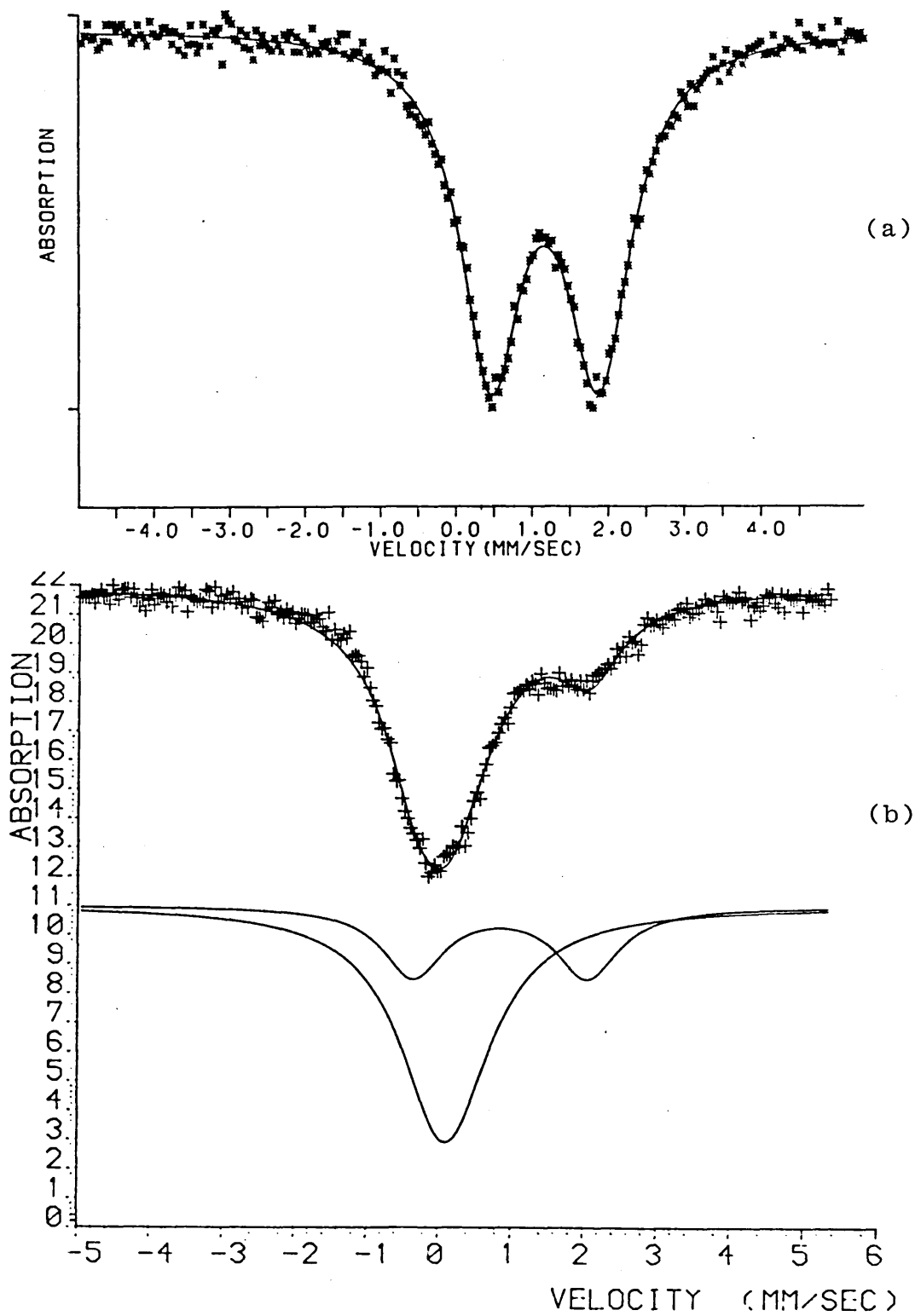


Figure 3.6 : Mössbauer absorption spectra of (a) neat TPTO and (b) TPTO (2.6% wt) in an elastomeric matrix

the excess Grignard reagent was hydrolysed with dilute sulphuric acid. Solvent extraction of the liquor with diethyl ether yielded solutions that were amenable to GC analysis. This procedure was also carried out on the authentic phenyltins Ph_3SnX (where $\text{X} = \text{Cl}, \text{Ac}, \text{OSnPh}_3$) and $\text{Ph}_n\text{SnCl}_{4-n}$ (where $n = 1$ and 2) and it was found that no dephenylation was actually induced by the analytical method. The experimental conditions are given in Table 3.9 and the resolution attained for the stannanes $\text{Ph}_n\text{SnPr}_{4-n}$ (where $n = 0 - 3$ and $\text{Pr} = n\text{-C}_3\text{H}_7^-$) is illustrated in Figure 3.7(a).

Table 3.9 : GC conditions used for the separation of derivatized phenyltins

Instrument : Perkin-Elmer 8310B Gas-chromatograph			
Detector : Flame ionization (FID, with H_2 at 16 p.s.i. and air at 20 p.s.i.)			
Column dimensions : 1.82 x 0.003 m, stainless steel			
Packing : 3% OV-1 ^a on Chromosorb WHP 80/100 mesh			
Carrier gas : N_2 at $35 \text{ cm}^3 \text{ min}^{-1}$			
Injector temperature : 350°C			
Detector temperature : 350°C			
Temperature programming conditions:			
<u>Stage</u>	(1)	(2)	(3)
Oven temperature/ $^\circ\text{C}$	200	230	300
Isothermal time/min	1.2	1.2	1.0
Ramp rate/ $^\circ\text{C min}^{-1}$	20	20	-

a, OV-1 contains dimethyl silicone gum

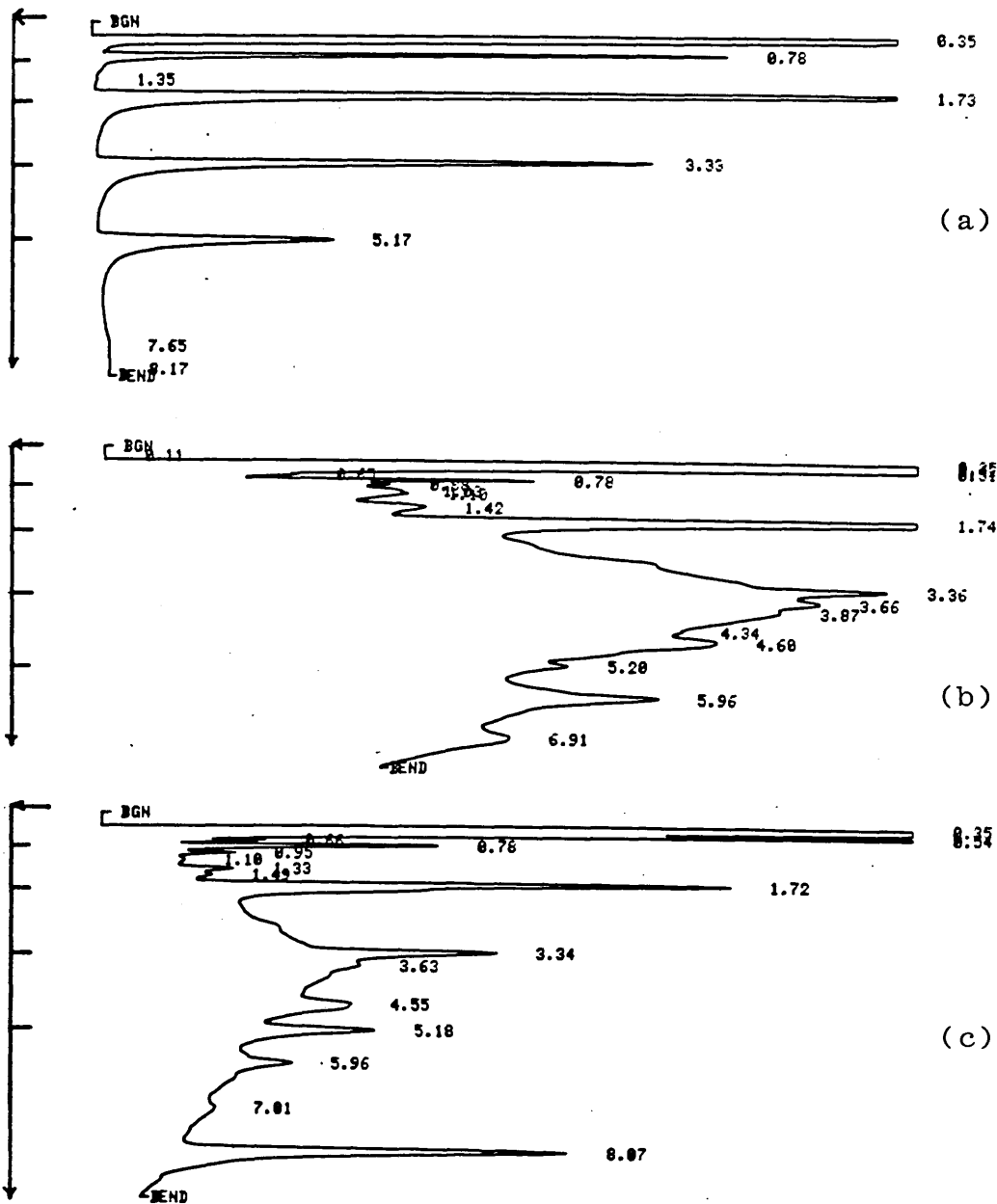


Figure 3.7 : Chromatograms obtained from (a) derivatised standards, (b) AFR 3646 and (c) AFR 3644. Figures represent retention time in minutes

Retention times, derived from Figure 3.7(a), for the derivatized standards are given in Table 3.10.

Table 3.10 : Retention times (t_R) for n-propylated stannanes

Standard	t_R (± 0.03 min)
SnPr ₄	0.78
PhSnPr ₃	1.73
Ph ₂ SnPr ₂	3.33
Ph ₃ SnPr	5.17

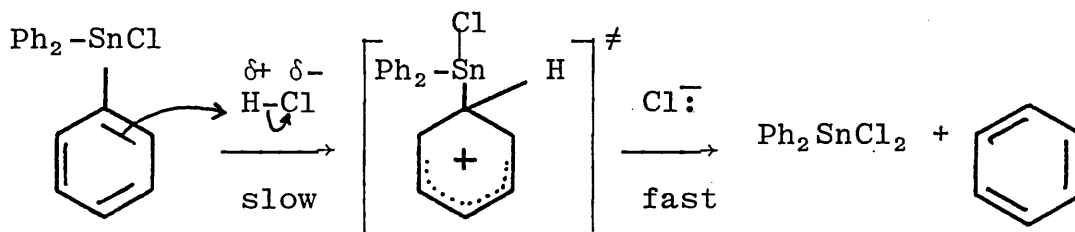
It is immediately clear from authentic elastomer chromatograms, Figures 3.7(b) and (c), that the analytical method per se is not ideal for the quantitative determination of tin species in the elastomer extracts. Without the inclusion of additional sample clean-up operations, a whole range of unidentified organics have been separated on the GC column along with the stannane derivatives.

The method is, however, adequate for the qualitative identification of the tin moieties by correlation of t_R values with those given in Table 3.10 for the standards. Despite the complexity of the extract chromatograms, all stages of the dephenylation of the original Ph₃Sn⁻ moiety can be identified and the monophenyltin derivative would appear to be the major degradation product. However, it is unlikely that the efficiency of stannane formation within the elastomer matrix and subsequent extraction into

ether, was the same for each tin moiety present. Consequently, the relative peak heights of each derivative on the elastomer chromatograms, were only used as an approximate guide in assessing the degree of degradation undergone by the original Ph_3Sn -biocides.

3.3.2 A Mössbauer Investigation of the Thermal Stability of some Phenyltin Compounds

Aryltin compounds will readily undergo Sn-C bond cleavage in the presence of halogens and halogen acids [9,11]. The accepted mechanism involves electrophilic substitution at carbon, thus:



Subsequent interaction with acid would be expected to produce the monoaryl derivative followed by the appropriate tin(IV) tetrahalide as the ultimate degradation product. The hydrogen chloride present in the neoprene elastomers is likely to react with the triphenyltin compounds added as potential biocides (Table 3.7), and produce a range of products consisting of tri-, di-, mono- and inorganic tin moieties.

The ease with which a series of triphenyltin derivatives underwent reaction with hydrogen chloride under the high

temperature conditions used in the elastomer curing process, was demonstrated by heating bis(triphenyltin)-oxide, diphenyltin oxide, tetraphenyltin, triphenyltin acetate, and triphenyltin chloride, respectively with excess quantities of hydrochloric acid (2 mol dm^{-3}) under refluxing conditions. Each system was held at 150°C for fifteen minutes after which the filtered residues were analysed by Mössbauer spectroscopy. The Mössbauer parameters were found to have been extensively modified in each case (Table 3.11) and the relevant Mössbauer spectra are shown in Figures 3.8(a) to (e).

The broad line widths evident in spectra (b) to (e) suggest that the relevant organotins have been converted to a mixture of products including triphenyltin chloride and diphenyltin dichloride. In spectrum (c) for the tetraphenyltin system, it was possible to obtain a significant improvement in the quality of computer fit by allowing the MOSFIT routine to model a series of quadrupole split doublets to the data, in addition to the obvious singlet at 1.25 mm s^{-1} .

Similar treatment of the triphenyltin acetate data, spectrum (d), indicated the possible existence of diphenyl and monophenyltin chlorides in the residue. Also, the thermal instability of bis(triphenyltin) oxide towards disproportionation when heated above its melting point ($119\text{--}123^\circ\text{C}$), was demonstrated by infrared and Mössbauer spectroscopic analysis of the residue obtained after heating this material at 150°C for thirty minutes.

Table 3.11 : ^{119}Sn Mössbauer data for triphenyltin compounds heated with excess hydrogen chloride under the elastomer curing conditions (figures in parentheses correspond to the pure compounds)

Organotin	δ $\pm 0.02 \text{ mm s}^{-1}$	ΔE_Q $\pm 0.02 \text{ mm s}^{-1}$	Γ $\pm 0.02 \text{ mm s}^{-1}$	Relative Area $\pm 5\%$
$(\text{Ph}_3\text{Sn})_2\text{O}$	1.32 (1.13)	2.45 (1.42)	1.07	100
$(\text{Ph}_2\text{SnO})_n^a$	1.28 (0.90) 1.28	3.10 (1.90) 2.38	1.04 1.00	69 31
Ph_3SnCl	1.08 (1.33)	2.00 (2.56)	1.10	100
$\text{Ph}_3\text{SnOCCH}_3^b$ $\begin{array}{c} \text{O} \\ \\ \text{O} \end{array}$	0.14 1.25 (1.30) 1.31	0.00 3.12 (3.35) 2.12	1.17 0.90 1.24	17 26 57
Ph_4Sn^c	1.26 (1.26) 1.11	0.00 (0.00) 2.48	1.42 1.04	91 9

- a, Data fitted as two unresolved quadrupole doublets
b, Data fitted as one singlet and two unresolved quadrupole doublets
c, Data fitted as one singlet and one quadrupole doublet

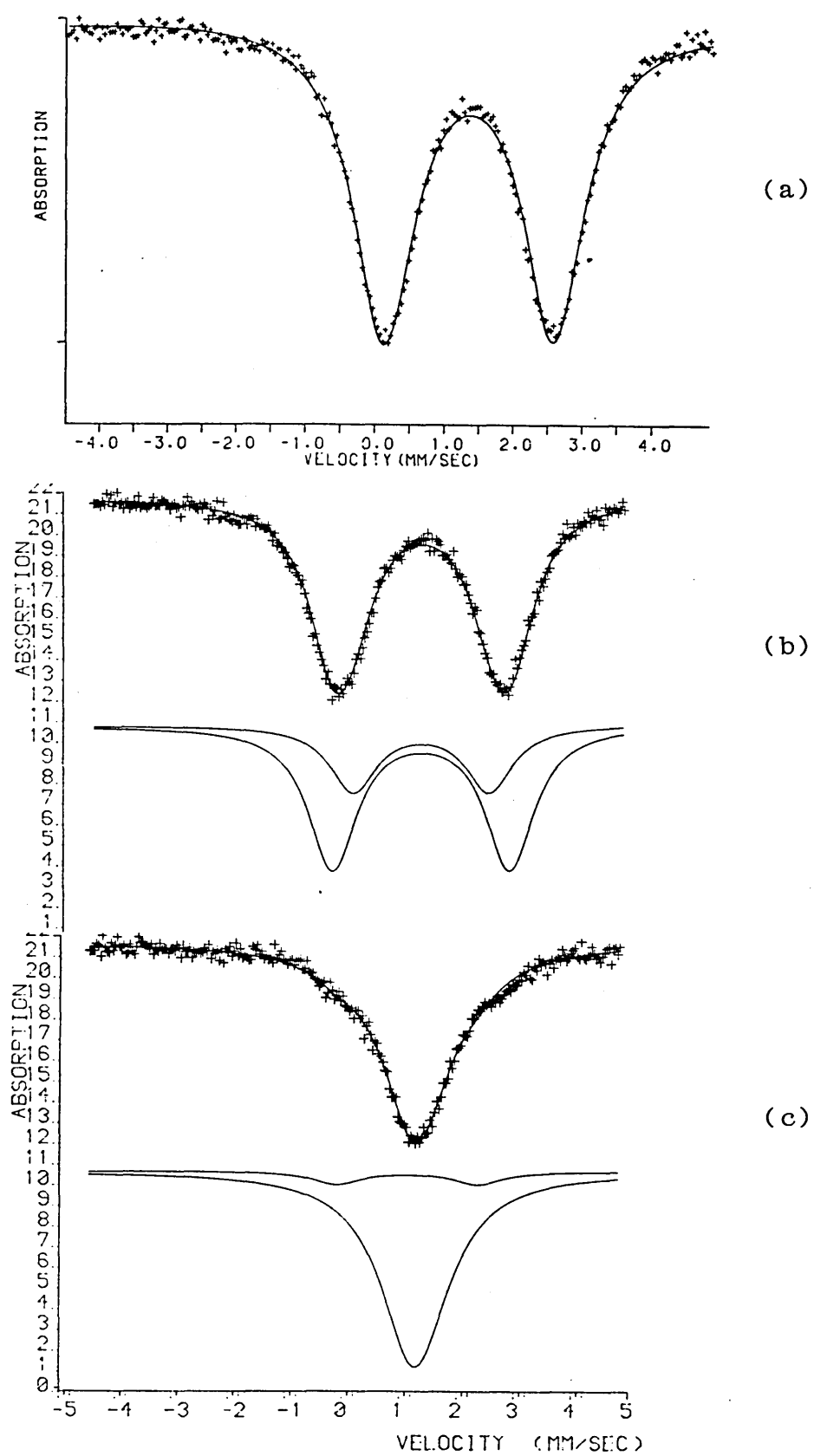


Figure 3.8 Tin-119 Mössbauer spectra obtained after heating the following with HCl at 150°C (a) $(\text{Ph}_3\text{Sn})_2\text{O}$, (b) Ph_2SnO and (c) Ph_4Sn

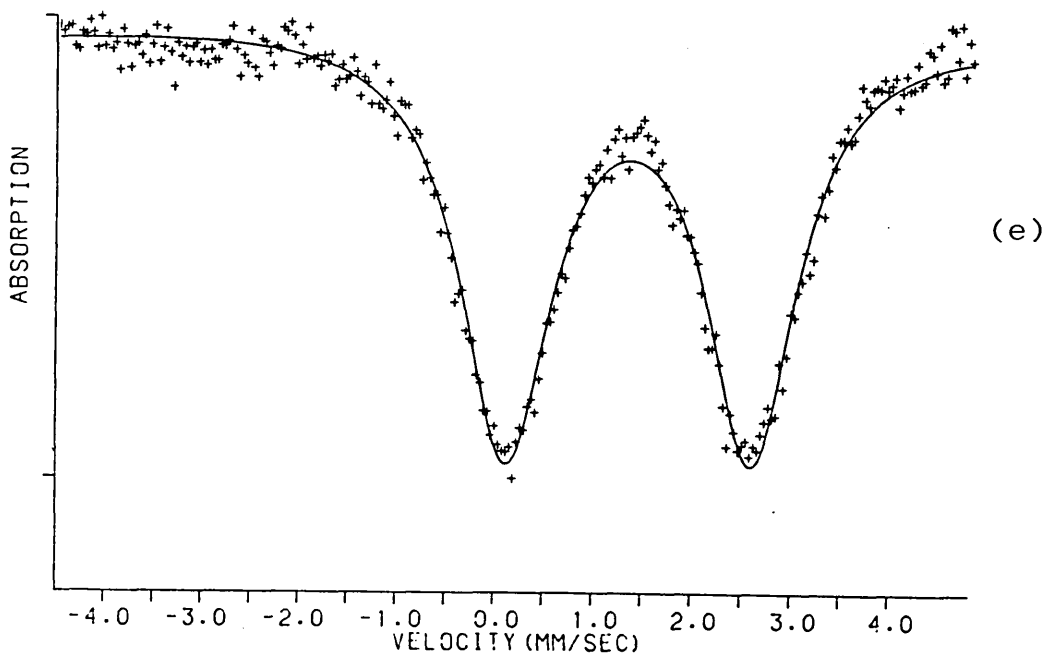
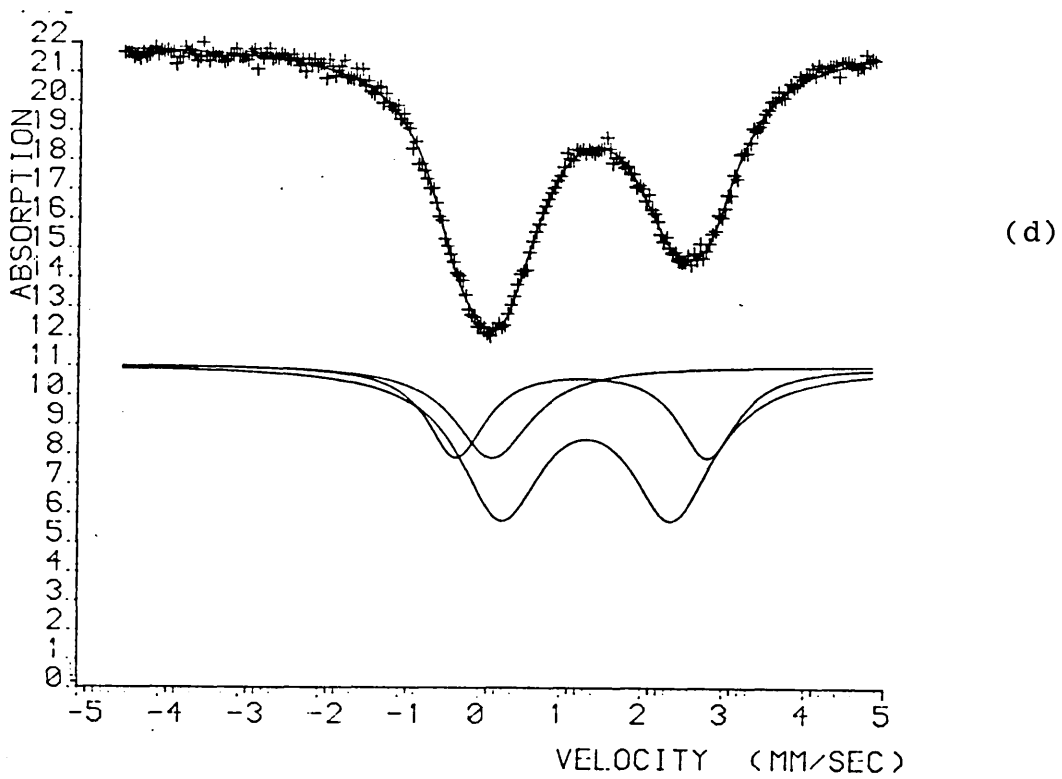
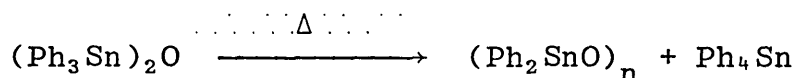


Figure 3.8 Tin-119 Mössbauer spectra obtained
after heating the following with HCl at
150°C (d) $\text{Ph}_3\text{SnOC}(:\text{O})\text{CH}_3$ and (e) Ph_3SnCl

The infrared spectra obtained from potassium bromide pellets in the range 1000 - 200 cm^{-1} , are shown in Figures 3.9 (a to c). The diminished intensity of the asymmetric Sn-O-Sn stretching mode at 770 cm^{-1} along with the appearance of characteristic $(\text{R}_2\text{SnO})_n$ Sn-O stretching modes at 575 cm^{-1} (ν_{as} Sn-O) and 415 cm^{-1} (ν_{s} Sn-O) in Figure 3.9 (c), clearly indicate the thermal disproportionation of the bis-oxide according to the reaction:



The Mössbauer spectrum obtained for the same residue was interpreted as a quadrupole doublet superimposed upon a singlet at $\sim 1.22 \text{ mm s}^{-1}$. The fitting parameters are given in Table 3.12 and the spectrum is shown in Figure 3.10.

Table 3.12 : ^{119}Sn Mössbauer Parameters for $(\text{Ph}_3\text{Sn})_2\text{O}$ after heating under the elastomer curing conditions

Compound	$\delta_{1,2}$ (mm s^{-1})	ΔE_Q^2 (mm s^{-1})	Γ (mm s^{-1})	Relative Area $\pm 5\%$
<u>Before Heating</u>				
$(\text{Ph}_3\text{Sn})_2\text{O}$ (pure)	1.13	1.42	1.01	100
Ph_2SnO (pure)	0.90	1.90	1.28	100
Ph_4Sn (pure)	1.26	0.00	1.06	100
<u>After Heating</u>				
$(\text{Ph}_3\text{Sn})_2\text{O}$	1.21	0.00	1.14	39
	0.85	1.80	1.64	61

1 Measured relative to BaSnO_3 , absorber at 80K

2 Errors = $\pm 0.02 \text{ mm s}^{-1}$

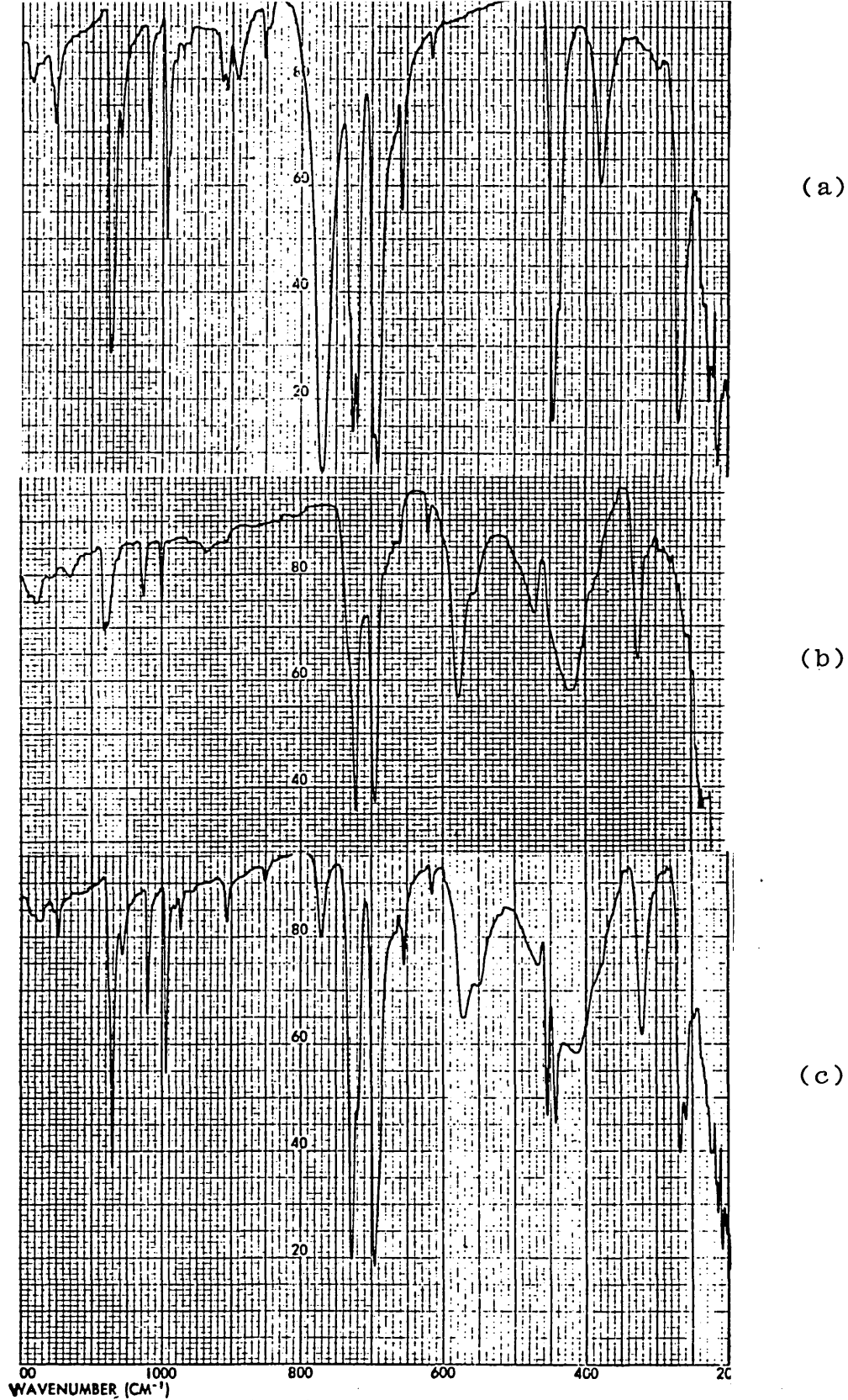


Figure 3.9 : Infrared spectra recorded for (a) pure $(\text{Ph}_3\text{Sn})_2\text{O}$, (b) pure $(\text{Ph}_2\text{SnO})_n$ and (c) $(\text{Ph}_3\text{Sn})_2\text{O}$ after heating at 150°C for 30 mins.

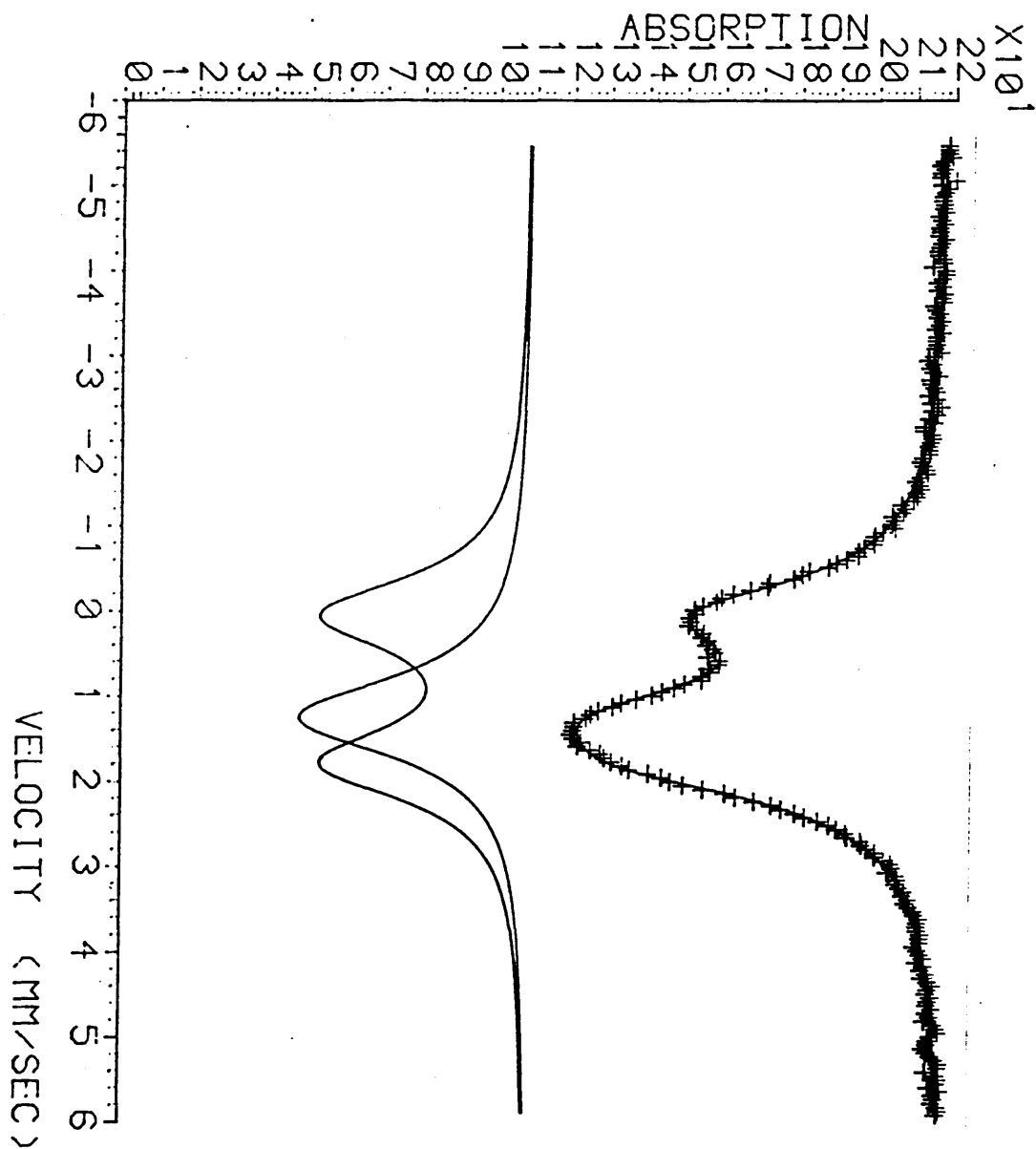


Figure 3.10 : Tin-119 Mössbauer spectrum of $(\text{Ph}_3\text{Sn})_2\text{O}$
after heating at 150°C for 30 minutes

3.3.3 ^{119}mSn Mössbauer Studies of the Fate of Triphenyltin Biocides Dispersed in Neoprene

Although the effect of heating triphenyltin-based toxicants in a hydrogen chloride environment has a marked effect on their Mössbauer parameters, this alone does not explain the extensive chemical breakdown evident in the authentic elastomer spectrum; Figure 3.6(b). Therefore, in an attempt to reveal additional chemical interactions that may exist between the triphenyltins and the base elastomer, neoprene films containing respectively Ph_3SnF , $(\text{Ph}_3\text{Sn})_2\text{O}$ and degradation products at 2.5% by weight were prepared according to the method described in Section 3.2.3. The tin-119 Mössbauer spectrum of each film was then recorded with the absorber maintained at a temperature of 80K. The isomer shift is quoted relative to barium stannate and all the data are associated with an experimental error of $\pm 0.05 \text{ mm s}^{-1}$; Table 3.13.

Table 3.13 : ^{119}Sn Mössbauer data from solvent cast neoprene films containing triphenyltin compounds at 2.5% wt. Parameters for the pure compounds are given in parentheses.

Organotin	δ (± 0.05 mm s $^{-1}$)	ΔE_Q (± 0.05 mm s $^{-1}$)	Γ (± 0.5 mm s $^{-1}$)	Relative Area $\pm 5\%$
Ph_3SnF^a	0.76 (1.29)	1.86 (3.69)	1.01	32
	1.30	3.58	0.94	68
$(\text{Ph}_3\text{Sn})_2\text{O}^b$	0.48 (1.13)	2.16 (1.42)	1.04	30
	0.86	2.28	0.88	29
	1.35	2.62	0.98	41
Ph_3SnCl^b	0.59 (1.33)	1.90 (2.56)	0.88	34
	0.87	2.10	0.88	30
$\text{Ph}_2\text{SnCl}_2^a$	1.42	2.52	0.82	36
	0.34 (1.37)	0.00 (2.86)	1.26	47
PhSnCl_3	0.84	1.86	1.02	53
	0.37 (1.10)	0.00 (1.75)	1.28	100
SnCl_4	0.43 (0.82)	0.00 (0.00)	1.28	100

a, Data fitted as 2-unresolved doublets

b, Data fitted as 3-unresolved doublets

The Mössbauer spectra obtained from these systems are presented in Figures 3.11(a) to (f).

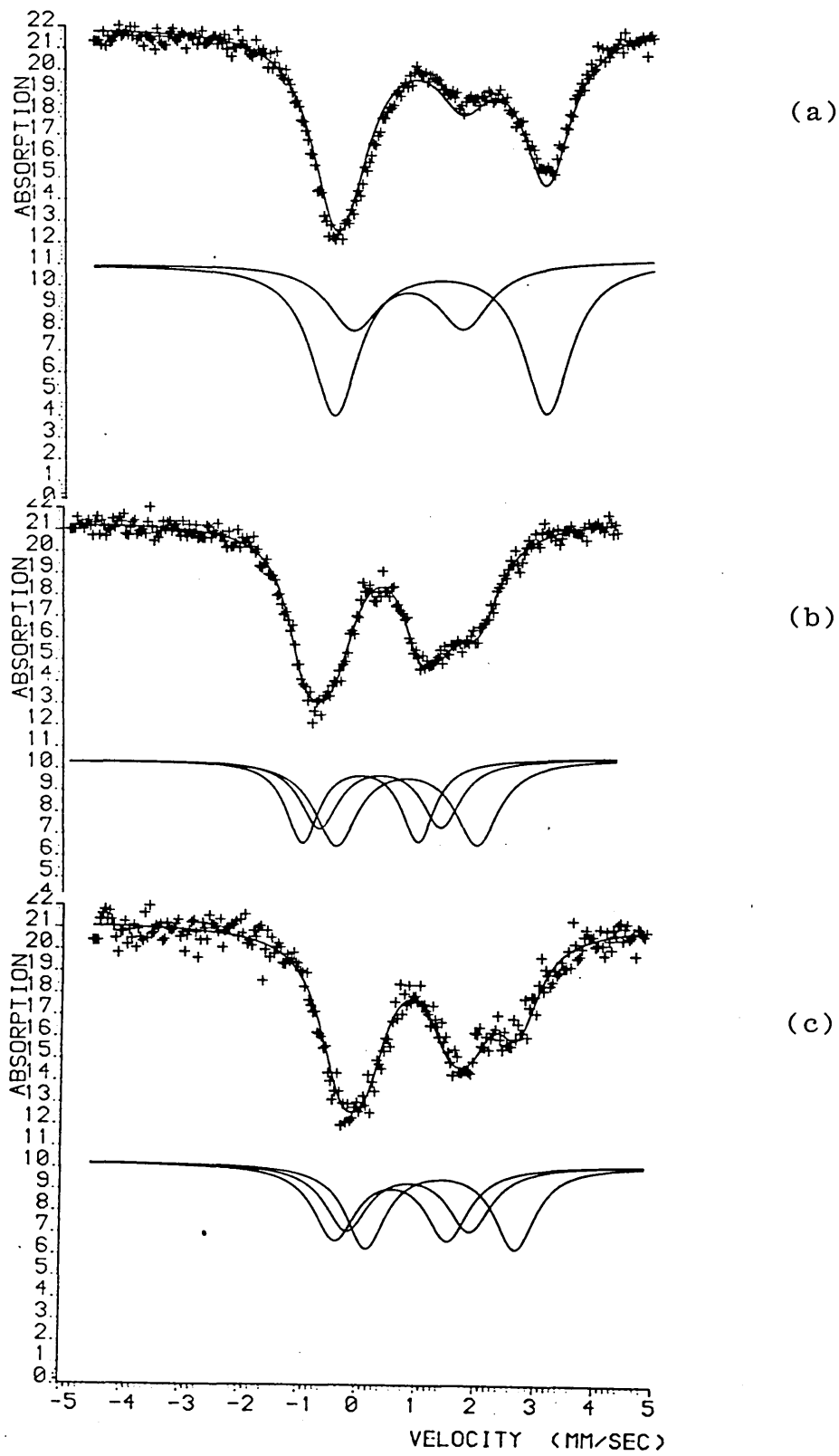


Figure 3.11 : ^{119}Sn Mössbauer spectra obtained from solvent cast neoprene films containing (a) Ph_3SnF , (b) $(\text{Ph}_3\text{Sn})_2\text{O}$ and (c) Ph_3SnCl

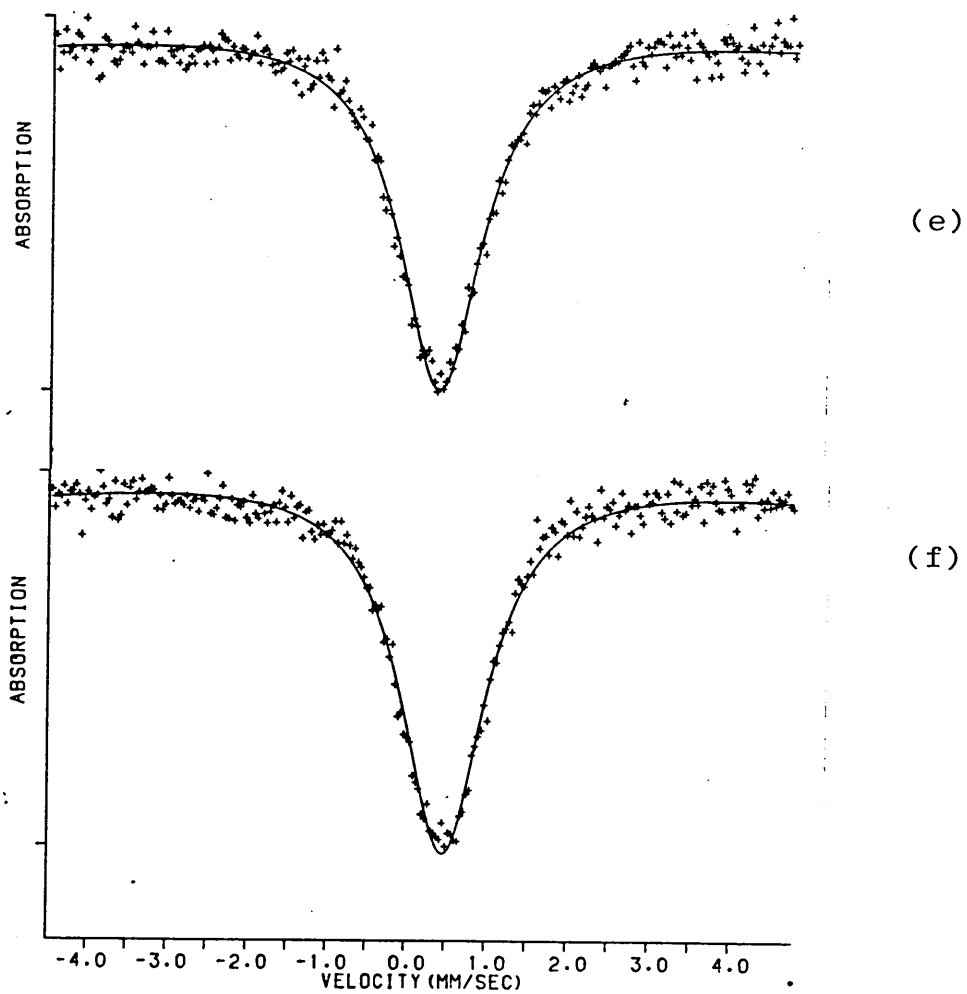
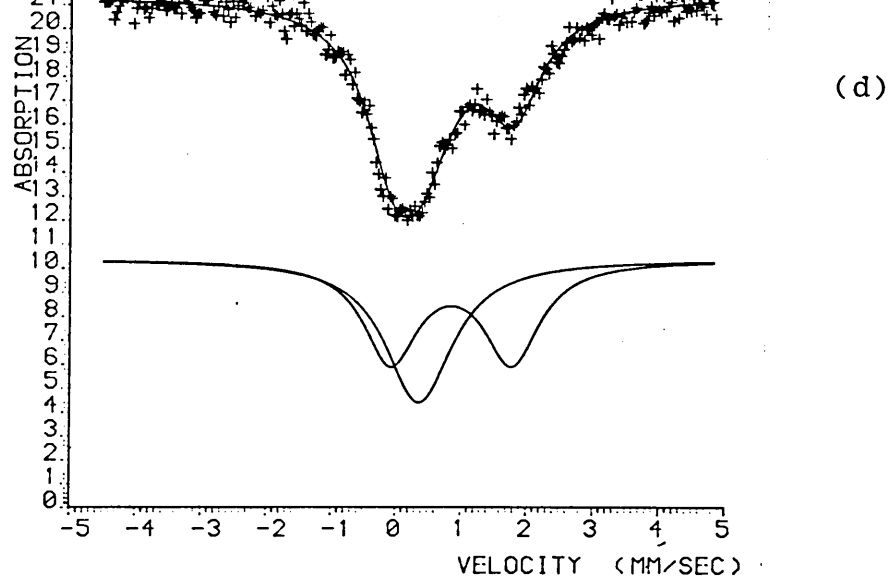


Figure 3.11 : ^{119}Sn Mössbauer spectra obtained from solvent cast neoprene films containing (d) Ph_2SnCl_2 , (e) PhSnCl_3 and (f) SnCl_4 .

The Mössbauer spectra demonstrate the gross chemical changes that have occurred in each organotin/polymer system, even under the mild experimental conditions used. Triphenyltin fluoride, Figure 3.11(a), appears to have undergone degradation to a diphenyltin moiety, possibly the chloro-fluoro derivative.

The form of the bis(triphenyltin)oxide and triphenyltin chloride spectra would indicate that these materials have undergone the same fate upon dispersion in neoprene, Figures 3.11(b) and (c). Further, the similarity of each spectrum would suggest that the bis-oxide undergoes conversion to the chloride prior to degradation. These spectra were initially interpreted as three overlapping quadrupole doublets arising from the presence of a mixture of organotin degradation products. The spectrum obtained for diphenyltin dichloride can be superimposed upon the inner doublet evident on the bis-oxide and mono-chloride spectra and provides indirect evidence of the presence of Ph_2SnCl_2 as a degradation production. Clearly, this material itself undergoes further degradation;

Figure 3.11(d) .

The addition of monophenyltin trichloride and stannic chloride was accompanied by a marked colour change in the neoprene matrix. The polymer solution was observed to change from amber-yellow to a red-brown colour and this was thought to arise from an increase in the degree of conjugation within the polymer. In addition, it was noted that of all the organotin-neoprene systems that

were studied, only the PhSnCl_3 - and SnCl_4 - dispersed elastomers were insoluble in dichloromethane. These observations are consistent with the formation of cross-links between the poly(chloroprene) chains.

3.4 Conclusions

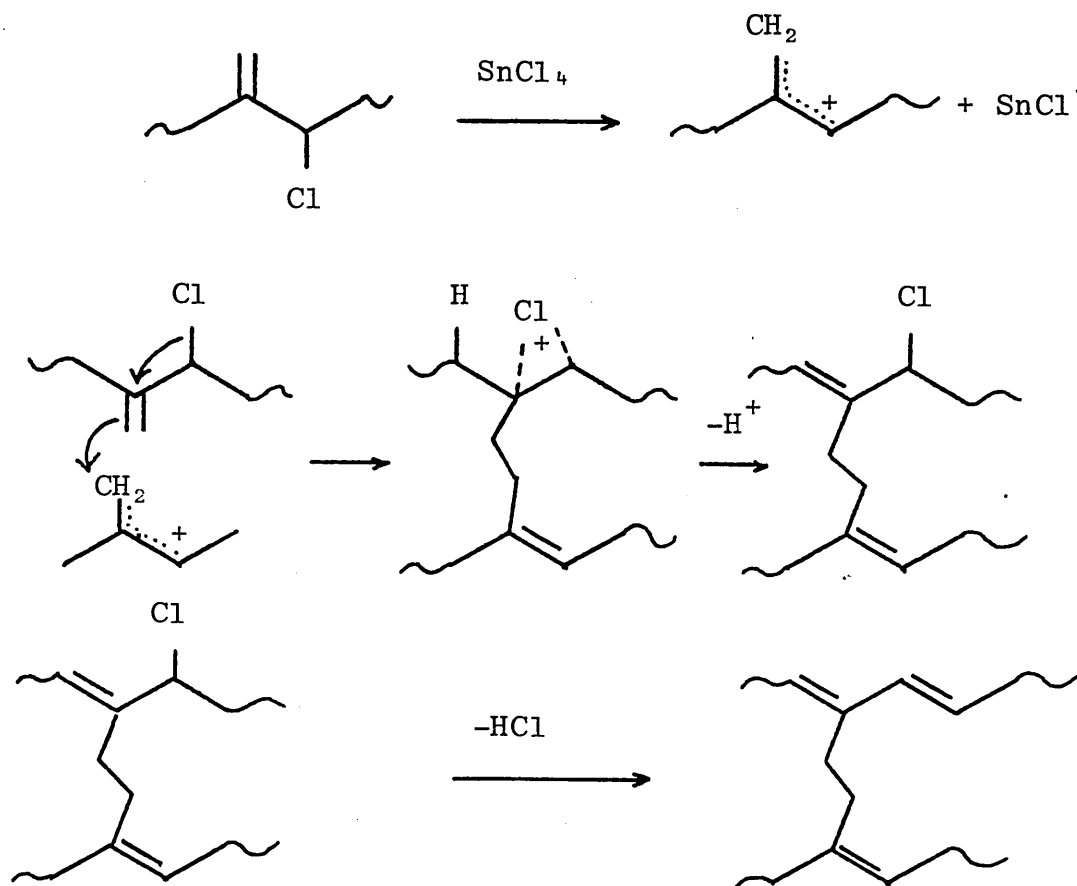
Tin-119 Mössbauer and N.M.R. studies have shown that a variety of tri-n-butyl and triphenyltin biocides undergo substantial chemical modification when dispersed into a marine antifouling coating matrix. The butyltin experiments indicate that the predominant conversion product in each case is tri-n-butyltin chloride; although most of the butyltin derivatives reveal significant amounts of tri-n-butyltin stearate and di-n-butyltin distearate as co-products.

The drastic degradation of a series of triphenyltin biocides within an authentic coating has been shown to involve successive Sn-C bond cleavage leading ultimately to the formation of stannic chloride.

Both the butyl and phenyltin derivatives were observed to interact strongly with the base polymer; poly(2-chloro-1,3-butadiene). The nature of the interaction in the butyltin systems is thought to involve coordination between the organotin moiety and the chlorine atoms of the elastomer. The phenyltins, however, reveal a much more complex system of chemical reactions involving Sn-C bond cleavage within the polymer matrix leading to a distribution of organotin degradation products. These experiments

illustrate the high reactivity of phenyltin compounds relative to the butyltin analogues in these antifouling systems.

The Lewis acidity of two tin compounds, monophenyltin trichloride and stannic chloride, has rendered these materials capable of cross-linking the polymer chains. The similarity of Mössbauer parameters suggests that monophenyltin trichloride is converted to stannic chloride which, subsequently, interacts with the polymer to produce cross-links. It is postulated that the mechanism involves the formation of a stabilised carbocation as proposed by Baldwin et al [27], by reaction of the allylic structural unit arising from the 1,2-addition of 2-chloro-1,3-butadiene, with stannic chloride:



The observed reduction in the isomer shift of SnCl_4 upon incorporation into neoprene, may be attributed to the formation of a hexachlorostannate complex within the polymer network, as a result of the foregoing cross-linking reactions. This effect has also been observed by Brooks et al [26] who noted that the isomer shift of SnCl_4 was reduced from 0.82 mm s^{-1} in the pure state to 0.30 mm s^{-1} when dispersed in PVC at 1.2% by weight. The broad line width observed for SnCl_4 in neoprene is probably due to individual molecules existing in different chemical environments. Some SnCl_4 may have formed a complex with residual HCl, some may be involved in simple coordination with chlorine atoms on the polymer chain and finally, some of the SnCl_4 has become involved in the curing process and been transformed into halogenostannate(IV) species. The carbon black, present as a major component in the antifouling coatings, was found to interact with the Bu_3SnX derivatives where $\text{X} = \text{OSnBu}_3, \text{OC}(\text{:O})\text{OSnBu}_3, \text{SSnBu}_3$ and stearate. Of the phenyltins examined, only triphenyltin hydroxide appeared to have been affected by dispersion into carbon black. Most of the Bu_3SnX spectra could be interpreted as unresolved quadrupole doublets superimposed upon each other. This suggested the formation of several different organotins (or the existence of single compounds with different tin-sites) in the carbon matrix. The chemical processes that are responsible for the observed structural changes are thought to arise from surface reactions between the organotin and functional groups which are known to be present on the carbon black

aggregates. The phenomenon of intercalation was briefly considered but the effect could not be demonstrated in the simple experiment described in this study.

3.5 References

1. W. P. Newmann, "The Organic Chemistry of Tin", Interscience Publishers, John Wiley and Sons, 1970.
2. S. J. Blunden, R. Hill and J. N. R. Ruddick, J. Organomet. Chem., 267, C5-8 (1984).
3. S. J. Blunden, R. Hill and D. G. Gillies, J. Organomet. Chem., 270, 39-44 (1984).
4. S. J. Blunden, D. Searle and P. J. Smith, Inorg. Chim. Acta, 98, 185-189 (1985).
5. P. J. Smith, R. F. M. White and L. Smith, J. Organomet. Chem., 40, 341 (1972).
6. A. G. Davies, L. Smith, P. J. Smith and W. McFarlane, J. Organomet. Chem., 29, 245 (1971).
7. J. J. Burke and P. C. Lauterbur, J. Am. Chem. Soc., 83, 326 (1961).
8. D. L. Alleston, A. G. Davies and M. Hancock, J. Chem. Soc., 5744-5748 (1964).
9. R. C. Poller, "The Chemistry of Organotin Compounds", Logos Press Ltd, 1970.
10. R. Okawara and M. Wada, in "Organotin Compounds", ed, A. K. Sawyer, Dekker, New York, 2, 253 (1971).
11. A. G. Davies and P. J. Smith in, "Comprehensive Organometallic Chemistry", eds, G. Wilkinson, F. G. A. Stone and E. W. Abel, Pergamon Press (1982).

12. D. L. Gardner and I. C. McNeill, Eur. Polym. J., 7, 569-591 (1971).
13. A. van Tongerloo and R. Vukov, Proc. Int. Rubber Conf., 70-79 (1979).
14. R. Vukov, Rubber Chem. and Tech., 57, 284-290, (1984).
15. I. Kuntz, R. L. Zapp and R. J. Pancirov, Rubber Chem. and Tech., 57, 813-825 (1984).
16. J. S. Brooks, R. W. Clarkson and D. W. Allen, J. Organomet. Chem., 243, 411-415 (1983).
17. R. V. Parish and R. H. Platt, Inorg. Chim. Acta, 4(1), 65-72 (1970).
18. J. B. Horn in "Rubber Technology and Manufacture - second edition, Eds., C. M. Blow and C. Hepburn, published for the Plastics and Rubber Institute by Butterworth Science, 202-218 (1982).
19. G. Ivan and M. Giurginca, Revue Roumaine de Chemie, 29(8), 639-646 (1984).
20. N. F. Cardarelli, Revs in Silicon, Germanium, Tin and Lead Compounds, 8(2/3), 169-189 (1985).
21. R. Schlögl and H. Boehm, Z. Naturforsch., 396, 112-114 (1984).
22. *ibid.*, 788-790.

23. A. K. Sijpesteijn, J. G. A. Luijten and G. J. M. van der Kerk in "Fungicides, An Advanced Treatise", ed, D. C. Torgeson, Academic Press, New York, 2, 331 (1969).
24. N. F. Cardarelli and S. J. Caprette, "Antifouling Coverings", U.S. Patent 3426473, Feb 11th 1969.
25. P. J. Smith, "Toxicological Data on Organotin Compounds", Int. Tin Res. Inst. Publ. No 538 (1978).
26. D. W. Allen, J. S. Brooks and J. Unwin, "Polym. Deg. and Stab.", 10, 79-84 (1985).
27. F. P. Baldwin, D. J. Buckley, I. Kuntz and S. B. Robinson, "Rubber Plast. Age.", 42, 500 (1961).

CHAPTER FOUR : SPECTROSCOPIC AND CHEMICAL ANALYSIS
OF A MARINE-EXPOSED ELASTOMER

4.1 INTRODUCTION

4.2 RESULTS AND DISCUSSION

4.3 AN ATTEMPT AT SURFACE ANALYSIS USING CONVERSION
ELECTRON MÖSSBAUER SPECTROSCOPY (CEMS)

4.3.1 Introduction

4.3.2 CEMS, Principles and Detection System

4.3.2.1 Detection System

4.4 DISCUSSION AND CONCLUSIONS

4.5 REFERENCES

4.1 Introduction

A sample of marine antifouling elastomer, originally incorporated with TBTO at ca 2.5% by weight, was obtained from the hull of a ship after 2.5 years service at sea. The sample formulation was based on the commercially available NOFOUL[®] recipe which is essentially the same as that given in Table 3.1 for the Admiralty prepared elastomers.

A transmission-mode Mössbauer spectrum was recorded in the usual way and the derivatization gas-chromatographic procedure, described in Section 3.3.1, was applied to the chemical characterization of degradation products.

Tin-119 NMR spectroscopy was also used to help identify the organotin species present in the coating matrix.

4.2 Results and Discussion

It was clear from the asymmetric line shapes and intensities that the folded Mössbauer data obtained from the ship sample represented a variety of different tin sites within the elastomer matrix. The best computer fit, corresponding to the lowest χ^2 value, was obtained by modelling the data as three-unresolved quadrupole doublets and one singlet. The fitted spectrum, along with the deconvoluted components are shown in Figure 4.1, and the fitting parameters are presented in

the accompanying table, 4.1. The fitting procedure involved constraining the paired line widths for each doublet but the isomer shift and splitting were allowed to vary throughout the regression analysis.

Table 4.1 Fitted parameters derived for the ship antifouling elastomer sample

δ $\pm 0.05 \text{ mms}^{-1}$	ΔE_Q $\pm 0.05 \text{ mms}^{-1}$	Γ $\pm 0.05 \text{ mms}^{-1}$	Relative Area, $\pm 5\%$
- 0.03	0.00	0.78	2
1.32	3.16	1.00	50
1.35	1.52	1.24	21
0.67	1.38	1.06	27

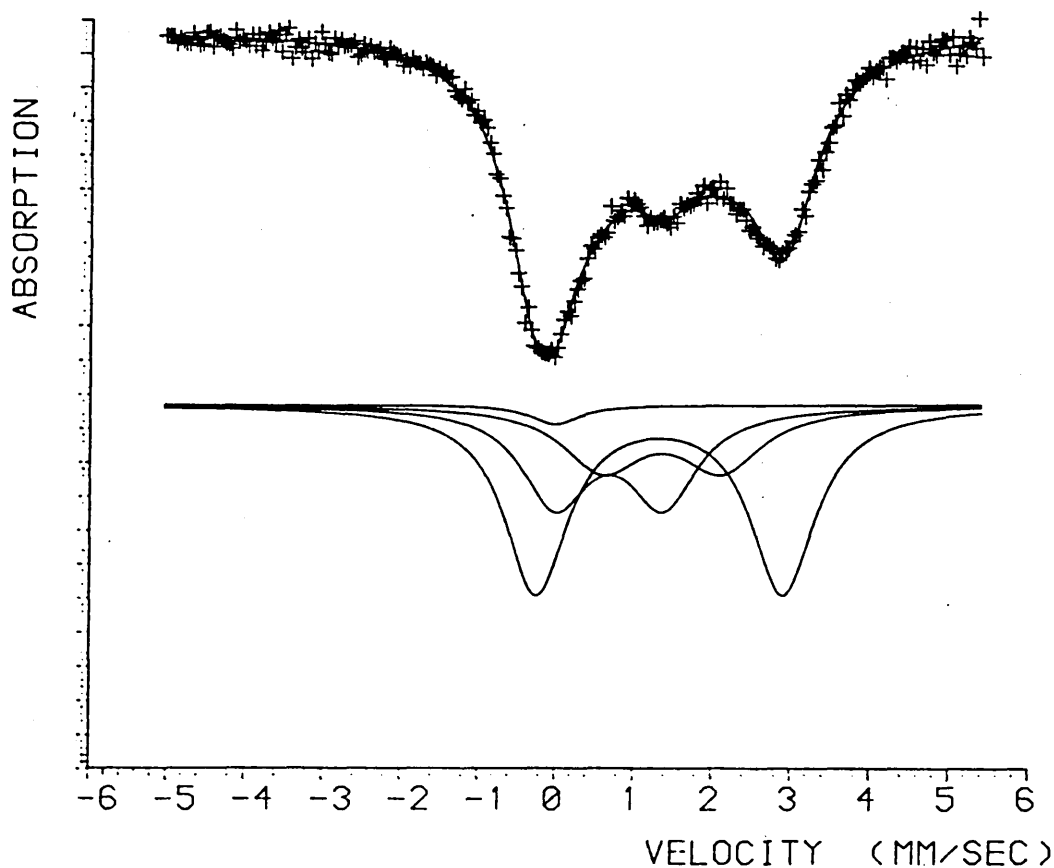


Figure 4.1 : Fitted data for the ship antifouling elastomer sample and deconvoluted components

Given that the coating had resided in an aqueous, mildly alkaline, medium for over two years, the presence of different tin sites was attributed to the formation of hydrolysis products within the elastomer matrix. The water absorption properties of neoprene coatings have already been investigated by Woodford who demonstrated that water could diffuse into a neoprene-based formulation to the extent of 5.9 - 8.4% by weight [1].

It is suggested, therefore, that these hydrolysis products are distributed throughout the bulk of the coating and are not merely confined to the near surface regions.

In order to corroborate these proposals and to attempt identification of the organotins evident in the Mössbauer spectrum, part of the sample was subjected to Soxhlett extraction in dichloromethane for two days. An aliquot of the resultant oil extract was redissolved in deuteriochloroform for tin-119 NMR analysis, and the remainder was derivatized according to the Grignard process described in Section 3.3.1 for subsequent gas-chromatographic analysis. The NMR data and chromatographic conditions are presented in Tables 4.2 and 4.3 respectively.

Table 4.2 : Tin-119 NMR data obtained from the ship antifouling elastomer extract

Signal	$\delta(^{119}\text{Sn})^a \pm 0.1 \text{ ppm}$
1	156.1
2	102.4
3	- 161.1

a Measured relative to tetramethyltin

Table 4.3 : Gas-chromatographic conditions used for the separation of n-butyltin moieties

Instrument :	Pye Unicam Series 104
Detector :	Flame Ionization
Column Length :	10 feet (glass)
Packing [†] :	10% SE-30 on 80-120 mesh Celite
Column Temperature :	200°C (isothermal)
Detector Temperature :	250°C
Carrier Gas :	Nitrogen at 40 cm ³ min ⁻¹
Hydrogen flow rate :	40 cm ³ min ⁻¹
Air Pressure :	15 p.s.i.

† The stationary phase, SE-30, consists of a methyl silicone gum.

Pure samples of tetra-n-propyltin (SnPr_4), tri-n-butyl-n-propyltin (Bu_3SnPr), di-n-butyl-di-n-propyltin (Bu_2SnPr_2) and n-butyltri-n-propyltin (BuSnPr_3) were prepared according to the Grignard method described in Section 3.3.1. Purity was checked chromatographically and by tin-119 NMR spectroscopy whereupon it was confirmed that the Grignard reaction conditions and subsequent isolation steps did not induce Sn-C bond cleavage.

Referring to Figure 4.2, the first chromatogram, (a), illustrates the baseline resolution obtainable for each stannane under the conditions used. Chromatograms (b) and (c) representing the marine-exposed elastomer residue, clearly indicate the presence of mono-, di- and tri-n-butyltin moieties within the coating matrix. These traces are to be compared with chromatogram (d) obtained from an authentic antifouling elastomer which had not been exposed to a marine environment. In this sample, there is no evidence of any monobutyltin having been formed during the compounding/curing processes. There are, however, measurable amounts of dibutyltin species and this may indicate that some thermally-induced Sn-C bond cleavage takes place during the coating formulation processes.

The apparent absence of tetrapropyltin derived from any inorganic tin compounds present (eg, SnO_2 , SnCl_4 , SnCl_6^{2-}) is probably due to the relative insolubility of such inorganic species in the solvent used for the Soxhlett extraction procedure.

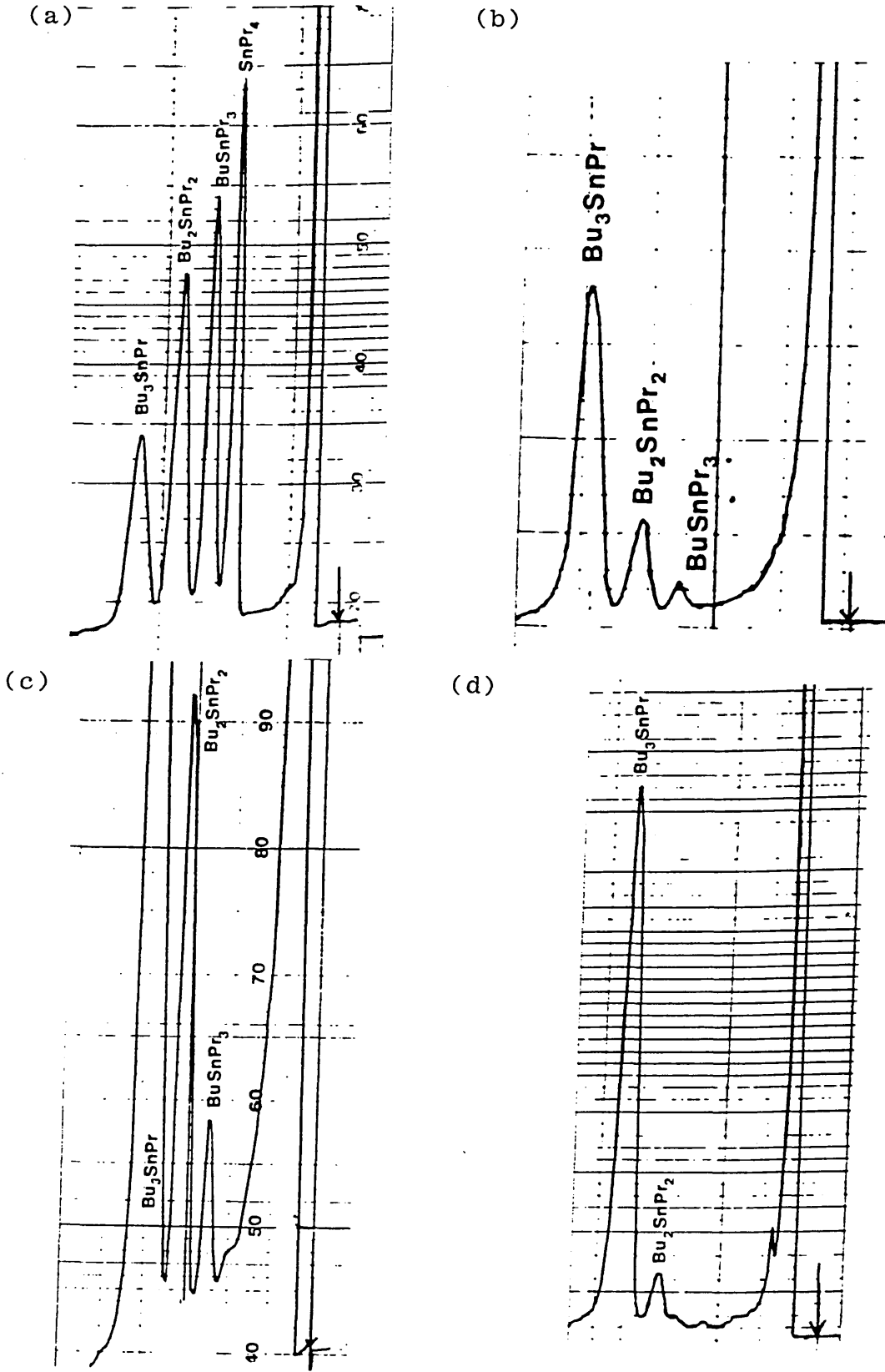


Figure 4.2 : Gas chromatograms for (a) n-propyltin standards, (b) ship elastomer extract, (c) ship extract and (d) elastomer extract from a non-exposed coating sample

4.3 An Attempt at Surface Analysis using Conversion Electron Mössbauer Spectroscopy (C.E.M.S.)

4.3.1 Introduction

The apparent existence of organotin(IV) degradation products in the marine-exposed elastomer prompted a study into the possible depth-selective distribution of hydrolysis products throughout the bulk of the coating. If hydrolysis-induced Sn-C bond cleavage does play a major role in the degradation of triorganotin biocides in these systems, then it would be reasonable to suppose that the majority of the hydrolysis products would be concentrated at the near surface regions of the coating matrix where water absorption at the elastomer-environment interface takes place.

Further, the possible surface enrichment of stannic oxide brought about by the exhaustive hydrolysis of organotin moieties continuously diffusing through the coating was also considered.

The following experiment demonstrated the use of Mössbauer spectroscopy in an alternative mode using an appropriate laboratory-built detection system.

4.3.2 C.E.M.S., Principles and Detection System

An alternative mechanism by which an excited state nucleus can relax, is by the process of Internal Conversion.

During the $I_e = 3/2$ to $I_g = 1/2$ transition of tin-119m,

only about 17% of the decay events result in the emission of the 23.8 keV γ -photon (Section 2.4.2). When internal conversion takes place, the nuclear energy is transferred to an L-shell electron which is then ejected with an energy of 19.6 keV. Subsequent electronic rearrangement also results in the emission of Auger electrons and x-ray photons. The major events during the decay of tin-119m are summarized in Table 4.4.

Table 4.4 : Major events during the decay of the I = 3/2 excited state of tin-119m

Emission	Energy keV	Number (per 100) Absorption Events
γ -photons	23.8	17
X-rays	3.6	9
L-conversion electrons	19.6	83
LMM-Auger electrons	2.8	74

The conversion electrons which are ejected following resonant absorption, are rapidly attenuated in matter and therefore only those which have originated from the near surface regions ($\sim 1 \mu\text{m}$ [2]) will be detected. Consequently, a Mössbauer spectrum, accumulated in "backscatter" mode, consists of a plot of emission intensity versus Doppler velocity and is characteristic of the uppermost regions of the substrate.

4.3.2.1 Detection System

Conversion electrons from the surface of the marine-exposed (ship) sample were detected using a Channeltron electron multiplier. The backscatter spectrum for this surface was then compared with that obtained from a freshly prepared surface within the bulk of the same sample. This was accomplished by slicing off the marine-exposed surface at a depth of about 0.5 mm.

The experimental arrangement is shown to scale in Figure 4.3.

Gamma rays from the tin-119 source entered the vacuum chamber, maintained at less than 10^{-4} torr, through an aluminised Mylar window. The absorber was mounted on a copper block machined so that its surface was oriented at 45° to the incident beam. This block was fixed directly to a copper rod cold-finger which, when immersed in liquid nitrogen, cooled the block and sample to 77 K by conduction. The channeltron detector, type X919BL, fixed in a nylon holder, was arranged so that its front entry window was parallel to and at a distance of 20 mm from the absorber. Around the entry window was placed a hemispherical grid accelerator; the positioning was such that the channeltron was just beyond the focal point of the hemisphere. When held at a positive potential with respect to the absorber, this grid provided a significant improvement in counting efficiency with no decrease in signal to noise ratio. During operation of the detector,

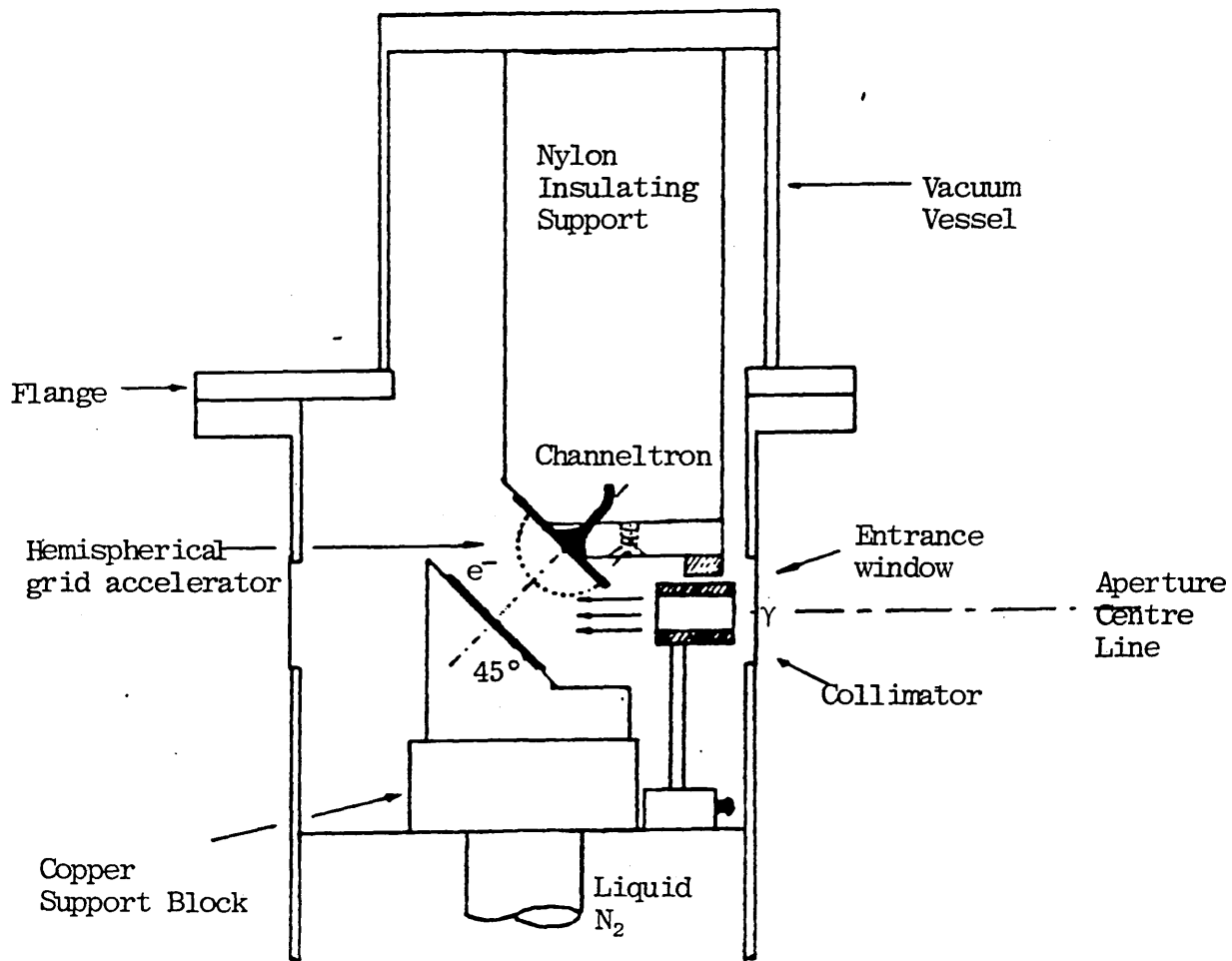


Figure 4.3 : Cross-section of vacuum system and target detector system

positive potentials of 2604 volts and 50 volts were applied to the channeltron and the hemispherical grid respectively. The system was then evacuated to about 10^{-5} torr before cooling the sample area to 77 K. Under these conditions, spectra of the quality shown in Figures 4.4(a) and (b) were obtained in about six days.

4.4 Discussion and Conclusions

The results of the transmission-mode Mössbauer experiment together with the tin-119 NMR and gas-chromatography data, clearly demonstrate the long-term environmental degradation of tributyltin species in a typical commercial antifouling coating matrix. The degradation processes were shown to involve the successive dealkylation of the original triorganotin moiety and it is believed that hydrolytic Sn-C bond cleavage is the principal mechanism by which these reactions occur.

Several workers have considered the environmental degradation of triorganotin compounds in aquatic media and the hypothetical degradation pathways for TBTF and TBTO have been presented by Cardarelli and Evans [3] who illustrated how stannic oxide is formed as the final degradation product. Similarly, the environmental degradation of TBTO was considered by Sheldon [4], to involve the initial formation of the triorganotin carbonate, by reaction with carbon dioxide, followed by successive debutylation to yield stannic oxide:

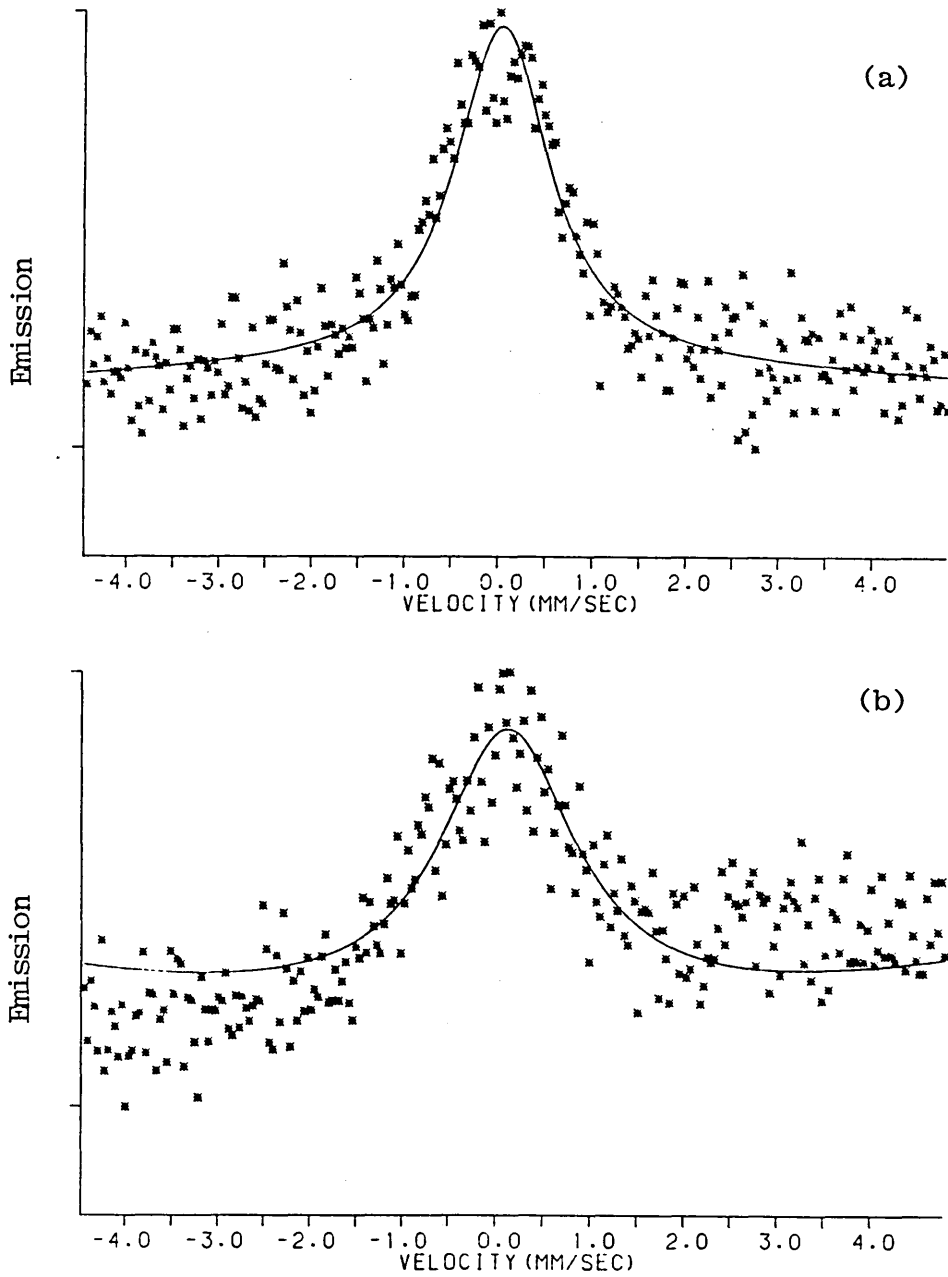
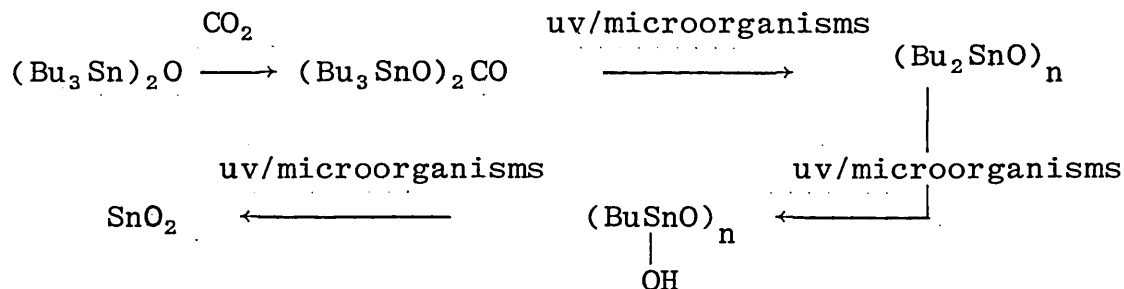
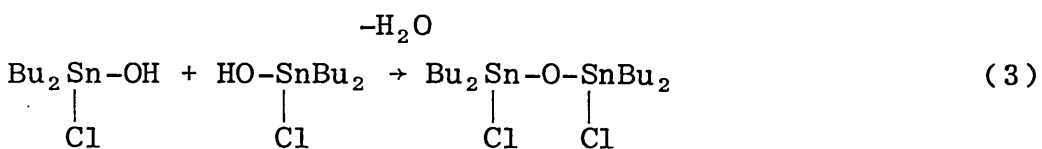
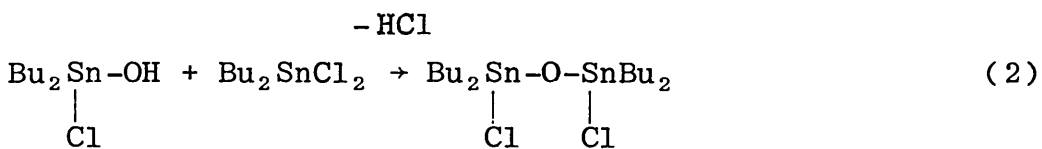
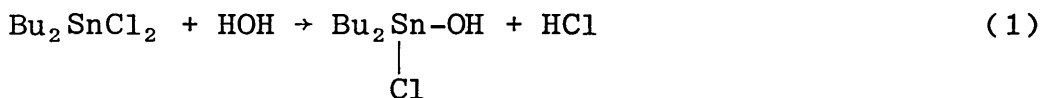


Figure 4.4 : Backscatter spectra obtained from the ship elastomer sample (a) marine exposed surface, (b) a freshly prepared surface

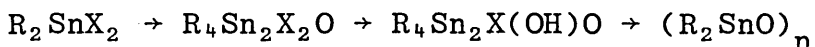


The first stage of this degradation scheme was supported, to some extent, by the work of Laughlin et al [5] who used tin-119 NMR spectroscopy to demonstrate the presence of tributyltin-carbonate, -oxide and -chloride in a chloroform extract from a sea water sample (pH ~ 8) originally containing TBTO.

The subsequent hydrolysis of the diorgano and mono-organotin hydrolysis products has also been studied by other workers [6-8]. For example, Gibbons et al demonstrated that when dibutyltin dichloride is stirred with water, an insoluble compound is formed which corresponds to the appropriate bis[dibutylhalotin(IV)] oxide. The following routes were suggested to account for these observations:



Alleston et al have studied the intermediates formed during the hydrolysis of dialkyltin(IV) compounds and have proposed polymeric dibutyltin oxide as the last product in the exhaustive hydrolysis of dibutyltin dichloride under basic conditions. The generalised reaction scheme was presented as follows:



Migdal [8] extended this work to show that hydrolysis of tetrabutyl-1,3-dichlorodistannoxane leads to the formation of α, ω -dichlorooligostannoxanes of the type $Cl(SnBu_2O)_n SnBu_2Cl$ where n is controlled by the molar ratio of base to distannoxane.

Monoalkyltins also yield a range of products when subjected to hydrolysis and Luijten [9] has observed mixtures of compounds which are intermediates between alkyltin trichlorides and alkanestannonic acids in aqueous media.

Considering the high water absorbing properties of neoprene-based antifouling coatings (5.9 - 8.4% wt [1]) and the findings of Sherman [10] who demonstrated the hydrolysis of TBTF within a commercial controlled-release formulation, it is likely that the transmission-mode Mössbauer spectrum obtained from the marine-exposed elastomer represents a complex range of degradation products formed by debutylation and hydrolysis reactions. The Mössbauer parameters corresponding to the best-fit

of the experimental data could not be related to specific organotin compounds of the types cited in the references, since time did not allow the preparation of appropriately dispersed authentic elastomer samples. However, the tin-119 NMR data given in Table 4.5 are consistent with the presence of tributyltin chloride, tributyltin stearate [$\delta(^{119}\text{Sn}) = + 102.4 \text{ ppm}$] and, possibly, dibutyltinbis(stearate) as extractable moieties. The formation of the bis(stearate) derivative in coating formulations was previously discussed in Section 3.2.2.

A sample of tetrabutyl-1,3-dichlorodistannoxane, one possible degradation/hydrolysis product, was prepared by fusing together equimolar amounts of dibutyltin dichloride and dibutyltin oxide. The resulting white solid melted in the range 104-107°C and was soluble in common non-polar solvents. Tin-119 NMR analysis of the material in deuteriochloroform solution produced a spectrum consisting of two resonances to high-field of tetramethyltin. Absorption in this region usually corresponds to compounds in which the tin atom has a coordination number of greater than four [11]. This was confirmed by tin-119 Mössbauer analysis of the pure compound in which the broadened line shapes indicated the presence of multiple tin sites. Lorentzian lines representing two unresolved quadrupole doublets were modelled to the data and the Mössbauer parameters, along with the NMR data, are given in Table 4.5. The relevant tin-119 NMR

and Mössbauer spectra are shown in Figure 4.5.

Table 4.5 : Tin-119 NMR and Mössbauer data obtained
for pure tetrabutyl-1,3-dichlorodistannoxane

$\delta(^{119}\text{Sn})^a$ $\pm 0.1\text{ppm}$	δ^b $\pm 0.02\text{mms}^{-1}$	ΔE_Q $\pm 0.02\text{mms}^{-1}$	ρ^c ± 0.05	Γ $\pm 0.02\text{mms}^{-1}$	Relative Mössbauer Line Area $\pm 5\%$
- 90.4	1.18	3.22	2.73	1.02	33
- 138.1	1.49	3.20	2.15	1.02	67

a Chemical shift measured relative to tetramethyltin in deuteriochloroform.

b Isomer shift measured relative to barium stannate with the absorber at 80 K.

c The ratio $\Delta E_Q/\delta$.

The NMR and Mössbauer data clearly demonstrate the presence of two non-equivalent tin sites in this molecule as indicated by Davies et al [12]. Further, their observation that the distannoxane possesses two pentacoordinate tin atoms distributed in a ladder network (I) is supported by the findings of Herber et al [13] who suggested that the coordination number can be obtained from ρ , the ratio of quadrupole splitting (ΔE_Q) to isomer shift (δ), and that for a value of ρ greater than 2.1, pentacoordination can be assumed.

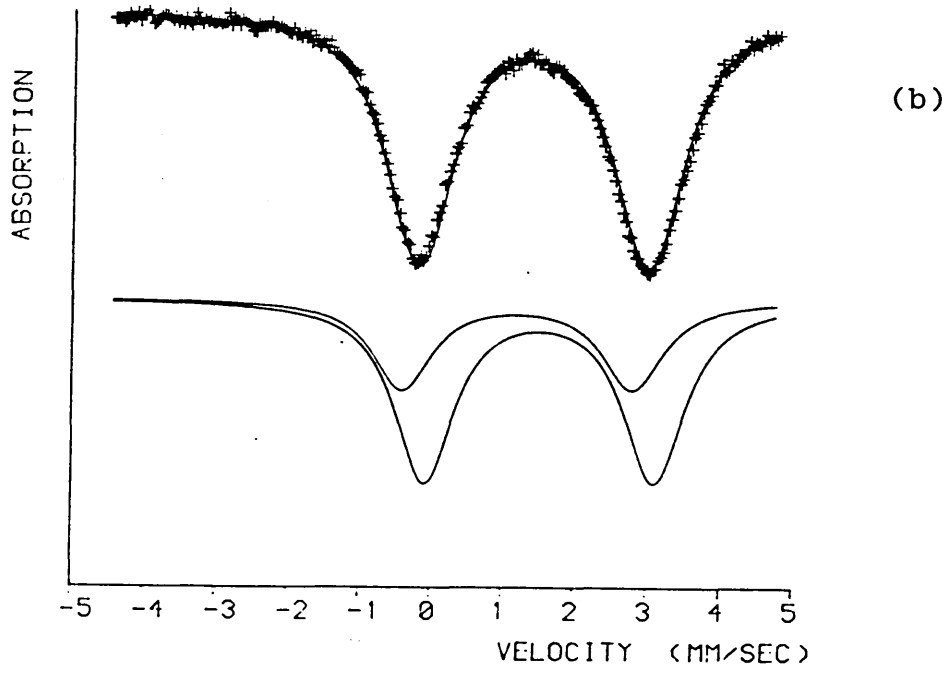
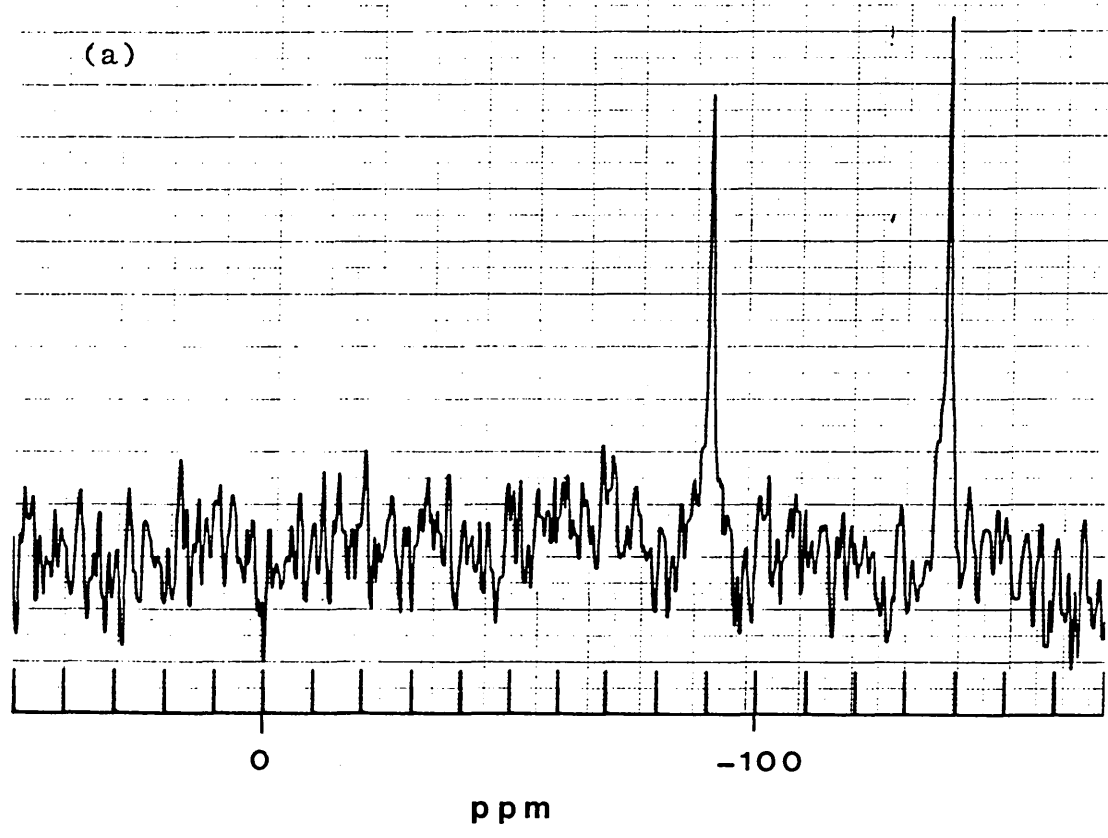
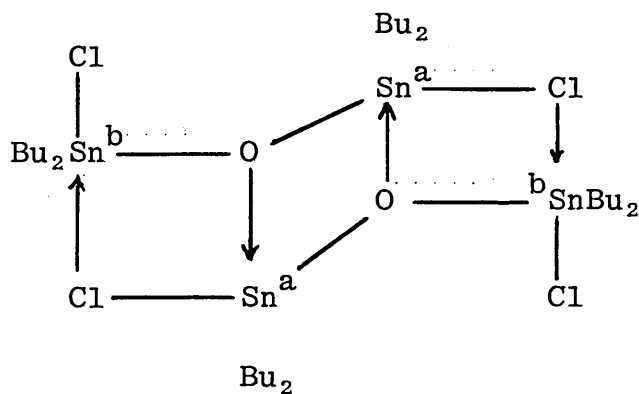


Figure 4.5 : (a) Tin-119 NMR and (b) Mössbauer spectra obtained for $(\text{ClBu}_2\text{Sn})_2\text{O}$



(I)

The difference in isomer shift for each doublet, illustrates the difference in s-electron density at each of the tin nuclei (a) and (b) as a result of coordination with the oxygen and chlorine atoms respectively. This example of a single organotin compound with chemically non-equivalent tin-sites, shows how a complex Mössbauer spectrum of the type obtained from the marine-exposed elastomer can easily result from the presence of relatively few degradation/hydrolysis products.

The backscatter spectra indicate the need for improvements in experimental design as the prolonged accumulation times, necessary because of the low surface tin concentration, led to large background counts and poor signal to noise ratios for each spectrum, Figures 4.4(a) and (b). In spite of this, however, both spectra were obviously dominated by a very broad absorption line at ca zero mm s⁻¹ and in that respect they differ markedly

to the transmission-mode spectrum in Figure 4.1.

The fitted parameters are given in Table 4.6.

Table 4.6 : Backscatter Mössbauer parameters obtained from a commercial antifouling elastomer sample; (a) marine-exposed surface (2.5 years) and (b) freshly exposed surface

Surface type	δ $\pm 0.05 \text{ mms}^{-1}$	ΔE_Q^1 $\pm 0.05 \text{ mms}^{-1}$	Γ $\pm 0.05 \text{ mms}^{-1}$	χ^2
(a)	- 0.01	0.00	1.24	154
(b)	+ 0.08	0.00	1.76	194

1 Data fitted as a broad singlet in each case, although the large line widths could indicate the existence of unresolvable quadrupole doublets

The zero velocity peak was attributed to the presence of stannic oxide formed as the final organotin(IV) degradation product and this is offered as supportive evidence for proposed hydrolytic degradation mechanisms discussed earlier.

The spectrum obtained from the freshly exposed surface of this sample did not reveal the presence of organotin moieties in quite the explicit manner that was hoped for. Indeed, the only indication that organotin compounds were present in addition to stannic oxide, came from the observed line broadening of the zero

velocity peak and the asymmetry in background counts about this region. It is quite clear that some backscatter has occurred in the positive velocity region of $2.5 - 4.0 \text{ mm s}^{-1}$. However, the signal to noise ratio is extremely poor; Figure 4.4(b).

The main difficulties in observing the organotin(IV) compounds (apparent in the transmission-mode spectrum) when using the backscatter technique arise from the very low concentrations of such materials in the scattering thickness ($\sim 1 \mu\text{m}$) and in the relatively low recoil-free fractions of organotins as compared with inorganic tin compounds such as stannic oxide. For example, Stockler [14] and Barbieri [15] have calculated the recoil-free fractions of several organotin(IV) compounds at 80 K and an approximate range for this quantity would appear to be $0.06 - 0.4$ depending on the particular compound studied. Herber, however, reports a recoil-free fraction for stannic oxide at room temperature of 0.497 ± 0.006 [16]. Since this quantity will increase substantially at the experimental temperature of 77 K, it is obvious that the presence of stannic oxide, even in small amounts, will dominate the resultant Mössbauer spectra. It is believed, therefore, that the Mössbauer spectra of organotin compounds which are present in the marine-unexposed elastomer sample, are masked by the spectrum obtained from the small but significant quantities of stannic oxide on the surface.

The Mössbauer data in Figure 4.4(b) for the freshly prepared surface were tentatively fitted as a singlet and a quadrupole doublet in order to improve the quality of fit in the positive velocity region. The following parameters were so obtained:

$$\delta_1 = 0.00 \text{ mm s}^{-1}, \Delta E_Q = 0.00 \text{ mm s}^{-1}, \Gamma = 1.22 \text{ mm s}^{-1},$$

Rel. Area 58%

$$\delta_2 = 1.49 \text{ mm s}^{-1}, \Delta E_Q = 2.82 \text{ mm s}^{-1}, \Gamma = 1.02 \text{ mm s}^{-1},$$

Rel. Area 42%

The statistical improvement in the quality of fit was evident in the reduced χ^2 value of 171 (cf $\chi^2 = 194$) and the Mössbauer parameters for the first quadrupole doublet are noticeably similar to those obtained for the tributyltin-containing elastomers discussed in Chapter 3. The modified fit is shown in Figure 4.6.

The only practical way of improving the quality of the backscatter spectra obtained in this study would be to employ much lower absorber temperatures, possibly by the use of a pumped helium or liquid helium-cooled cryostat, and to use a more active source than the one used here (initial activity 15 mCi). However, the exercise did demonstrate the potential utility of backscatter (C.E.M.S.) Mössbauer spectroscopy in surface analysis and with the refinements mentioned above, it should be possible to apply the technique to more informative studies of industrially important substrates bearing Mössbauer active isotopes.

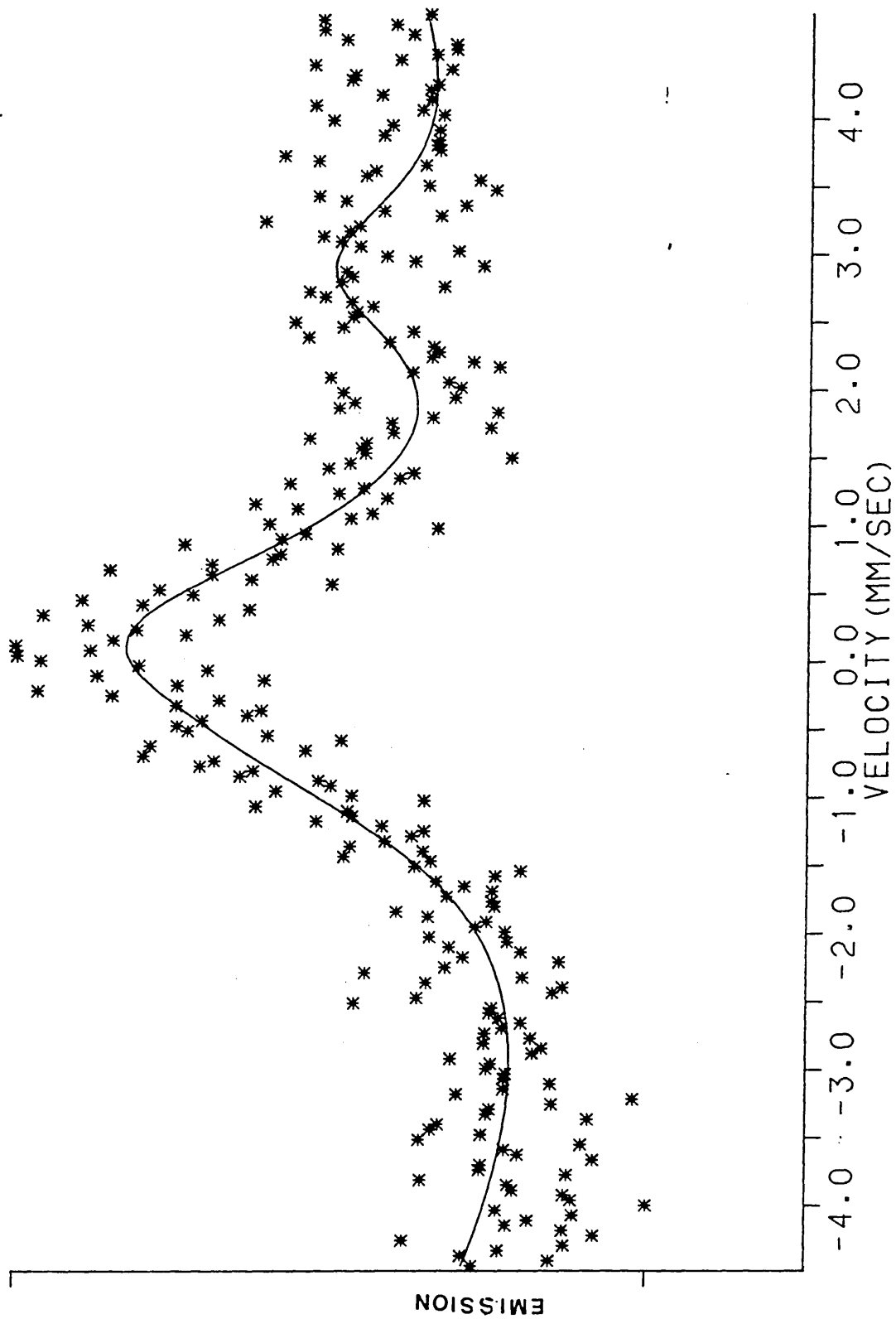


Figure 4.6 : Freshly exposed surface of marine anti-fouling elastomer obtained from ship's hull

4.5 References

1. J. M. D. Woodford, Dept. of Supply, Austral. Dfce. Stds. Semr. Dfce. Stds. Labs., Report 496 (1972).
2. H. M. van Noort, B. C. M. Meenderink and A. Molenaar, J. Electrochem. Soc., 133(2), 263-265 (1986).
3. N. F. Cardanelli and W. Evans in, "Controlled Release of Bioactive Materials", (ed) R. Baker, Academic Press, 357-385 (1980).
4. A. W. Sheldon, J. Paint Technol., 47, 54 (1975).
5. R. B. Laughlin, H. E. Guard and W. M. Coleman, Environ. Sci. Technol., 20, 201-204 (1986).
6. A. J. Gibbons, A. K. Sawyer and A. Ross, J. Org. Chem., 26, 2304-2306 (1961)
7. D. L. Alleston, A. G. Davies and M. Hancock, J. Chem. Soc., 5744-5748 (1964).
8. S. Migdal, D. Gertner and A. Zilkha, Can. J. Chem., 46, 2409-2413 (1968).
9. J. G. A. Luijten, Rec. Trav. Chim., 85, 873-878 (1966).
10. L. R. Sherman, J. App. Polym. Sci., 28, 2823-2829 (1983).
11. A. G. Davies, P. G. Harrison, J. Kennedy, T. N. Mitchell, R. J. Puddephatt and W. McFarlane, J. Chem. Soc. (C), 1136 (1969).

12. A. G. Davies, L. Smith, P. J. Smith and W. McFarlane,
J. Organomet. Chem., 29, 245-250 (1971).
13. R. H. Herber, H. A. Stockler and W. T. Reichle,
J. Chem. Phys., 42, 2447 (1965).
14. H. A. Stockler, H. Sano and R. H. Herber,
J. Chem. Phys., 47(5), 1567-1571 (1967).
15. R. Barbieri, L. Pellerito, A. Silvestri, G. Ruisi
and J. G. Noltes, J. Organomet. Chem., 210,
43-50 (1981).
16. R. H. Herber in "Chemical Mössbauer Spectroscopy",
ed, R. H. Herber, Plenum Press, New York and
London, 199-216 (1984).

CHAPTER FIVE : VARIABLE TEMPERATURE MÖSSBAUER STUDIES
OF TRI-N-BUTYL TIN CHLORIDE IN THE PURE
STATE AND IN ELASTOMERIC MEDIA

- 5.1 INTRODUCTION
- 5.2 THEORY
- 5.3 EXPERIMENTAL AND RESULTS
- 5.4 DISCUSSION
- 5.5 CONCLUSIONS
- 5.6 REFERENCES

CHAPTER 5 : VARIABLE TEMPERATURE MÖSSBAUER STUDIES OF
TRI-N-BUTYLTIN CHLORIDE IN THE PURE STATE
AND IN ELASTOMERIC MEDIA

5.1 Introduction

In Chapter 3, it was suggested that the major conversion product formed during the curing of the tri-n-butyltin-containing elastomers was tri-n-butyltin chloride (TBTC1). It was also noted, however, that the Mössbauer parameters for this compound in an elastomeric matrix differed from those of the pure compound and it was suggested that a possible biocide-polymer (or polymer component) interaction may have caused the discrepancy.

In this study, variable temperature Mössbauer spectroscopy (v.t. M.s.) was used to probe the vibrational behaviour of the tin nucleus of the TBTC1 molecule in three different systems. These were:

- (i) the pure state
- (ii) solvent cast into neoprene at 2.5% by wt.
- (iii) part of the authentic antifouling elastomer formulation; AFR 3644.

The aims of this work were to determine if there were any differences in the vibrational behaviour and whether these could be related to structural changes.

5.2 Theory

The recoil-free fraction (f) or the probability of an emission or absorption event occurring without phonon interactions was briefly discussed in Section 2.4.1.

A relationship between f and the mean square vibrational amplitude of the Mössbauer atom, $\langle X^2 \rangle$ was given as:

$$f = \exp \left[\frac{-4\pi \langle X^2 \rangle}{\lambda} \right] \quad (18)$$

Since this vibrational amplitude is temperature dependent, then f is also temperature dependent and it is possible to extract chemical information on the environment of the Mössbauer atom by monitoring f as a function of temperature, T .

The Debye model of solids [1] leads to an expression for f of the form:

$$f(T) = \exp \left\{ \frac{-3E_R}{2k_B\theta_D} \left[1 + 4 \left(\frac{T}{\theta_D} \right)^2 \int_0^{\theta_D/T} \frac{x dx}{(e^x - 1)} \right] \right\} \quad (19)$$

where the recoil energy (Chapter 2), $E_R = E_\gamma^2 / 2M_{\text{eff}}c^2$, θ_D is the Debye temperature of the solid and k_B is the Boltzmann constant.

In the high temperature limit where $T > \theta_D/2$,

$\int_0^{\theta_D/T} \frac{x dx}{(e^x - 1)}$ goes to θ_D/T and hence:

$$f(T) = \exp \left\{ \frac{-3E_R}{2k_B \Theta_D} \left[1 + 4 \left(\frac{T}{\Theta_D} \right)^2 \cdot \frac{\Theta_D}{T} \right] \right\} \quad (19a)$$

$$= \exp \left[\frac{-3E_R}{2k_B \Theta_D} - \frac{6E_R T}{k_B \Theta_D^2} \right] \quad (20)$$

Therefore, for an ideal monatomic isotropic cubic solid, the slope of the plot of $\ln f(T)$ versus temperature would be given by:

$$\frac{d[\ln f(T)]}{dT} = - \frac{6E_R}{k_B \Theta_D^2} \quad (21)$$

Clearly, since the materials examined in this study do not fulfil the Debye criteria, ie that they be composed of a monatomic isotropic array of atoms, it would be unreasonable to attach too much physical significance to the Debye temperature extracted from equation (21). For comparative purposes, however, it is justifiable to assume that the smaller the Debye temperature, the larger is the mean square displacement of the Mössbauer atom. Thus, by comparing the slopes derived from $f(T)$ versus T plots, it should be possible to characterise the tightness with which the tin atom is bound in the lattice, and hence the degree of molecular association.

For thin absorbers (Section 2.4.3, Mössbauer thickness, $t \ll 5$), the area, A , under the spectra envelope and $f(T)$ are linearly related and the Debye model predicts

that plots of $\ln A(T)$ versus temperature are linear.

Under these conditions, the thin absorber approximation leads to:

$$\frac{d \ln(A)}{dT} = \frac{-6E_R}{k_B \theta_D^2} = \frac{-3E_\gamma^2}{(M_{\text{eff}} c^2) k_B \theta_D^2} \quad (22)$$

The two unknowns in equation (22) are the Debye temperature and M_{eff} , the effective vibrating mass of the absorbing atom.

5.3 Experimental and Results

Mössbauer spectra were recorded over the temperature range 12.5 - 60 K using the Displex cryostat and Air Products temperature controller described in Chapter 2.

The method of calculating an appropriate sample mass that fulfilled the thin absorber criterion was illustrated in Chapter 2. Table 5.1 lists the sample masses used in this study and the validity of the thin absorber approximation is tested for assumed f -values of 0.06 and 0.4:

Table 5.1 : Sample masses and Mössbauer thickness values for TBTC1 in various systems

Absorber	TBTC1 (mg)	^{119}Sn Content (mg cm $^{-2}$)	t (f = 0.06)	t (f = 0.4)
TBTC1 (pure)	78.7	0.79	0.17	1.12
Neoprene ^a	14.2	0.09	0.02	0.13
AFR 3644 ^b	45.6	0.29	0.06	0.41

a Solvent-cast neoprene film containing TBTC1 at 2.5% by weight

b Authentic marine antifouling elastomer containing TBTC1 at 2.5% by weight

In Table 5.1 it is observed that $t \ll 5$ for all absorbers and, therefore, it is valid to assume that the temperature dependence of the Mössbauer absorption line area ($A(T)$) is linearly related to the temperature dependence of the recoil-free fraction and equation (20) may be re-written:

$$A(T) = A_0 \exp \left(\frac{-3E_R}{2k_B \Theta_D} - \frac{6E_R T}{k_B \Theta_D^2} \right) \quad (23)$$

The gradient of the logarithmic form of this expression (equation 22) was determined for each absorber by calculating the total absorption area and plotting $\ln A$ (normalised) as a function of temperature. For each absorption peak, the normalised area was obtained by evaluating:

$$A = \Gamma_{\text{exp}} \frac{(\text{Background Counts} - \text{Counts at Absorption})}{\text{Background Counts}}$$

where Γ_{exp} was the experimental full width at half height for each absorption line.

To facilitate data comparison, the calculated absorption line areas for each sample were normalised to the base temperature value of 12.5 K. Thus, graphs were actually plotted of $\ln[A(T)/A(12.5K)]$ versus temperature. The experimental results are given in Table 5.2 and the corresponding plots are shown in Figures 5.1(a) - (c).

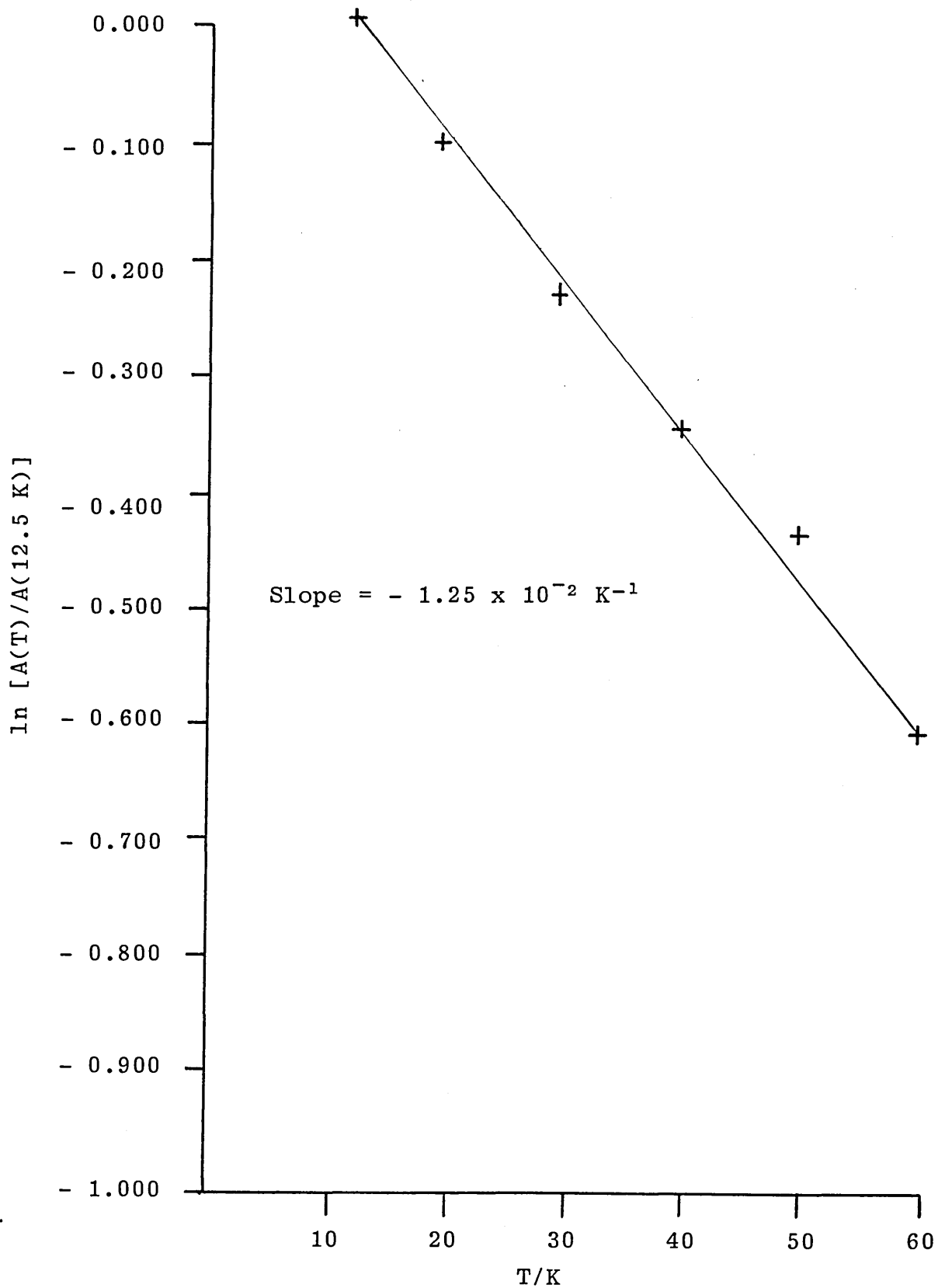


Figure 5.1(a) : Temperature dependence of normalised absorption line area for neat TBTC1

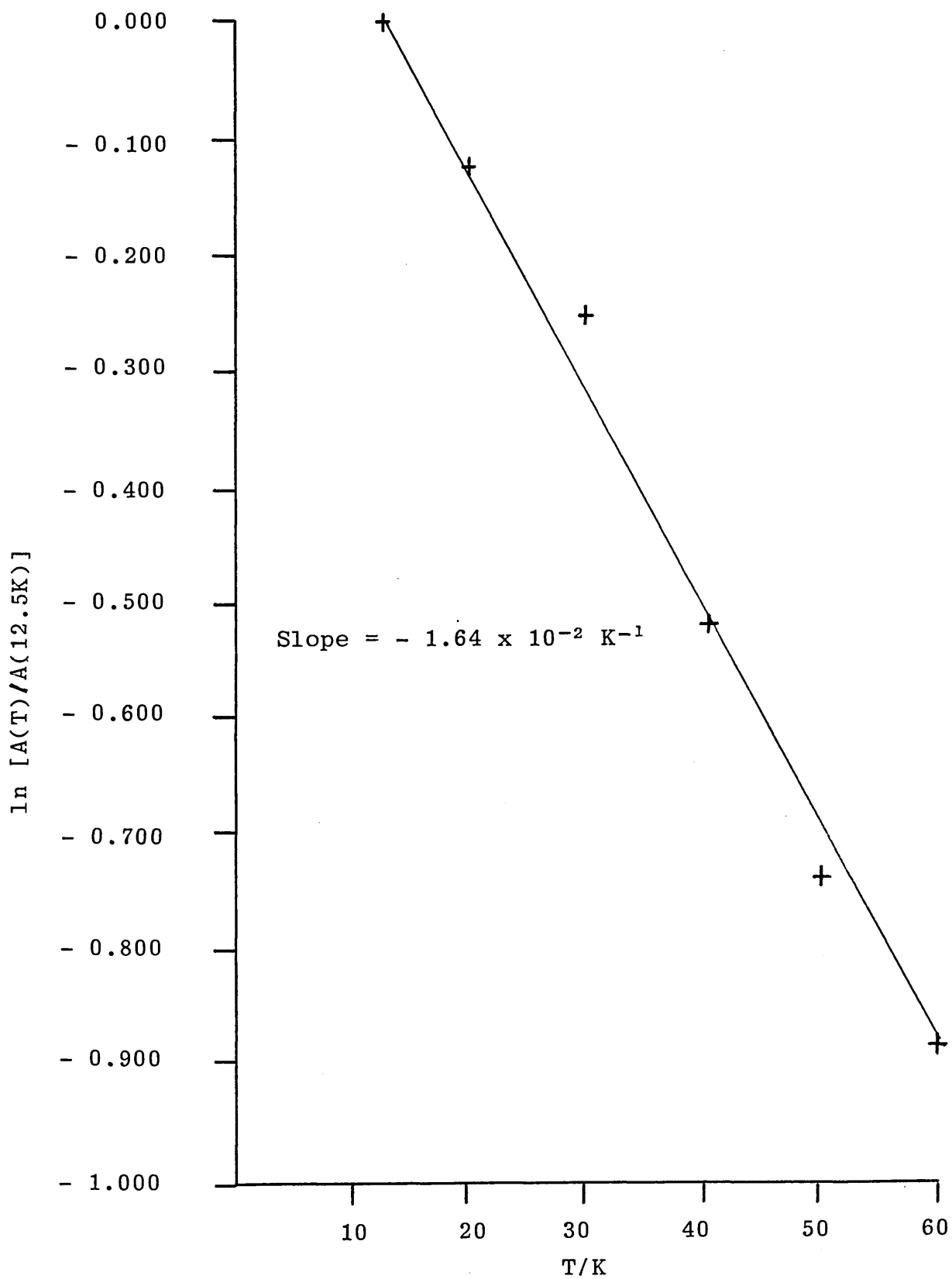


Figure 5.1(b) : Temperature dependence of normalised absorption line area for TBTC1 dispersed in neoprene at 2.5% wt.

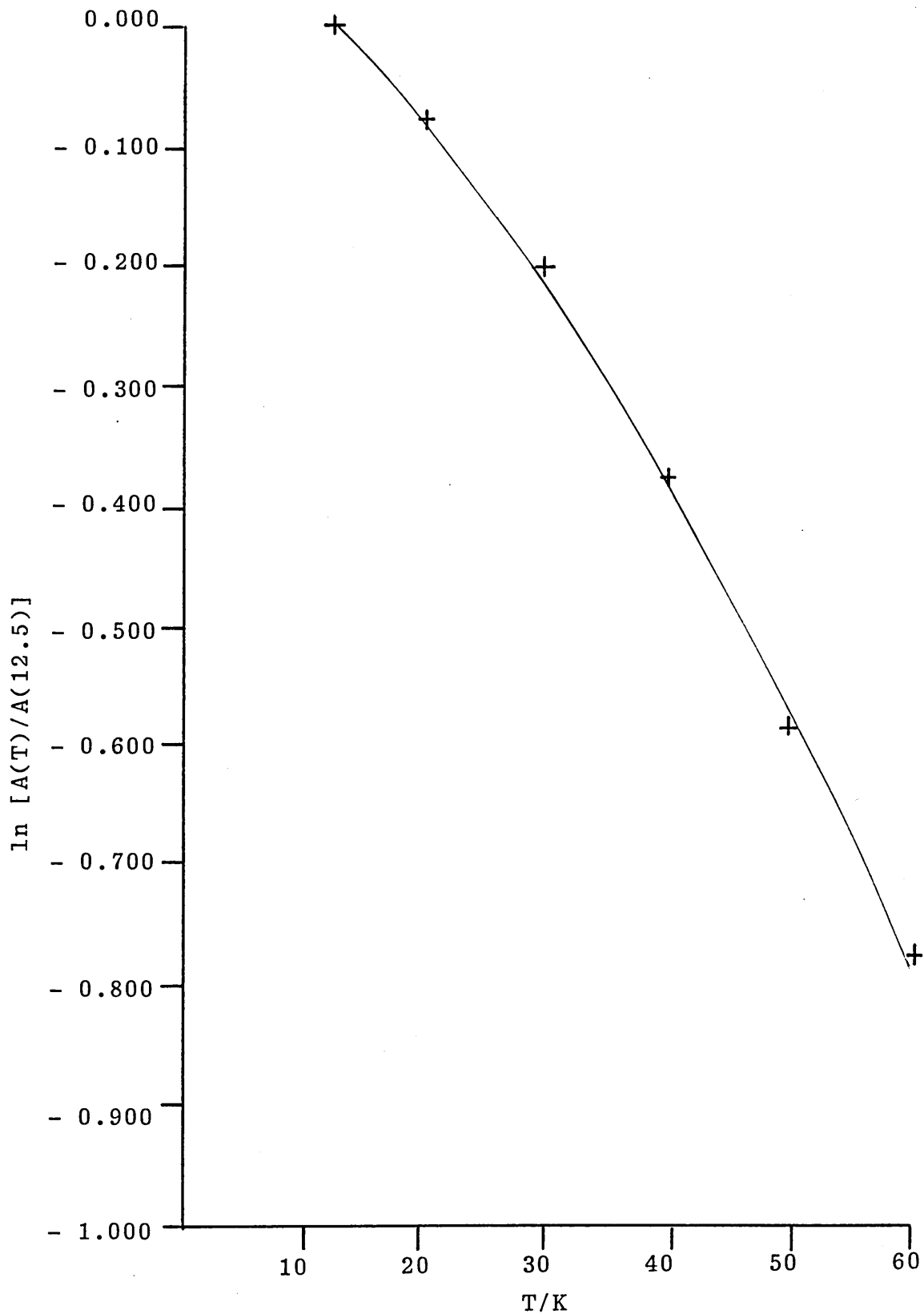


Figure 5.1(c) : Temperature dependence of normalised absorption line area for TBTC1 in an authentic antifouling coating (AFR 3644)

Table 5.2 : Variable temperature Mössbauer absorption
line areas for the TBTCI experiments
recorded over a temperature range of
12.5 - 60 K

T (± 1.0 K)	ln[A(T)/A(12.5 K)]		
	Pure TBTCI	Neoprene	AFR 3644
12.5	0.000	0.000	0.000
20.0	- 0.102	- 0.126	- 0.0786
30.0	- 0.227	- 0.251	- 0.203
40.0	- 0.348	- 0.523	- 0.382
50.0	- 0.443	- 0.736	- 0.588
60.0	- 0.614	- 0.876	- 0.778

5.4 Discussion

The temperature dependence of the recoilless fraction for neat TBTCI and the solvent-cast neoprene system was observed to be practically linear over the experimental temperature range, and it was, therefore, justifiable to apply the Debye model in the high temperature limit to obtain an estimate of θ_D for these materials.

The function lnA(T) for the authentic antifouling elastomer sample was, however, non-linear over the same temperature range and since there were no significant variations in isomer shift (δ) or quadrupole splitting (ΔE_Q) with temperature, this non-linearity was not

Table 5.3 : Mossbauer parameters obtained from the
TBTC1 variable temperature studies

Absorber	δ (± 0.05 mm s^{-1})	ΔE_Q (± 0.05 mm s^{-1})	Γ (± 0.05 mm s^{-1})	ρ^a (± 0.05)
Pure TBTC1	1.54	3.44	0.89	2.23
Neoprene System	1.47	2.97	1.11	2.02
AFR 3644	1.40	2.80	0.98	2.00

a ρ is the ratio $\Delta E_Q/\delta$ (Section 4.2). For $\rho > 2.1$, pentacoordination at the tin atom can be assumed. Values less than 2.1 indicate four-coordination.

See R. Herber, H. A. Stockler and W. T. Reichle, J. Chem. Phys., 42, 2447 (1965).

considered to be the result of structural changes in the TBTC1 molecule (Table 5.3). To explain the deviation from non-linearity, it was necessary to consider the apparently anharmonic nature of the potential in which the tin atoms were vibrating. In the antifouling elastomer such vibrational anharmonicity was considered to be the likely result of either coordinative interactions between TBTC1 molecules and the chlorine sites of the polymer backbone and/or bonding interactions between TBTC1 and the highly abundant, surface active carbon black particles. The temperature dependence of $\ln A$ was very marked in this system suggesting a large degree of

vibrational anisotropy.

Boyle et al [2] observed a non-linear temperature dependence for the recoilless fraction of metallic tin in the temperature range θ_D to $4\theta_D$, where θ_D for tin is 142 K. They demonstrated that the non-linearity was due to anharmonicity in the $\langle X^2 \rangle$ of the tin atom. The effect of thermal expansion on the Debye-Waller factor, W , was considered by Zener and Belinsky [3] and it was shown that:

$$2W \approx \frac{3E_0^2 T}{Me^2 k \theta_D^2} \left[1 + \frac{2V\beta}{3RK} \left(T - \frac{3}{8} \theta_D \right) \right] \quad (24)$$

where R is the gas constant, K is the isothermal compressibility, β is the high temperature volume expansion coefficient and V is the molar volume. The recoilless fraction, f , is related to the Debye-Waller factor by the expression:

$$f = \exp(-2W) \quad (25)$$

and it was therefore possible to fit the experimental results to an equation of the form:

$$\ln A = K - AT - BT^2 \quad (26)$$

where the quadratic term takes into account vibrational anharmonicity. It was then possible to apply Newton's Approximation:

$$(\theta_D)_{n+1} = (\theta_D)_n - F[(\theta_D)]/F'[(\theta_D)] \quad (27)$$

where:

$$F[(\theta_D)] = \frac{3B\theta_D^3}{8} + A\theta_D^2 - \frac{3E_0}{Mc^2k_B} \quad (28)$$

$$\text{and } F'[(\theta_D)] = \frac{9B\theta_D^2}{8} + 2A\theta_D \quad (29)$$

to evaluate an estimate of θ_D for each experiment. The final values for the parameters K, A, B and θ_D are given in Table 5.4.

The small magnitude of the B coefficient in the fit for neat TBTC1 indicates the linearity of the function $\ln A(T)$ for this experiment. Consequently, the data were refitted according to the linear relationship:

$$\ln A(T) = \frac{-3E_R}{2k_B\theta_D} - \frac{6E_R T}{k_B\theta_D^2} \quad (30)$$

as predicted by the Debye model in the high temperature limit. Linear regression analysis of the data yielded an equation of slope $d\ln(A)/dT = -1.25 \times 10^{-2}$ which, when substituted into equation (22) and taking M_{eff} as the relative molecular mass of TBTC1, produced a Debye temperature of 72.4 K. This was in excellent agreement with the value predicted by the anharmonic oscillator model used previously. Thus, the Debye model, in the high temperature limit, appeared to predict adequately the lattice vibrational behaviour of neat TBTC1 and it was considered justifiable to apply equation (20) to a

Table 5.4 : Parameters derived from fitting $\ln A = K - AT - BT^2$ to experimental data in the range 12.5 - 60 K, and calculated values of recoilless fraction at 80 K

Absorber	K	ΔK ($\times 10^2$)	A ($\times 10^2$ K)	ΔA ($\times 10^2$ K)	B ($\times 10^5$ K ²)	ΔB ($\times 10^5$ K ²)	θ_D (K)	$\Delta\theta_D$ (K)	f ($M_{eff} = 325.49u$)	Δf
Neat TBTCI	0.15	5.5	1.24	0.35	- 0.048	4.79	72.7	10.3	0.30	0.09
Solvent-cast Neoprene	0.24	7.99	1.81	0.51	1.48	6.92	59.5	8.4	0.17	0.08
AFR 3644	0.11	2.87	0.68	0.18	14.26	2.53	77.5	13.4	0.34	0.11

calculation of the recoil-free fraction at the commonly adopted experimental temperature of 80 K. As the variable temperature studies were conducted over the range 12.5 - 60 K, it had to be assumed that linearity was maintained up to 80 K.

Since the recoil energy, E_R , may be expressed as $E_\gamma^2/2M_{\text{eff}}c^2$, equation (20) may be re-written:

$$f(T) = \exp \left[\frac{-3E_\gamma^2}{2M_{\text{eff}}c^2k_B} \left(\frac{1}{2\theta_D} + \frac{2T}{\theta_D^2} \right) \right] \quad (31)$$

where the effective vibrating mass, M_{eff} , must, at this stage, be assumed to equal the relative molecular mass of TBTC1.

Thus, for $\theta_D = 72.4$ K, $E_\gamma = 23.875$ keV, $M_{\text{eff}} = 325.49$ u and $T = 80$ K,

$$f(80K) = \exp \left[\frac{-3(23.875 \times 10^3)^2 \times 1.602 \times 10^{-19}}{2 \times 325.49 \times 931.5 \times 10^6 \times 1.381 \times 10^{-23}} \cdot \left(\frac{1}{2 \times 72.4} + \frac{2 \times 80}{(72.4)^2} \right) \right]$$

$$f(80K) = \exp (- 32.71 \times 0.037)$$

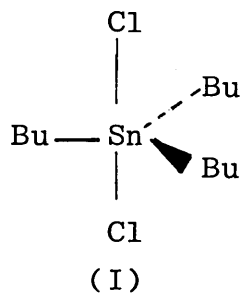
$$f(80K) = \exp (-1.21)$$

$$\therefore \underline{f(80K) = 0.30}$$

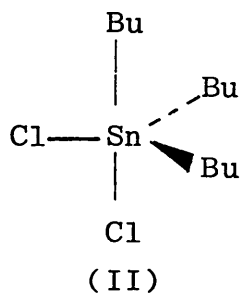
5.5 Conclusions

Variable temperature studies of TBTCl in three different systems have revealed that:

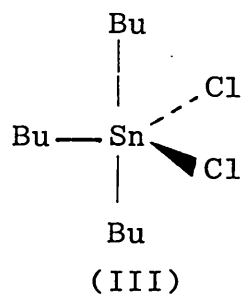
- (a) in the pure state, in the range 12.5 - 60 K, TBTCl molecules autoassociate via chlorine bridging bonds to produce pentacoordinate tin moieties. The absence of any line broadening in the Mössbauer spectra suggests that this auto-association leads to either quite long-chain polymeric structures in which the terminal groups (ie four coordinate tin moieties) do not make a significant contribution to the spectral envelope or, the TBTCl moieties have paired up to produce dimeric structures based on the cis- or mer-pentacoordinate geometries. The structures to be considered can be readily distinguished by comparing the magnitude of the observed quadrupole splitting with those obtained from partial quadrupole splitting (p.q.s.) calculations using the additive model proposed by Bancroft et al for the five-coordinate structures given below [4]:



trans-



cis-



mer-

The derived expression for $\Delta E_{Q(I)}$, $\Delta E_{Q(II)}$ and $\Delta E_{Q(III)}$ are:

$$\Delta E_{Q(I)} = 2[Cl]^{tba} + 2[Cl]^{tba} - 3[Bu]^{tbe} \quad (32)$$

$$\Delta E_{Q(II)} \approx \frac{2[Bu]^{tba} - 8[Bu]^{tbe} + 2[Cl]^{tba} + 5[Cl]^{tbe}}{\sqrt{13}} \quad (33)$$

$$\Delta E_{Q(III)} \approx \frac{-8[Bu]^{tba} - [Bu]^{tbe} + 7[Cl]^{tbe}}{\sqrt{7}} \quad (34)$$

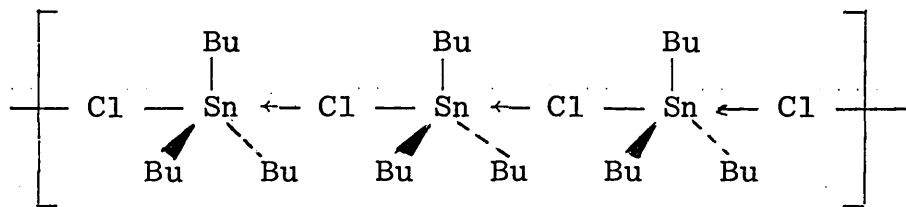
where:

$$\begin{aligned} [Bu]^{tbe} (\text{trigonal-bipyramidal-equatorial}) &= - 1.13 \text{ mm s}^{-1} \\ [Bu]^{tba} (\text{trigonal-bipyramidal-apical}) &= - 0.94 \text{ mm s}^{-1} \\ [Cl]^{tbe} (\text{trigonal-bipyramidal-equatorial}) &= + 0.20 \text{ mm s}^{-1} \\ [Cl]^{tba} (\text{trigonal-bipyramidal-apical}) &= 0.00 \text{ mm s}^{-1} \end{aligned}$$

Thus:

$$\begin{aligned} \Delta E_{Q(I)} &= 3.39 \text{ mm s}^{-1} \\ \Delta E_{Q(II)} &= 2.26 \text{ mm s}^{-1} \\ \Delta E_{Q(III)} &= 3.80 \text{ mm s}^{-1} \end{aligned}$$

Clearly, $\Delta E_{Q(I)}$ corresponding to the trans-trigonal bipyramidal structure is in closest agreement with the experimentally measured value of 3.44 mm s^{-1} and this would suggest that at temperatures below 60K, TBTC1 molecules autoassociate to form polymer structures containing linear Cl—Sn—Cl bridging bonds:



$$\Delta E_Q(\text{observed}) = 3.44 \pm 0.05 \text{ mm s}^{-1}, \text{ p.q.s.}$$

$$\Delta E_Q(\text{calc}) = 3.39 \text{ mm s}^{-1}$$

Within this polymer structure, the linear temperature dependence of $\ln A$ indicates that the tin atoms are able to vibrate isotropically about their mean positions. The resultant increase in effective vibrating mass is consistent with observed high value of $f(80\text{K})$.

- (b) In the solvent-cast neoprene experiment, the variable temperature data, when fitted to the anharmonic oscillator model (equation 26), demonstrated a very small anharmonic, B , term which was well within the error limits (ΔB) associated with this fit. The temperature dependence of $\ln A$ was, therefore, regarded as a linear function in the temperature range studied. The substantially reduced quadrupole splitting parameter (Table 5.3) relative to the pure compound, suggests that the associated structure described previously is largely broken down by dilution in the neoprene matrix, The ratio,

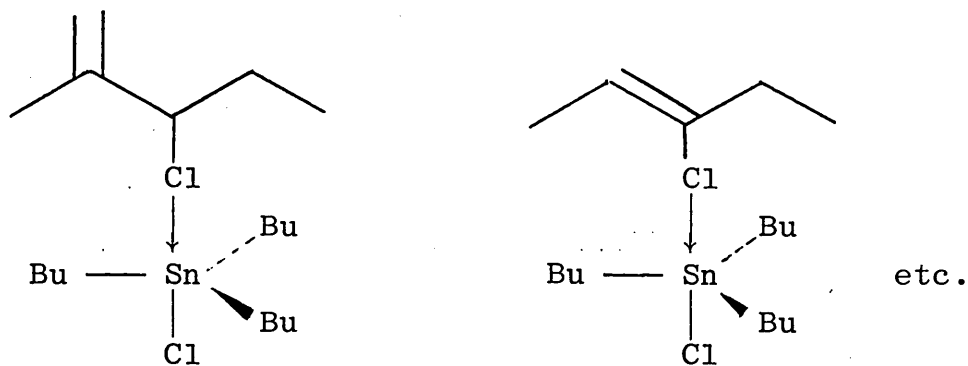
$\rho = 2.02$, indicates that the TBTC1 now exists as a four coordinate compound and, since its vibrational behaviour is apparently harmonic, the evidence also indicates that TBTC1 has been dispersed as discrete tetrahedral molecules in the polymer medium. The reduced value of the Debye temperature and the recoilless fraction (Table 5.4) indicate a significant rise in the mean square vibrational amplitude of the tin atom, which would be consistent with the enhanced vibrational freedom possessed by a non-associated form of TBTC1.

- (c) In the antifouling coating formulation, the ratio, $\rho = 2.00$, suggests that the tin nuclei exist in four-coordinate geometries and the TBTC1 molecules must, therefore, be present as discrete moieties in this matrix. Reference to Table 5.4, however, reveals that the change in coordination from five to four has not been accompanied by an expected decrease in recoilless fraction, f . Indeed the calculated value of $f(80K) = 0.34$ is typical of the five-coordinate geometry exhibited by neat TBTC1 at this temperature. Therefore, it can only be assumed that although the TBTC1 molecules do exist as four-coordinate structures, each moiety is under the influence of some constraining force(s) that is effectively restricting the vibrational freedom of the tin

nuclei. These constraints are evident in the non-linear temperature dependence of $\ln A$ which indicates the nuclei are vibrating within an anharmonic potential.

One possible explanation for the anomalously high f -value and its pronounced non-linear variation with temperature (Table 5.4), could be the existence of a moderately strong polymer-organotin interaction. This type of association was not evident in the solvent-cast neoprene experiment. However, the dispersion of TBTC1 by solvent casting was not carried out under the elevated temperature and pressure conditions employed in the usual curing process.

The small ρ value indicates that the four-coordinate geometry of the TBTC1 moiety is preserved during this interaction, but the forces involved are clearly sufficiently binding to substantially reduce the vibrational freedom of the nucleus. In the light of this information, therefore, structures based on autoassociation into polymers or dimers, as well as those involved coordination of the tin atoms with available chlorine sites on the polymer chains must be excluded, eg:



An alternative explanation involves interaction of the organotin with the carbon-black filler abundant in coating formulation. Yurchenko et al [5] in their studies of a series of tin(II)-containing transition metal complexes, observed significant increases in the recoilless fractions for these compounds when adsorbed onto surface active materials such as silica (SiO_2), alumina (Al_2O_3) and magnesia (MgO). They postulated the existence of strong chemical bonds between the complexes and the surface active groups such that each molecule was effectively "anchored" into position on the substrate.

It is possible that similar surface reactions occur in the elastomer formulation between the organotin and the carbon-black particles. If physical or chemisorptive bonding forces operate, then it is conceivable that this anchoring process is responsible for the high f-value and the anisotropic nature of such bonding has resulted in the non-linearity of the function $\ln A(T)$.

The concept of intercalation was introduced in Section 3.2.4, although the existence of this effect with TBTC1 in carbon-black and synthetic graphite was not demonstrated using x-ray diffractometry. If the elevated temperature and pressure conditions of the polymer curing process are energetically favourable towards expansion of the interplanar spacing in graphite carbon, then in principle, it would be possible for compounds including TBTC1 to become intercalated between the carbon atom layers.

Whether or not this has indeed occurred, remains to be demonstrated. However, it is appreciated that the highly anisotropic nature of the bonding [6] between host and guest species would be consistent with a non-linear temperature dependence of $\ln A$.

Although these variable temperature studies have revealed additional bonding interactions between TBTC1 and one or more of the coating ingredients, the actual nature of these interactions has not been unambiguously elucidated. It is apparent that whether the interactions are based upon a neoprene/organotin or perhaps a carbon black/organotin association, the four coordinate geometry of the tin nucleus is preserved indicating that for the majority of the TBTC1 there is no coordinative bonding with other ligands in the system. Primary evidence for

this conclusion comes from small ρ -value and the
absence of line broadening due to different tin sites.

5.6 References

1. See for example, N. N. Greenwood and T. C. Gibb, "Mössbauer Spectroscopy", Chapman and Hall, (1971).
2. A. J. F. Boyle, D. St. Burbury, C. Edwards and H. E. Hall, Proc. Phys. Soc. 77, 129 (1960).
3. C. Zener and S. Bilinsky, Phys. Rev., 50, 101 (1936).
4. G. M. Bancroft, V. G. Kumar Das, Tsun K. Sham and M. G. Clark, J. Chem. Soc., Dalton, 643-654 (1976).
5. E. N. Yurchenko, V. I. Kuznetsov and E. Burgina, Theor. Exp. Chem., 21, 186-192 (1985).
6. R. H. Herber and H. Eckert, in "Chemical Mössbauer Spectroscopy", (ed) R. H. Herber, 133-175 (1984).

CHAPTER SIX : THE EFFECTS OF ORGANOTIN TOXICANTS ON

THE CURING OF NEOPRENE-BASED ANTIFOULING

ELASTOMERS

6.1 INTRODUCTION

6.2 EXPERIMENTAL

6.2.1 Torque Rheometry

6.2.2 Results

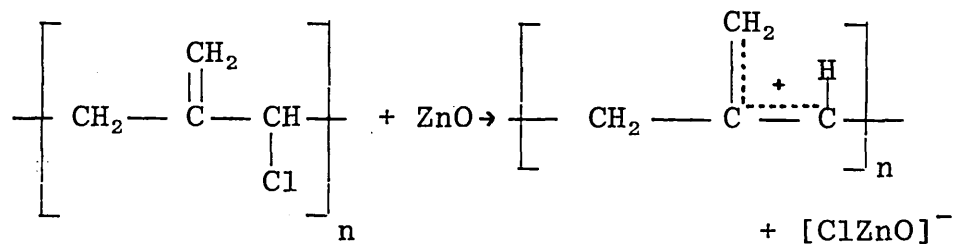
6.3 DISCUSSION AND CONCLUSIONS

6.4 REFERENCES

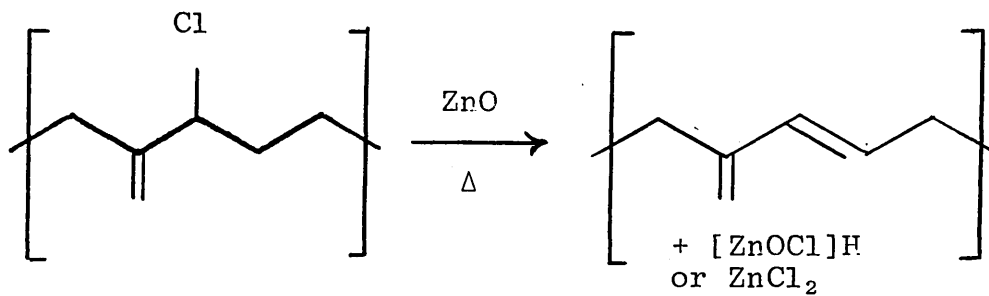
CHAPTER 6 : THE EFFECTS OF ORGANOTIN TOXICANTS ON THE
CURING OF NEOPRENE-BASED ANTIFOULING
ELASTOMERS

6.1 Introduction

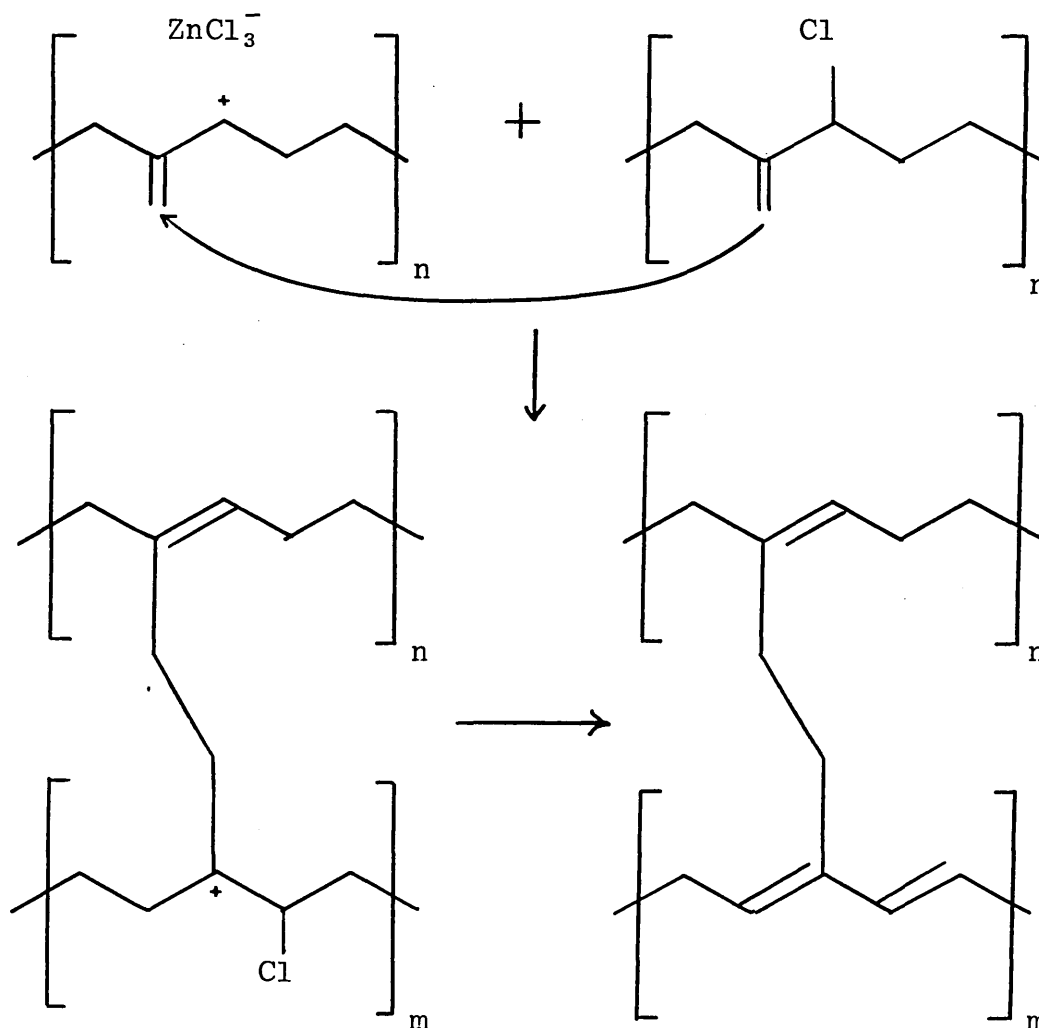
The crosslinking system employed in curing the basic neoprene formulation given in Section 3.1 (Table 3.1) consists of a combination between zinc oxide, calcined magnesium oxide and the organic accelerator tetramethylthiuram disulphide (TMTD). Although the chemistry behind the crosslinking reaction is still not fully understood, it has been postulated that the initial step in zinc oxide crosslinking is the formation of an allylic carbocation by the reaction of the allylic chloride moiety with the zinc species [1]:



In a similar study of zinc oxide crosslinking, Vukov has suggested that the curing mechanism involves initial dehydrochlorination to produce diene structures and zinc oxychloride or zinc chloride as the Lewis acid catalysts required for the crosslinking reaction [2]:



Crosslinking is then considered to proceed via a cationically induced oligomerization reaction to produce carbon-carbon bonds in a manner similar to that originally proposed by Paldwin et al [3]:



Kuntz et al also demonstrated that the rate of the crosslinking reaction in zinc oxide cured chlorobutyl rubber was increased by a factor of three following the addition of a small amount of stearic acid [1]. The important role played by this material in the kinetics of the curing processes is thought to arise from its ability to solubilize the zinc species in the elastomer by converting it to zinc stearate. The formation of elastomer-soluble zinc mercaptide species such as zinc bis(dimethyldithiocarbamate) in TMTD accelerated systems is also well recognised [4].

It is clear, then, that any side reactions that interfere with the formation of these solubilized forms of zinc must have some effect on the curing kinetics of neoprene crosslinking.

The aims of the following experiments were to demonstrate the effects of the presence of various organotin biocides on the cure characteristics of the basic coating formulation, and also to indicate how some organotins may interfere with the crosslinking reaction by consuming some of the components necessary for the solubilization of zinc in the elastomer matrix.

6.2 Experimental

6.2.1 Torque Rheometry

It is possible to monitor the cure characteristics of a coating formulation by observing the change in viscosity at constant temperature of the mix as a function of time. The principles behind this method of testing can be appreciated from the operation of the most widely used curemeter; the Mooney viscometer.

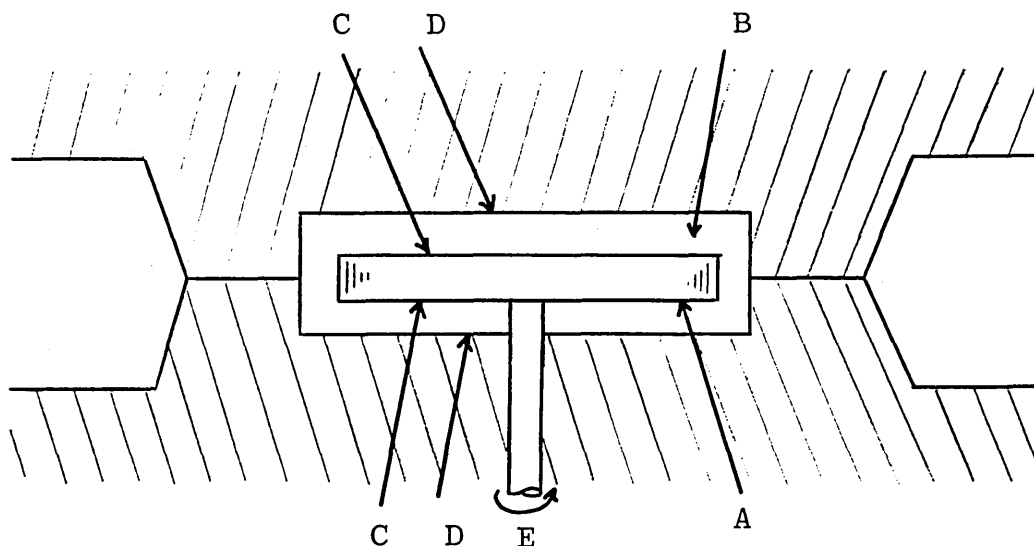


Figure 6.1 : Diagram of the Mooney Viscometer

As the disc-shaped rotor, A, turns inside the cylindrical chamber, B (formed by two mating dies), filled with the coating formulation, shear forces are produced between surfaces C and D. The resulting torque on shaft E gives a measure of the viscosity of the mix and this is plotted on a time-stiffness curve from which it is possible to deduce:

- (i) the minimum stiffness, representing the effective viscosity of the unvulcanized mix;
- (ii) scorch time, given as time taken for a fixed small rise above the minimum stiffness. The scorch time indicates just how long a particular formulation can be held at a given processing temperature (150°C in these experiments) before the onset of curing makes further processing difficult;
- (iii) equilibrium stiffness, representing the elastic modulus of the fully cured elastomer;
- (iv) time to an arbitrary "fractional modulus", of 90% of the equilibrium (or maximum) modulus, and representing a technical cure.

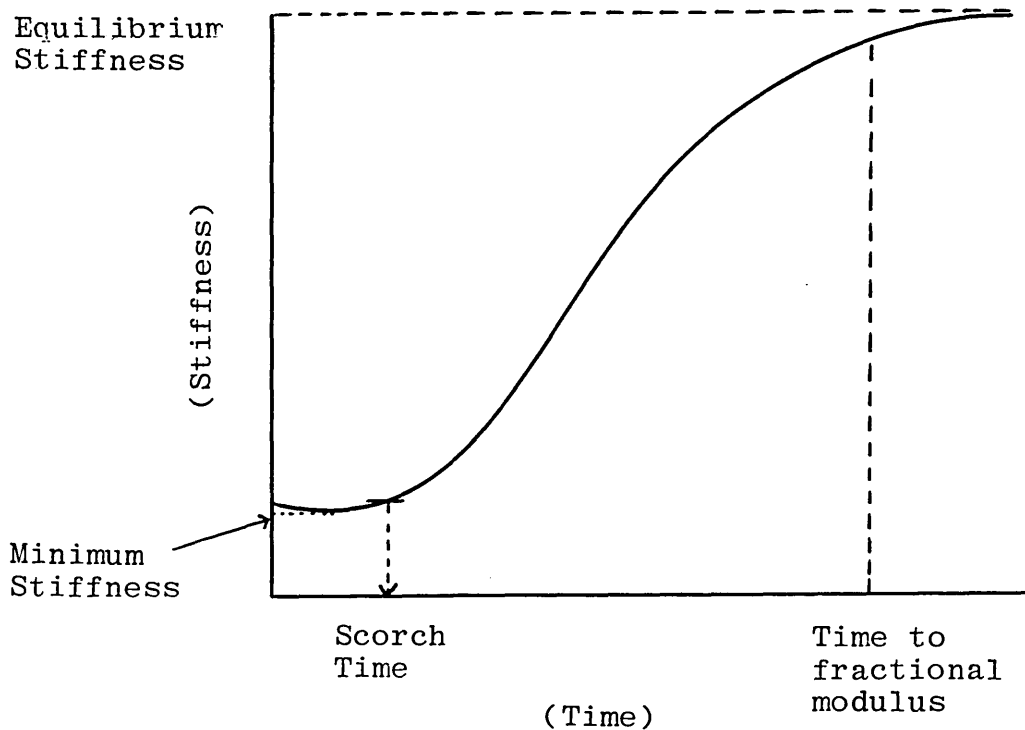


Figure 6.2 : Determination of plasticity, scorch and cure characteristics by curemeter

Torque rheograms were obtained for the following elastomer formulations at a constant temperature of 153°C and over a time-scale of thirty minutes:

<u>Elastomer Code</u>	<u>Containing at 2.5% wt</u>	
<u>AFR:</u>		
2754	No biocide (blank)	
3126	(Bu ₃ Sn) ₂ O	(TBTO)
3647	Bu ₃ SnCl	(TBTC1)
3642	Bu ₃ SnF	(TBTF)
3646	(Ph ₃ Sn) ₂ O	(TPTO)
3644	Ph ₃ SnCl	(TPTC1)
3645	Ph ₃ SnF	(TPTF)
3643	Ph ₃ SnOCCH ₃ O	(TPTAc)

6.2.2 Results

The torque rheograms obtained from the above systems are presented in Figures 6.3(a) to (h).

- (a) In the basic coating formulation containing no biocide, the onset of curing took place after approximately 2.5 minutes and proceeded rapidly to a technical full cure after about 7.5 minutes. The plateau region beyond this time was well-defined, indicating that the crosslinking reactions were effectively complete.

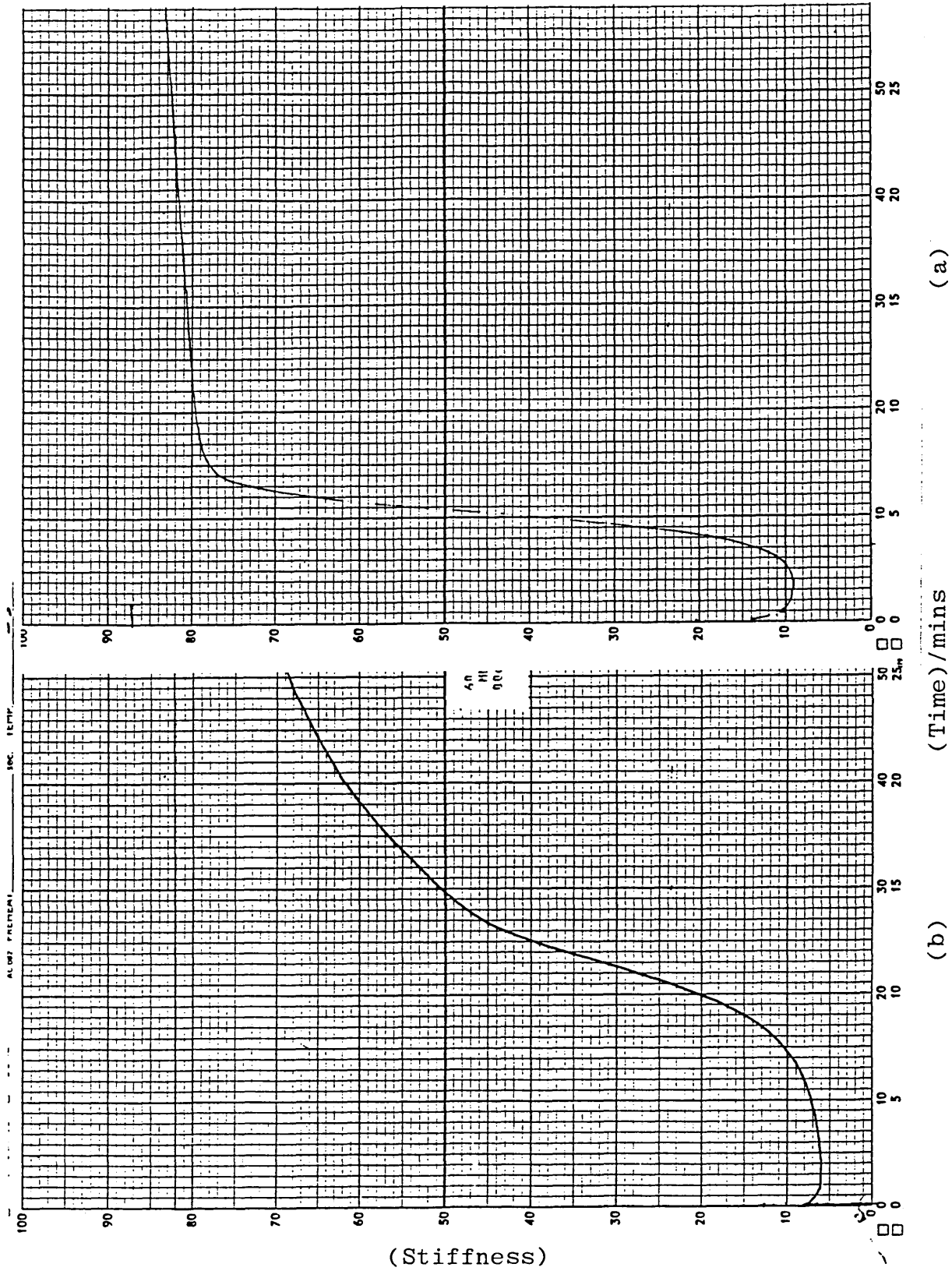


Figure 6.3 : Torque rheograms obtained from antifouling elastomer mix containing (a) no biocide, (b) TBTO at 2.5% by wt.

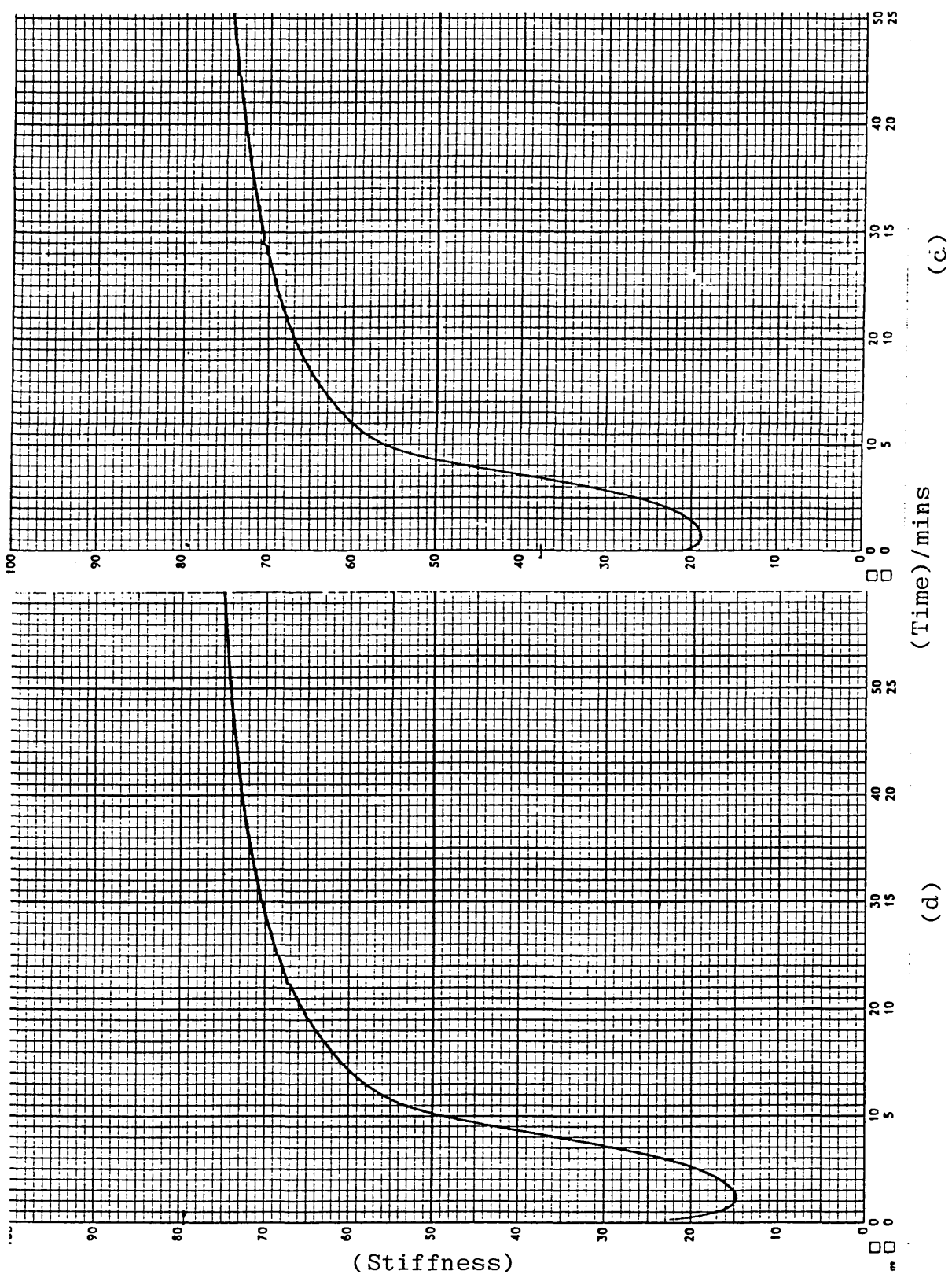


Figure 6.3 : Torque rheograms obtained from antifouling elastomer mix containing (c) TBTF and (d) TBTC1 at 2.5% by wt.

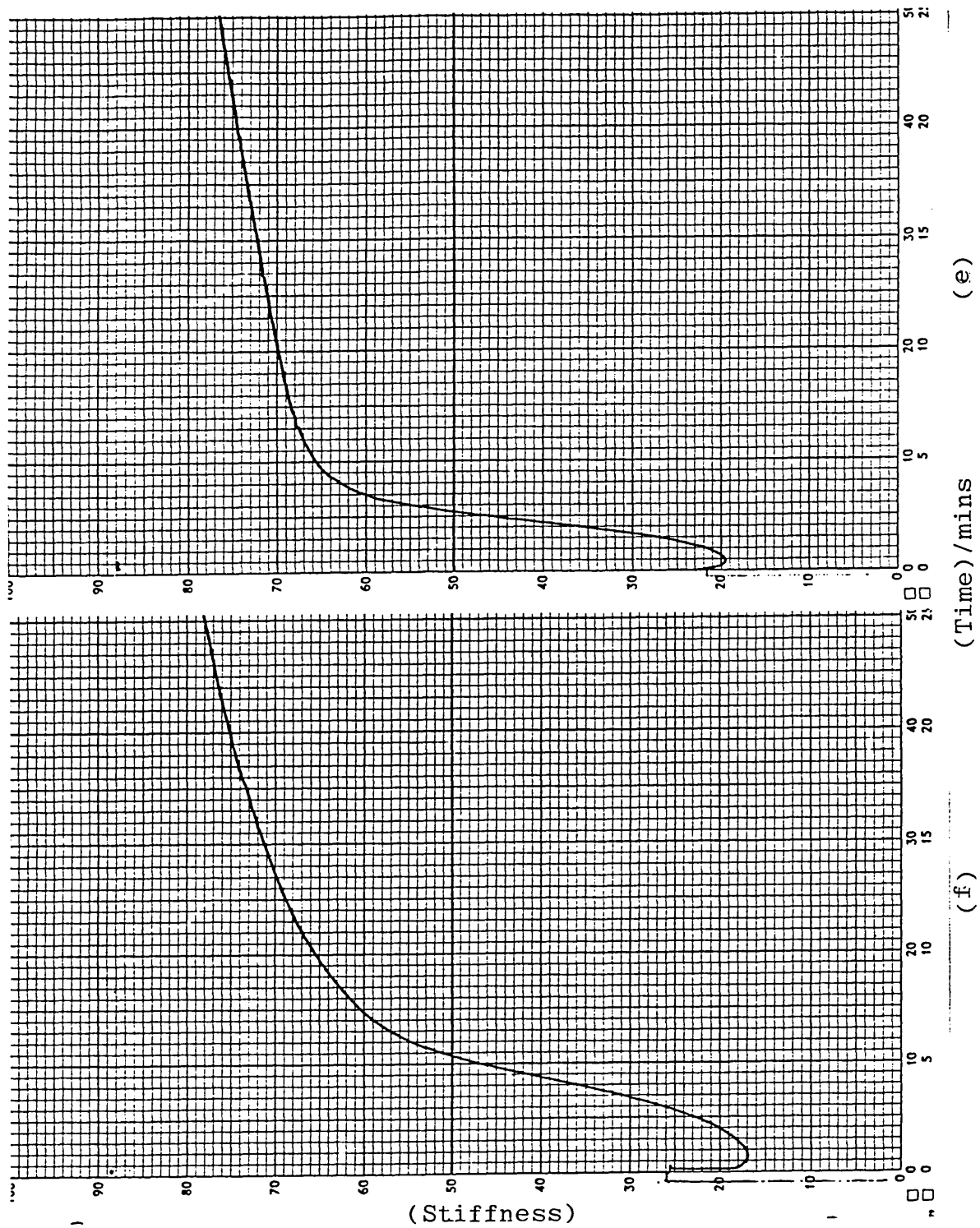


Figure 6.3 : Torque rheograms obtained from antifouling elastomer mix containing (e) TPTCl and (f) TPTO at 2.5% by wt.

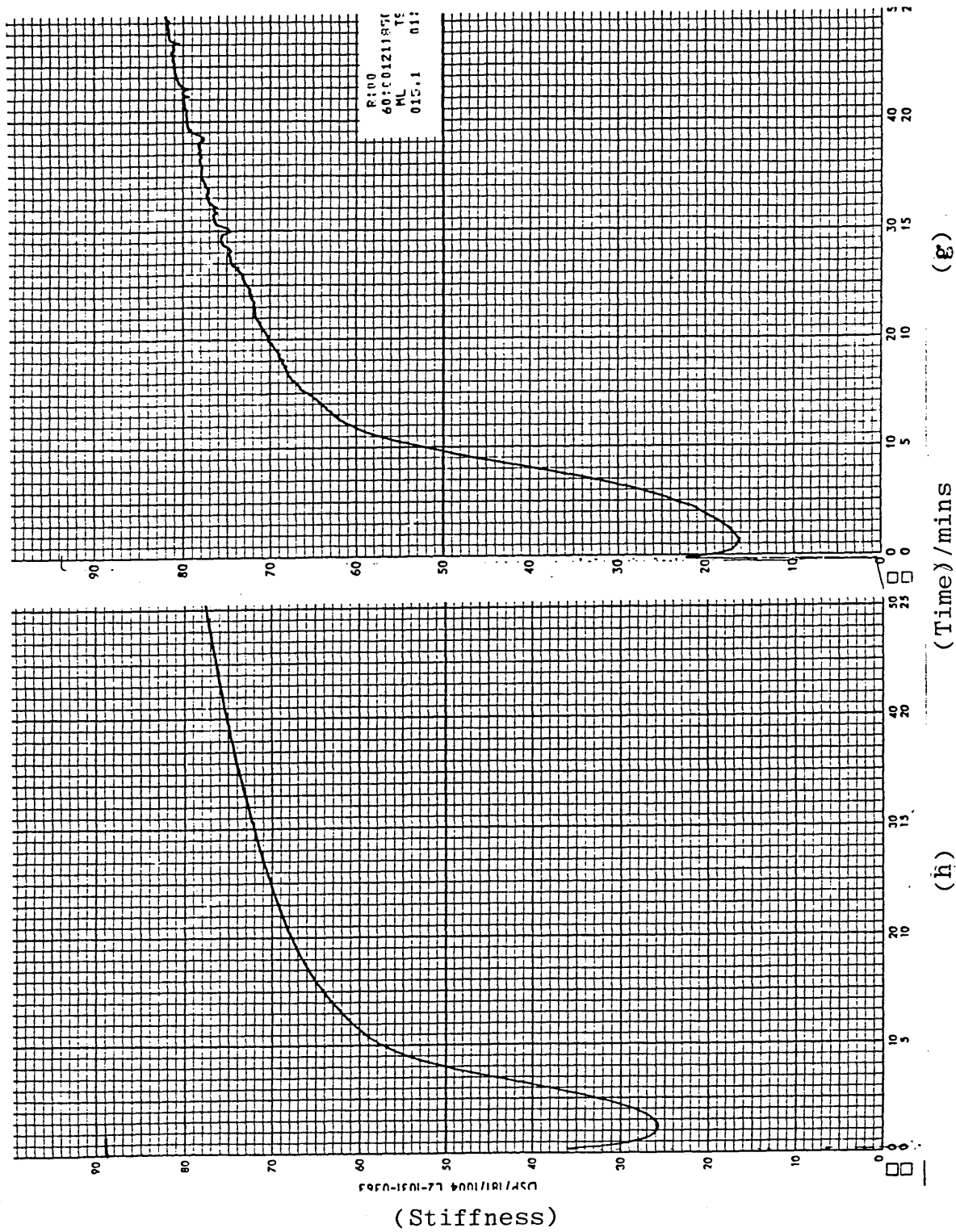


Figure 6.3 : Torque rheograms obtained from antifouling elastomer mix containing (g) TPTAc and (h) TPTF at 2.5% by wt.

- (b) The formulation containing TBTO as the active biocide illustrated markedly different curing characteristics to the basic formulation (a). The scorch time was increased to about 7 minutes and crosslinking occurred at a significantly lower rate, as shown by the reduced slope of the rising curve, and to a lesser degree as indicated by the absence of a plateau in the stiffness versus time behaviour.
- (c)/ In the formulations containing (c) TBTF and
(d) TBTC1, the onset of curing occurred between 1.5 and 2.5 minutes of heating. The cure rate appeared to be similar to that of the biocide-free formulation; however, the plateau region was less sharply defined in both cases.
- (e) The onset of curing in this system containing TPTC1, took place after only 1 minute and proceeded quite rapidly to full cure after about 5 minutes. The curing behaviour changed markedly after a 4-5 minute time period when the stiffness was observed to change only slightly with time.
- (f) The formulation containing TPTO demonstrated a slightly longer scorch time (2.5 minutes) compared with the previous example and less well-defined changes in curing characteristics. A technical full cure was not observed over the 30 minute time-scale of the experiment.

(g)/ The curing behaviour for these formulations
(h) containing (g) TPTAc and (h) TPTF, was similar to that observed for the TPTO-containing system. Both systems were characterized by a short scorch time and a gradual change in stiffness with the build-up of crosslinking density.

6.3 Discussion and Conclusions

From the rheograms presented in Figures 6.3(a) to (h), it is evident that the presence of both tributyltin (TBT) and triphenyltin (TPT) biocides does have an influence on the curing behaviour of the basic formulation AFR 2754. The most dramatic effects are exhibited by the TBTO-containing system in which the organotin has led to an almost doubling of the scorch time and substantial retardation in the rate of cure. The prolonged scorch time suggests that initiation of the curing process is being delayed and in order to rationalize this observation, it is necessary to consider the initial stages of the cationic curing mechanism as proposed by Baldwin et al [3]. The success of the crosslinking reaction, requires the prior formation of a zinc-containing Lewis acid catalyst, ie either zinc oxychloride or zinc dichloride. It is possible that a competing reaction between TBTO and the labile chlorine atoms of the polymer effectively consumes the chlorine atoms available for catalyst formation. The resulting loss of initial reactivity would account for the observed increased scorch time and decreased rate of

crosslinking evident on the rheogram, Figure 6.3(a).

Additional interferences with the initial curing reactions may result from an interaction with stearic acid and/or the organic accelerator TMTD. Reactions of this type would interfere with the solubilization of zinc within the elastomer and thereby limit its availability for catalyst formation. The reaction with stearic acid was demonstrated in Section 3.2.2 where the presence of tributyltin stearate and dibutyltin bis(stearate) could be inferred from the tin-119 NMR spectrum of the appropriate elastomer. In order to determine whether TBTO and TMTD could react together under the polymer curing conditions, both these materials were heated together in equimolar amounts at 150°C for thirty minutes. The resulting product consisted of a brown, non-viscous liquid and a brown solid. These phases (both offensively smelling!) were separated and analysed by infrared, tin-119 NMR and Mössbauer spectroscopies, Figures 6.4 - 6.6.

It is apparent from the fully decoupled tin-119 NMR spectra that there are at least five non-equivalent tin sites distributed between the solid and liquid reaction products, Figure 6.4. The absence of the characteristic asymmetric Sn-O-Sn stretching band at $\approx 770 \text{ cm}^{-1}$ in the infrared spectra suggests that all of the TBTO has been consumed in the reaction with TMTD (Figure 6.5). Indeed, the presence of an infrared band at 360 cm^{-1} in the liquid product is typical of the

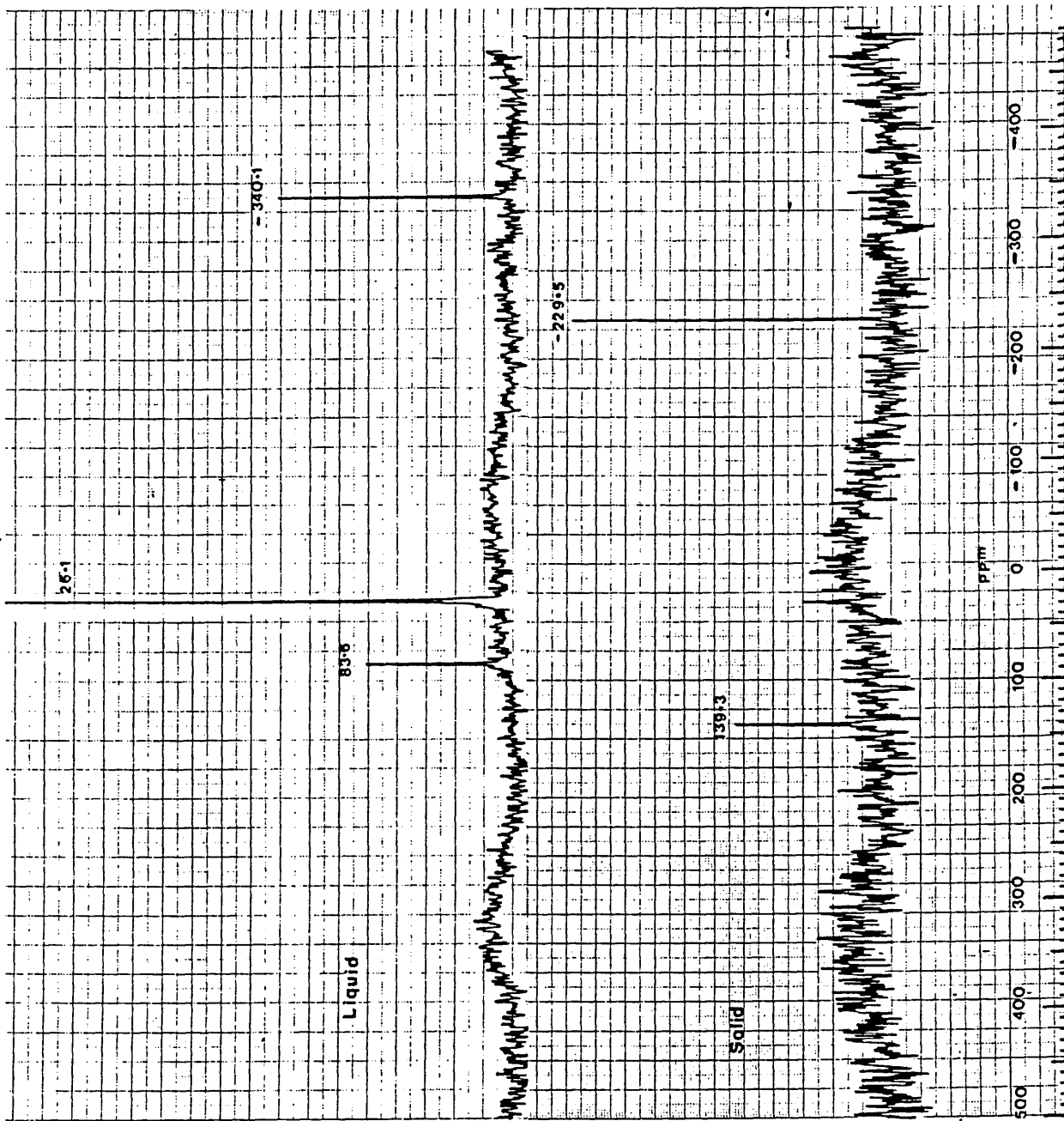


Figure 6.4 : Tin-119 NMR spectra of the residues obtained from the TBTO-TMTD reaction

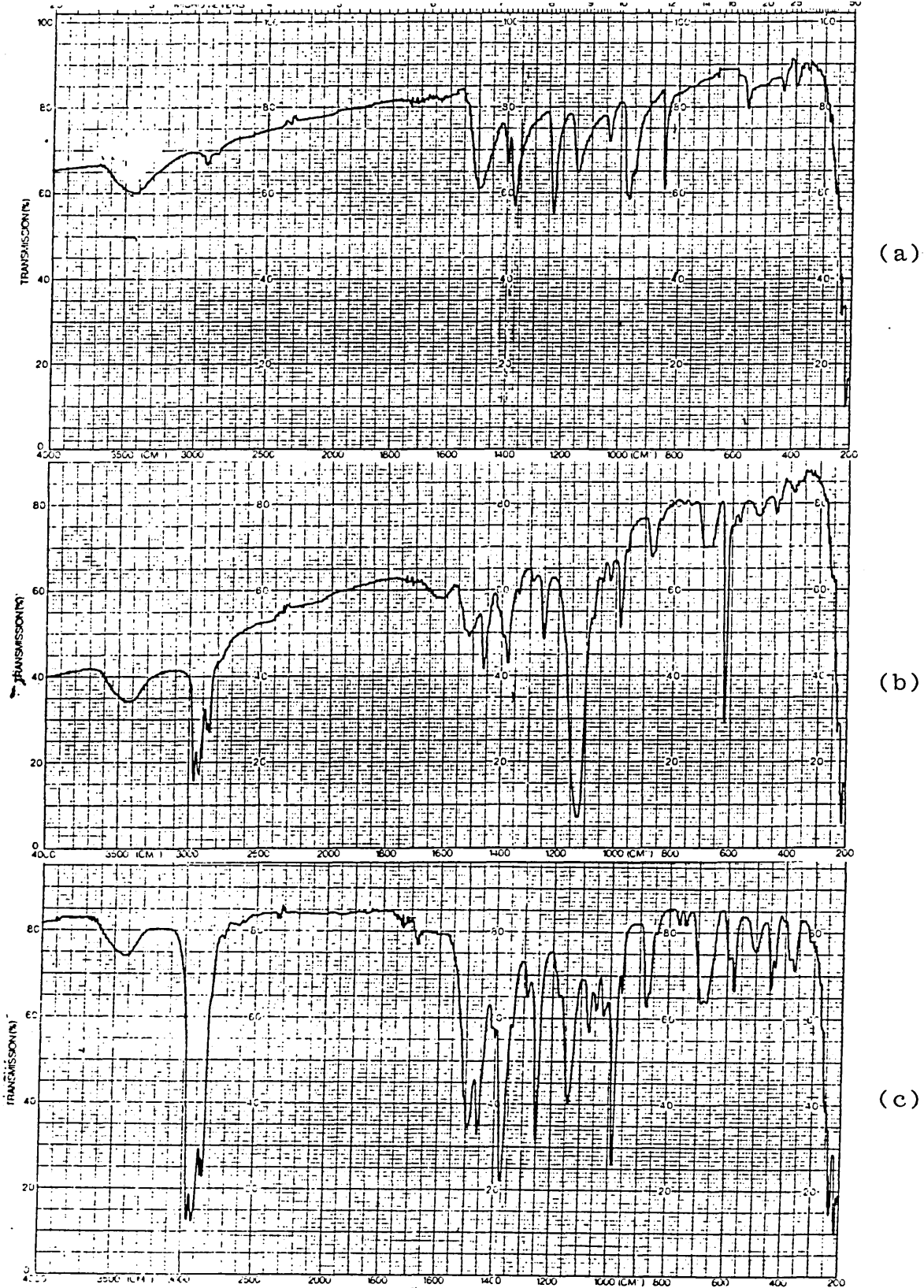


Figure 6.5 : Infrared spectra recorded in the range 200-4000 cm^{-1} of (a) pure TMTD, (b) solid reaction product with TBTO and (c) liquid reaction product with TBTO

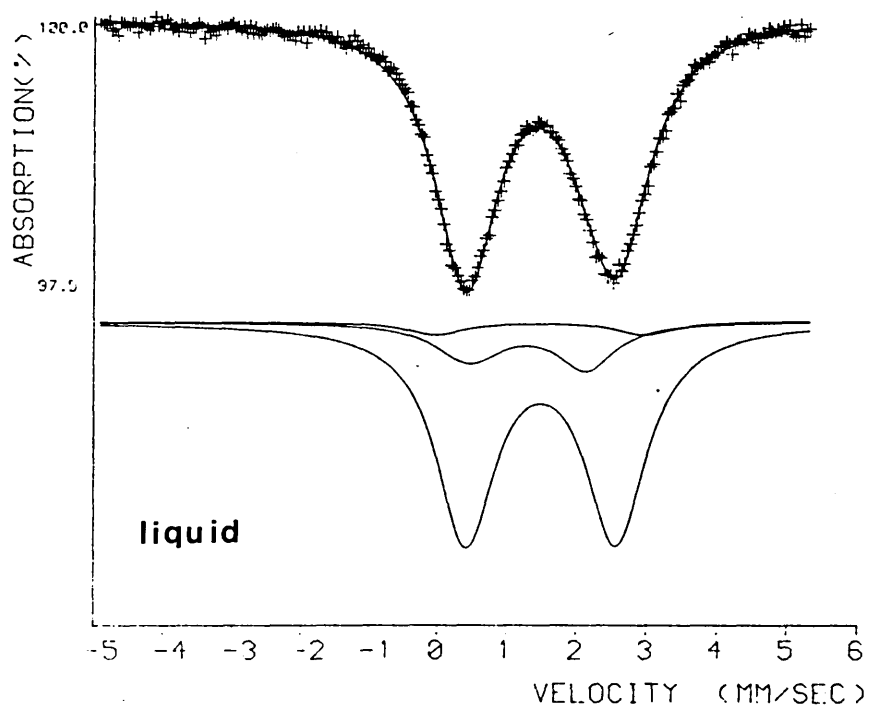
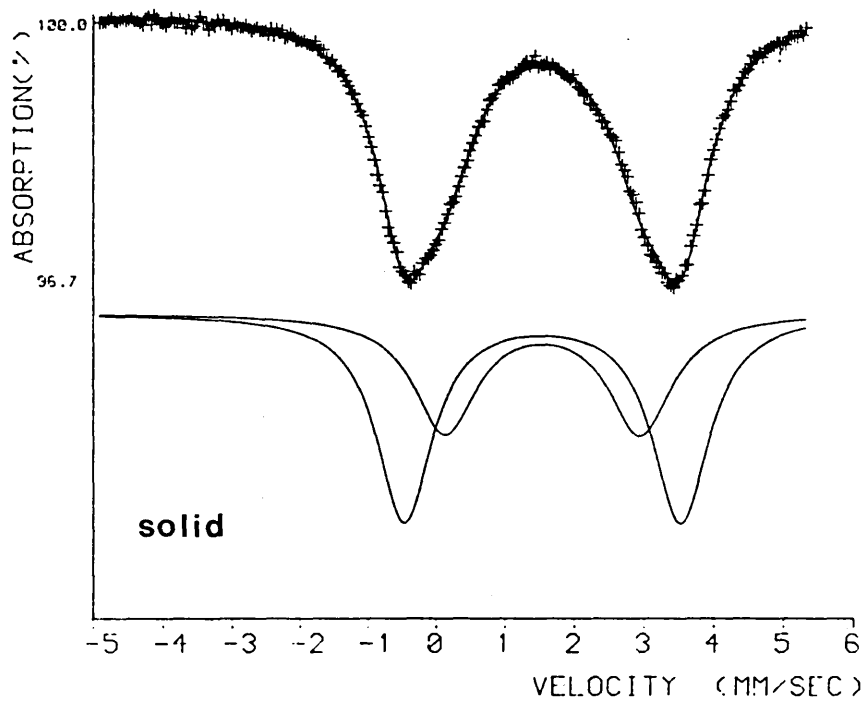
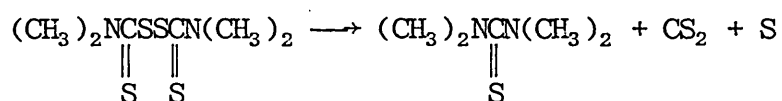


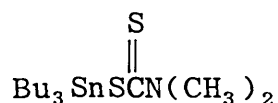
Figure 6.6 : Tin-119 Mössbauer spectra obtained from the solid and liquid residues of the TBTO-TMTD reaction

asymmetric Sn-S-Sn stretching mode, for which the normal range is 360-386 cm⁻¹. The corresponding tin-119 NMR spectrum shows a signal at + 83.7 ppm which suggests that bis(tributyltin) sulphide (TBTS) is present in the liquid phase [$\delta(^{119}\text{Sn})$ for TBTS in CDCl₃ solution is + 84.0 ppm]. The formation of this compound can be explained by examining some of the products formed in the thermal degradation of TMTD. Bateman et al [4] suggest that the decomposition of TMTD under typical curing conditions proceeds according to the reaction:



Since TBTO is known to react readily with carbon disulphide [5] and with thioureas [6] to produce TBTS, the presence of this compound, as indicated in both the infrared and tin-119 NMR spectra, is not unexpected.

The intense tin-119 NMR resonance at + 26.2 ppm in the liquid TBTO-TMTD product was attributed to the presence of tributyltin dimethyldithiocarbamate (TBT.dtc) and this was confirmed by preparing an authentic sample of this compound according to the method of Srivastava and Rastogi [7]:



TBT.dtc

The yellow oil obtained by mixing together equimolar quantities of tributyltin chloride and sodium dimethyldithiocarbamate dihydrate in ethanol, gave rise to a single resonance in the fully decoupled tin-119 NMR spectrum at + 27.3 ppm which is consistent with a four coordinate geometry about the tin atom [8]. The Mössbauer parameters of this compound were $\delta = 1.43 \text{ mm s}^{-1}$ and $\Delta E_Q = 2.24 \text{ mm s}^{-1}$, both in good agreement with those quoted by Hill and Smith [9], $\delta = 1.36 \text{ mm s}^{-1}$ and $\Delta E_Q = 2.23 \text{ mm s}^{-1}$.

In the time available, it was not possible to identify the compounds responsible for the high field tin-119 NMR resonances at - 340.1 ppm and - 229.5 ppm of the liquid and solid phases, respectively. However, the large upfield shifts are typical of those observed for dialkyltin bis(dialkyldithiocarbamate) species [10] in which the tin atom is probably hexacoordinate [11]. Since debutylation under the polymer curing conditions was evident in the chromatographic studies of Section 4.2, the possible formation of dibutyltin bis(dimethyldithiocarbamate) cannot be ruled out.

The Mössbauer data for the solid and liquid products were best computer fitted as two and three unresolved quadrupole doublets respectively. The fitted parameters are given in the table following:

Absorber	δ ± 0.02 (mm s ⁻¹)	ΔE_Q ± 0.02 (mm s ⁻¹)	Γ ± 0.02 (mm s ⁻¹)	ρ ± 0.05	Relative Area $\pm 5\%$
Solid	1.65	3.86	0.96	2.34	61
Residue	1.66	2.72	1.09	1.64	39
Liquid	1.61	2.08	1.02	1.29	79
Residue	1.43	1.63	1.06	1.13	16
	1.59	2.92	0.99	1.84	5

Table 6.1 : Tin-119 Mössbauer parameters obtained from the solid and liquid products of the TBTO-TMTD reaction

According to the ρ -values given in the table, the solid residue contains tin atoms in both four and five (or six) coordinate geometries [12]. The isomer shift and quadrupole splitting are typical of those exhibited by dialkyltin bis(dithiocarbamate) complexes in which the tin atom exists in a trans octahedral geometry. Reference to some of the data presented by Fitzsimmons [11] for analogous dibutyltin compounds supports the proposed formation of dibutyltin bis(dimethyldithiocarbamate):

Organotin	δa ± 0.2 (mm s ⁻¹)	ΔE_Q ± 0.2 (mm s ⁻¹)
Bu ₂ Sn[S ₂ CNPh ₂] ₂	1.72	3.21
Bu ₂ Sn[S ₂ CN(CH ₂ Ph) ₂] ₂	1.69	3.38
Bu ₂ Sn[S ₂ CN(CH ₂) ₄] ₂	1.53	3.06

a Measured relative SnO₂

Table 6.2 : Tin-119 Mössbauer parameters obtained for some dibutyltin dithiocarbamate complexes.
Data taken from reference [11]

The ρ -values calculated for the liquid residue components are indicative of four coordinate moieties and are consistent with the proposed formation of tributyltin dimethyldithiocarbamate, Bu₃SnS₂CNMe₂, and TBTS. The ρ -value for the third tin-component, however, is at variance with the structural implications of the high-field tin-119 NMR resonance at - 340.1 ppm which is more typical of a five or six geometry [10].

The effects of TBTC1 and TBTF on the cure kinetics of neoprene are not as dramatic as those exhibited by TBTO and this could imply that the nature of the interference also involves a competing crosslinking reaction between TBTO and the allylic chlorine moiety to produce ether crosslinks. This process, originally proposed by Kanakkanatt [13] would effectively consume some of the labile chlorine atoms available for zinc Lewis acid catalyst formation needed for efficient carbon-carbon crosslinking.

In the triphenyltin-containing systems, (Figures 6.3(f) to (h)), the scorch time of the basic formulation appears to have been substantially reduced. As the scorch time is related to the rate of initiation of crosslinking which is itself dependent upon the presence of Lewis acid catalysts, it is possible that the degradation products discussed in Section 3.3.1 have a catalytic effect on the curing kinetics. In particular, the degradation products, monophenyltin trichloride and stannic chloride, may initiate a cationic crosslinking reaction via the mechanism mentioned in Section 3.4.

In conclusion, it is clear that the fate of organotin biocides of the type R_3SnX in a typical neoprene coating, is subject to a variety of influences based upon:

- (i) the fundamental chemistry of the polarised Sn-X bond. For example, it may be able to participate in oxidative insertion reactions as illustrated in the formation of tributyltin carbonate from TBTO [5]. Exchange reactions such as the conversion of TBTO to TBTS in the presence of a thiourea are also possible [6] as are reactions involving nucleophilic attack at tin, eg, the formation of tributyltin dimethyldithiocarbamate from TBTC1;
- (ii) the stability of the Sn-C bonds and the susceptibility of the α -carbon atom in the R_3Sn^-

moiety to attack from electrophilic species;

(iii) the ability of the tin atom to expand its coordination number above four and form complexes with neutral and anionic ligands. Suitable ligands in the coating matrix will include: TMTD, tetramethylthiourea, dimethyldithiocarbamate radicals, carboxylate ions, chloride ions and the amine antioxidant "octamine". In this context, therefore, it is likely that the triphenyltin derivatives, being stronger Lewis acids [14] than the tributyltin analogues, will exist as complexed species within the coating matrix. Complex formation will be even more likely for the more strongly accepting diphenyltin and monophenyltin degradation products revealed in the chromatographic studies of Section 3.3.1.

The distribution of organotin products within a coating matrix will be governed by the relative amounts of reactive species present. It is clear that the chloride ion, from the dehydrochlorination reaction, plays a major role in the fate of the organotin biocides since tributyltin chloride was detected in all of the tributyltin-containing elastomers (Section 3.2.2). In addition, the presence of stearic acid has led to the formation of significant amounts of tributyl and dibutyltin stearate in the elastomer matrix.

In the triphenyltin-containing elastomers, the predominant reactions appear to involve scission of the Sn-C bonds leading to extensive degradation of the organotins.

The degradation products, in the form of the proposed complexed moieties, could not be extracted from the coatings for useful tin-119 NMR analysis and this may indicate the existence of a coordinative interaction between the tin species and the chlorine atoms of the polymer chains. Such a process could effectively bind the organotins into the elastomer matrix, thereby reducing their availability for extraction.

The reactive medium provided by a typical antifouling coating formulation, has been shown to lead to extensive chemical and structural modifications of the incorporated organotin biocides. In the triphenyltin-containing coatings, particularly, a range of organic and inorganic tin compounds have been produced and these will undoubtedly possess markedly different biocidal properties to the parent organotin.

6.4 REFERENCES

1. I. Kuntz, R. L. Zapp and R. J. Pancirov, Rubber Chem. and Technol., 57, 814-825 (1984).
2. R. Vukov, Rubber Chem. and Technol., 57, 284-290 (1984).
3. F. P. Baldwin, D. J. Buckley, I. Kuntz and S. B. Robinson, Rubber Plast. Age, 42, 500 (1961).
4. L. Bateman, C. G. Moore, M. Porter and B. Saville in "The Chemistry and Physics of Rubber-like Substances", (ed) L. Bateman, Maclaren and Sons Ltd, London (1963), Chapter 15.
5. A. J. Bloodworth, A. G. Davies and S. C. Vasishtha, J. Chem. Soc. (C), 1309-1313 (1967).
6. R. A. Cardona, E. J. Kupchik and H. E. Hanke, J. Organomet. Chem., 24, 371-374 (1970).
7. T. N. Srivastava and R. B. Rastogi, Indian J. Chem., 16(A), 221-223 (1978).
8. M. Nadvornik, J. Holecek, K. Handlir and A. Lychka, J. Organomet. Chem., 275, 43-51 (1984).
9. R. Hill and P. J. Smith, Int. J. Wood. Preserv., 3(2), 77-82 (1983).
10. A. G. Davies, P. G. Harrison, J. D. Kennedy, T. N. Mitchell, R. J. Puddephatt and W. Mcfarlane, J. Chem. Soc. (C), 1136-1141 (1969).

11. B. W. Fitzsimmons, A. A. Owusu, N. J. Seeley and A. W. Smith, J. Chem. Soc. (A), 935-937 (1970).
12. R. H. Herber, H. A. Stockler and W. T. Reichle, J. Chem. Phys., 42, 2447 (1965).
13. S. V. Kanakkanatt, P. P. Patnode and N. F. Cardarelli, Macromol Reprint, 1, 614-619 (1971).
14. A. G. Davies and P. J. Smith in "Comprehensive Organometallic Chemistry" (eds), G. Wilkinson, F. G.A. Stone and E. W. Abel, Pergamon (1982), Chapter 11.

CHAPTER SEVEN : GENERAL CONCLUSIONS

The initial studies made on a selection of tri-n-butyltin (TBT)-containing elastomers showed that each biocide suffered the same fate upon incorporation into a neoprene-based antifouling coating formulation. Using supportive information obtained by tin-119 nuclear magnetic resonance spectroscopy and gas chromatographic analysis, the structural modifications evident in the tin-119m Mössbauer spectra were attributed to the formation tri-n-butyltin chloride, tri-n-butyltin stearate and smaller amounts of di-n-butyltin di-stearate, during the polymer mixing and curing operations. It was evident from the Mössbauer data that the structural properties of these organotins in the elastomer matrix differ from those of the pure compounds under identical experimental conditions.

The dispersion of a selection of TBT and triphenyltin (TPT) biocides into uncured neoprene by solvent casting, led to marked structural changes being observed for all of the original biocides. The Mössbauer parameters for the TBT compounds were all of similar magnitude, consistent with the presence of single four-coordinate tin moieties within the elastomer matrix. Some line broadening was evident in the bis(tri-n-butyltin)sulphide system which may have indicated the presence of multiple tin sites in this system.

The selection of TPT biocides dispersed in neoprene all suffered extensive chemical breakdown via Sn-C bond cleavage even under the relatively mild conditions of the solvent casting procedure. It was also observed that neoprene films containing 2.5% by weight of (i) monophenyltin trichloride and (ii) stannic chloride were both insoluble in the solvent (dichloromethane) originally used for the casting process. This was taken as evidence for the Lewis acid catalysed formation of cross-links between the polychloroprene chains.

Dispersion into the filler material - carbon-black, was also accompanied by changes in local structure for several TBT compounds. Tri-n-butyltin fluoride proved to be the exception, as the Mössbauer parameters for the dispersed system were identical to those for the pure compound within experimental error. Similar studies with TPT compounds indicated that simple dispersion into carbon-black was not accompanied by any of the structural changes observed for the TBT systems. It was concluded that the TBT compounds were able to undergo chemical reactions with the surface active groups, which have been identified on carbon-black particles, to produce a distribution of organotin moieties. The failure of the TPT systems to undergo similar reactions implies that steric factors may play an important role in the relative reactivity of carbon-black towards organotins. The concept of intercalation, which may again be subject to steric constraints, was also considered but the effect was not demonstrated experimentally.

A series of TPT biocides were shown to suffer extensive chemical breakdown upon incorporation into the anti-fouling formulation. From the identical form of the Mössbauer spectra obtained from these samples, it was concluded that each of the biocides underwent initial conversion to the same triaryltin compound followed by subsequent degradation to yield the same distribution of products in each system. Gas chromatographic analysis of the elastomers following direct alkylation revealed the presence of tri-, di-, monophenyl and inorganic tin compounds as degradation products. None of the phenyltin compounds could be detected in Soxhlett extracted residues by tin-119 NMR spectroscopy and this was thought to indicate the existence of a binding interaction between the tin compounds and one or more of the components in the elastomer formulation.

Spectroscopic and chromatographic analysis of a commercial antifouling elastomer sample (NOFOUL[®]), obtained after 2.5 years exposure to a marine environment showed that the long-term degradation of the original bis(tri-n-butyltin)oxide biocide involved successive debutylation to produce stannic oxide as the ultimate degradation product. A number of degradation pathways involving hydrolytic Sn-C bond cleavage were presented in order to account for the distribution of tin compounds evident in the transmission-mode Mössbauer spectrum and in the gas chromatographic analysis of extracts.

A backscatter-mode spectrum of the marine-exposed surface was characterized by a single emission line at $\approx 0 \text{ mm s}^{-1}$ and this was attributed to the presence of stannic oxide. This surface was then sliced away to a depth of about $\frac{1}{2}$ mm and the sample was re-examined by backscatter Mössbauer spectroscopy. The resulting spectrum was still dominated by an emission at zero velocity, indicating the presence of stannic oxide even at this depth within the sample; however, the presence of organotin compounds could be inferred from the broadening evident in this emission line plus the large asymmetry in background radiation. The poor sensitivity towards the detection of organotins was attributed to their very low surface concentrations and their small recoilless fractions in comparison with that of stannic oxide.

Variable temperature Mössbauer studies of tri-n-butyltin chloride (TBTC1) revealed a strong binding interaction within an authentic antifouling elastomer. In the pure state, partial quadrupole splitting calculations showed that TBTC1, below 60 K, associated to produce a polymeric structure in which chlorine bridging bonds produce a five coordinate geometry about the tin centre. Application of the Debye model of solids to the vibrational behaviour of this polymer, led to a calculated value of the recoilless fraction at 80 K of 0.30. Upon dispersion into uncured neoprene by solvent casting, the recoilless fraction of TBTC1 was observed to fall

from 0.30 to 0.17. Similarly, the ratio of quadrupole splitting to isomer shift (ρ -value) was reduced from 2.33 for the pure compound to 2.02 in the neoprene-dispersed state. It was concluded that, upon dispersion, the five coordinate polymeric structure of the pure compound is broken down to produce discrete four coordinate TBTC1 molecules throughout the polymer matrix. In both the pure and dispersed states, the temperature dependence of the recoilless fraction showed the vibrational freedom of the organotin moiety to be isotropic.

The calculated recoilless fraction at 80 K for TBTC1 in the authentic coating matrix is 0.34 and this is typical of a tin nucleus existing in a five coordinate geometry. The ρ -value, however, of 2.00 is consistent with a four coordinate structure and it was therefore necessary to consider the possible existence of constraining forces which effectively restricted the vibrational freedom of the tin moiety in this matrix. These constraining forces were thought to arise from interactions between the tin and either the base polymer or the carbon-black filler. The anisotropic nature of any chemisorptive bonding on carbon-black particles or the possible formation of an intercalation compound, could account for the observed anharmonic vibrational behaviour of the tin nucleus in the coating system.

The interaction of several TBT and TPT biocides with the curing system of the basic coating formulation was studied by examining the rheology of each mix. All of the biocides had some effect upon the final degree of cure. However, of the TBT compounds, bis(tri-n-butyltin)oxide showed the greatest influence on the cure characteristics of the basic mix. The onset of curing was delayed and this is considered to be the result of (i) interfering reactions between the organotin and the organic accelerator and/or stearic acid, such that the concentration of elastomer-soluble zinc Lewis acid catalyst was lowered, or (ii) a competing cross-linking reaction involving the insertion of ether linkages between the allylic moieties of the polymer backbone.

The TPT compounds appeared to significantly reduce the scorch time of the basic formulation and, considering the extensive chemical breakdown undergone by these organotins, it is considered likely that the formation of monophenyltin moieties and stannic chloride would have a catalytic effect on the initiation of cross-linking.

In conclusion, the TBT biocides appear to undergo conversion during the polymer processing conditions to produce mainly tri-n-butyltin chloride, tri-n-butyltin stearate and smaller amounts of di-n-butyltin distearate irrespective of the nature of the anionic radical originally bound to the TBT moiety. The efficiency of the TBT formulations as antifouling coatings will, therefore, be largely dependent upon

the relative amount of non-toxic diorganotin formation and on the rate of diffusion of the triorganotin compounds through the bulk coating. This latter property will be strongly influenced by the degree of polymer/filler binding which is evident from the variable temperature Mössbauer studies.

The extensive chemical degradation undergone by the TPT biocides indicates that these materials are not suited to dispersion into neoprene-based elastomers under standard processing conditions. The degradation products, including significant amounts of inorganic tin, are essentially non-toxic, and are also strongly bound within the elastomer matrix. As well as the reduction in toxicological properties, low leaching rates are also likely to be a problem with coatings incorporating TPT compounds as biocides.

Areas for future work should include studies into the development of effective antifouling coatings in which the chemical identity of the original biocide is preserved upon incorporation into the matrix. One approach might be to employ a less reactive base elastomer (eg natural or nitrile rubber) employing a different or milder curing process to that used in the neoprene systems. Another approach would be to develop an organometallic elastomer in which different triorganotin moieties (eg tripropyl, tributyl and triphenyl) having a range of biocidal activities towards target organisms, could be leached to provide antifouling protection. Suitable

curing systems would, again, have to be developed in order to avoid the chemical degradation problems evident in the neoprene systems.

Current concern over the harmful effects of triorganotins (TBT compounds in particular) on certain non-target organisms such as shellfish species and phytoplankton, indicates a need for studies into the mode of action of these compounds when exerting their biocidal effects. Mössbauer spectroscopy has been applied to studies in numerous biological systems and it would seem the ideal technique to adopt for the in situ structural analysis of triorganotin biocides in actual organisms. The potential contributions to structure-activity studies could be usefully exploited in the development of more specific biocides and thereby alleviate some of the environmental problems that are the subjects of current legislation and debate.

ACKNOWLEDGEMENTS

The author wishes to express his sincere gratitude and best wishes to his supervisors, Dr J S Brooks and Dr D W Allen, for their helpful guidance and advice during the course of this research. He also acknowledges the financial support given by the Science and Engineering Research Council and the Admiralty Research Establishment (A.R.E.), Portsmouth.

The author would also like to thank Dr J T Gisborne and Mr B C Ochiltree of the collaborating establishment, for the many helpful discussions during my visit to the A.R.E. and for the supply of materials used in this research.

For providing a pleasant working environment and many even more pleasant social environments, the author is grateful to all the staff and research students in the Departments of Chemistry and Applied Physics. In particular, special thanks go to Mr R Smith, Principal Technician in the Department of Applied Physics, for his invaluable assistance with the practical aspects of this work, Mr S K Osborne, Research Technician in the Department of Chemistry, for his resourcefulness and endless patience, and to Miss A Hughes, Secretary in the Department of Applied Physics for converting into legible form the hieroglyphics that made up the original draft of this thesis.

COURSES AND CONFERENCES ATTENDED

1. Conferences

The Royal Society of Chemistry Mössbauer Discussion
Group meetings at:

- (i) University of Oxford, 2-4 July 1984
- (ii) University of East Anglia, 8-10 July 1985
- (iii) University of Nottingham, 7-9 July 1986 where
I presented a paper entitled "Tin-119m
Mössbauer Studies of the Fate of Organotin
Biocides in Marine Antifouling Elastomers".

Courses

- 2. Methods of Surface Analysis - a one day short course
held at Loughborough University of Technology on
8 February 1984.
- 3. Introduction to Mössbauer Spectroscopy - 10 x 2 hour
lectures held at Sheffield City Polytechnic in February
1984.
- 4. Computing lectures held at Sheffield City Polytechnic
in October 1983:
 - (i) Introduction to the IBM 4341 mainframe computer
 - (ii) Programming in BASIC.
- 5. MSc lectures in Applied Microelectronics (17 x 1 hour)
held at Sheffield City Polytechnic in October 1984.



The fate of organotin toxicants in neoprene-based elastomeric marine anti-fouling coatings: ^{119m}Sn Mössbauer and ^{119}Sn n.m.r. spectral studies

David W Allen,* Stephen Bailey,* John S Brooks†

Departments of Chemistry* and Applied Physics†, Sheffield City Polytechnic, Pond Street, Sheffield S1 1WB
and

Brian F Taylor

Department of Chemistry, The University, Sheffield S3 7HF

The need to protect ocean-going vessels, navigational buoys and delicate underwater installations from the effects of marine fouling has led to the development and widespread use of elastomeric coatings incorporating triorganotin toxicants. Typical of these are the neoprene-based coatings of the 'NOFOUL'® variety, containing both bis(tri-*n*-butyl)tin-oxide (TBTO) and -sulphide (TBTS), developed in 1964 by the B F Goodrich Company. More recent formulations omit the use of TBTS since it is more expensive than TBTO and offers no additional biocidal activity.^{1,2} It has been suggested that the TBTO is involved in the elastomer-curing process, undergoing conversion into tributyltin chloride (TBTC1), considered to be the active agent in preventing fouling, being released slowly when the elastomer is immersed in water.³ However, apart from this suggestion, little would seem to be known of the fate of TBTO and other related organotin compounds in such matrices, which also commonly contain many other reactive components, for example stearic acid and sulphur compounds, with which the organotin reagents could combine under the fabrication conditions (150°C, under pressure). In this

Communication, studies are described of the fate of various organotin toxicants, when incorporated into cured neoprene matrices, using ^{119m}Sn Mössbauer and ^{119}Sn n.m.r. spectroscopy.

Various organotin toxicants, TBTO, tributyltin stearate (TBTSt), bis(tributyltin) carbonate (TBTCO) and TBTC1 were incorporated into an anti-fouling rubber composition at ca 2.6 per cent *w/w*, respectively and the materials cured at 150°C under standard conditions. The resulting rubber sheets were examined initially by ^{119m}Sn Mössbauer spectroscopy enabling investigation of the environment of the tin atom to be studied *in situ* without further chemical treatment. The Mössbauer spectra were recorded using a constant acceleration spectrometer with a room temperature, 15 mCi barium stannate source. Samples of elastomer, and appropriate reference compounds, were held in perspex discs and cooled to 80 K using a continuous flow liquid nitrogen cryostat with helium exchange gas. The Mössbauer parameters for the various samples are presented in the Table, the quoted experimental errors of $\pm 0.02 \text{ mm sec}^{-1}$ (for pure compounds) and $\pm 0.05 \text{ mm sec}^{-1}$ (for the elastomers) in

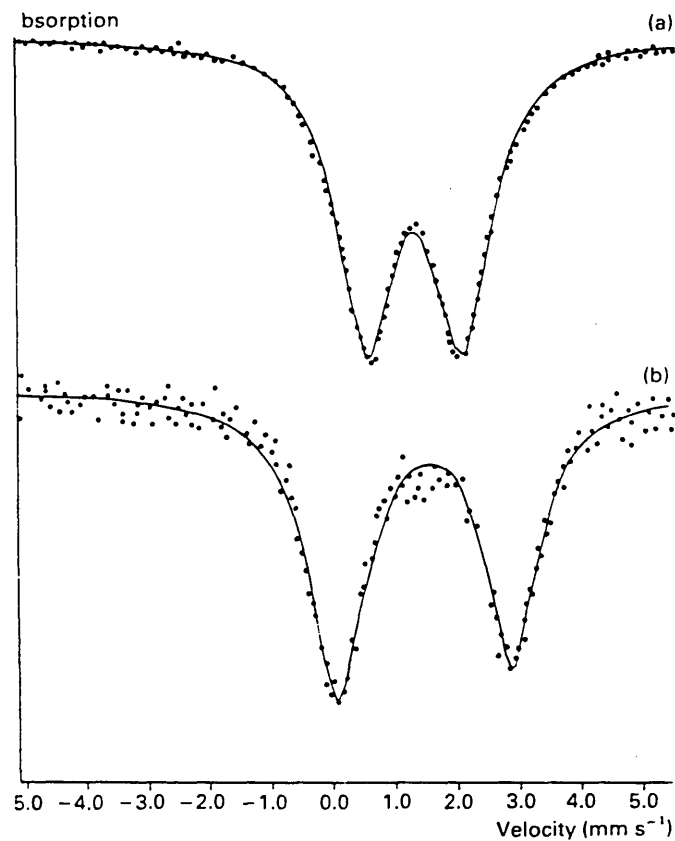


Figure 1. Mössbauer absorption spectra of (a) neat TBTO and (b) TBTO (2.6 per cent w/w) in an elastomeric coating matrix

The measured values of isomer shift (δ), quadrupole splitting (ΔE_Q) and full width at half-height (Γ) take into account errors associated with non-linearities, calibration, zero-velocity determination and computer-fitting.

It is clear that on incorporation into the neoprene rubber matrix, TBTO, TBTCO and TBTS_t undergo significant structural change. In the Figure, the spectra of pure TBTO and the elastomer prepared from a composition including TBTO, are compared for illustration. The similarity of the Mössbauer parameters for this group of toxicants indicate that all appear to undergo conversion into the same organotin species during fabrication of the elastomer. The Mössbauer parameters are identical, within experimental error, with those of a sample of tributyltin chloride dispersed in the same elastomeric matrix. It is noteworthy that the spectrum of the latter compound in the

elastomer is also different from that of the pure material. This difference is likely to be a consequence of dispersal of the chloride, resulting in a breakdown of intermolecular interactions present in the pure material at 80 K, which give rise to a pseudopolymeric five coordinate tin site.

In order to confirm the presence of TBTC1 in the elastomers, the cured materials were Soxhlet-extracted with dichloromethane. After evaporation of the extracts, the residues were dissolved in deuteriochloroform and the ¹¹⁹Sn n.m.r. spectra recorded. In each case, the major signal was observed at δ 156 ppm (Me_4Sn as external reference, $\delta = 0$), identical with that for TBTC1.

Thus it would seem clear that on incorporation of the above organotin toxicants into the elastomer matrix these compounds have participated in the curing process, and have been converted *via* reaction with hydrogen chloride arising from dehydrochlorination of the base polymer under curing conditions, to form tributyltin chloride as the predominant species present.

Received 9 September 1985

References

- 1 Cardarelli, N.F., 'Controlled release pesticide formulations', CRC Press, 1976
- 2 Evans, C.J., & Hill, R., *Rev. Silicon, Germanium, Tin, Lead Comp.*, 1983, **7**, 57-125
- 3 Kanakkanatt, S.V., Patnode, P.P., & Cardarelli, N.F., *Int. Congr. Pure App. Chem., Macromol. Reprint*, 1971, **1**, 614-9
- 4 Blunden, S.J., Hill, R., & Ruddick, J.N.R., *J. Organomet. Chem.*, 1984, **267**, C5-8

Table 1. ¹¹⁹Sn Mössbauer data for organotin compounds in anti-fouling neoprene elastomers at 80 K

Toxicant	Isomer shift ^d (δ/mms^{-1})	Quadrupole splitting (Δ/mms^{-1})	Line width (Γ/mms^{-1})
In elastomers (2.6 per cent w/w) ^a			
TBTO	1.40	2.82	1.09
TBTS _t	1.44	2.82	0.99
TBTCO	1.43	2.84	0.97
TBTC1	1.41	2.78	1.05
Pure materials ^b			
TBTO	1.25	1.53	1.11
TBTS _t	1.45	3.65	0.95
TBTCO ^c	(1.38)	2.70	(1.08)
	(1.43)	3.79	(0.88)
TBTC1	1.52	3.42	1.06

^a $\Gamma \pm 0.05 \text{ mm sec}^{-1}$; ^b errors $\pm 0.02 \text{ mm sec}^{-1}$; ^c computer fitted as two unresolved doublets, consistent with ref 4; ^d measured relative to $\text{BaSn}(\text{O}_3)_2$

Drastic degradation of triphenyltin toxicants in neoprene-based elastomeric marine anti-fouling coatings: ^{119m}Sn Mössbauer and chemical speciation studies

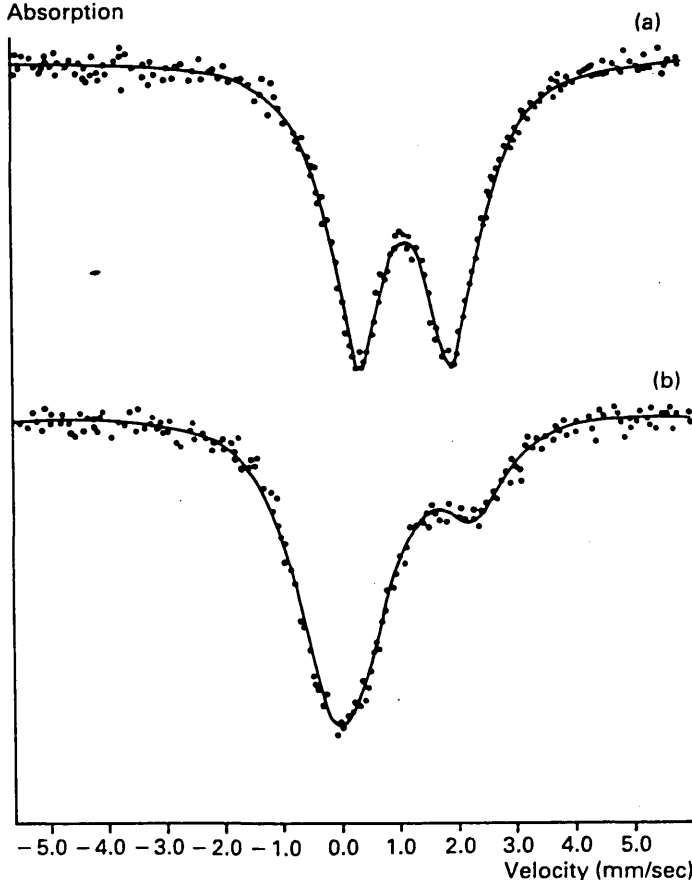
David W Allen,* Stephen Bailey* and John S Brooks†

Departments of Chemistry* and Applied Physics,† Sheffield City Polytechnic, Pond Street, Sheffield S1 1WB

In a recent Communication,¹ the authors reported a study of the fate of various tributyltin toxicants on incorporation into cured neoprene marine antifouling matrices, using ^{119m}Sn Mössbauer and ^{119}Sn n.m.r. spectral studies. It was shown that each tributyltin toxicant Bu_3SnX ($\text{X} = \text{OSnBu}_3$, stearate and carbonate) undergoes predominant conversion into tributyltin chloride during the compounding/curing processes. Now, a similar study of the fate of a range of triphenyltin compounds Ph_3SnX ($\text{X} = \text{F}$, Cl , OAc , OSnPh_3) on incorporation into neoprene antifouling compositions has been conducted and major differences have been found in the behaviour which have important implications for the future application of these systems.

Triphenyltin compounds Ph_3SnX ($\text{X} =$ an anionic group) are known to be active biocides and, therefore, have been of interest for their effectiveness as marine antifouling agents in elastomeric coatings used to protect ocean-going vessels, navigational buoys and other delicate underwater installations.² Various triphenyltin toxicants Ph_3SnX ($\text{X} = \text{F}$, OAc , Cl , OSnPh_3) have been incorporated into an antifouling neoprene rubber composition at *ca* 2 per cent by weight, respectively, and the materials cured at 150°C under standard conditions. The resulting rubber sheets have been examined initially by ^{119m}Sn Mössbauer spectroscopy, which enables the environment of the tin atoms to be studied *in situ* without further chemical modification or extraction. Mössbauer spectra were recorded using a constant acceleration spectrometer with a room temperature 15mCi barium stannate source, as

Figure Mössbauer absorption spectra of (a) neat TPTO and (b) TPTO (2.6 per cent w/w) in an elastomeric coating matrix



described in an earlier paper.¹

The Mössbauer results for the pure triphenyltin compounds are identical with literature values,³ each spectrum appearing as a quadrupole-split doublet. The spectrum of each tin-containing elastomer is, however, markedly different from that of the appropriate pure substance and the spectra of the elastomer samples are all identical. Each spectrum is clearly an unresolved composite representing the superimposed spectra of a number of degradation products. Illustrative spectra of pure bis(triphenyltin)oxide (TPTO) and an elastomer incorporating this substance are presented in the Figure.

The drastic changes in the Mössbauer spectra indicate that a substantial proportion of the starting material has been converted into an unresolved range of degradation products, most probably various chlorotin(IV) species arising from progressive dephenylation of the triphenyltin substrate followed by possible complexation with hydrogen chloride in the polymer matrix. The authors have shown that when phenyltin trichloride is dispersed in neoprene, its Mössbauer spectrum is modified from a well-resolved quadrupole doublet for the pure compound to a singlet with a small positive isomer shift (*ca* 0.3 mmsec⁻¹). Similarly, when stannic chloride is dispersed in neoprene, the isomer shift is reduced from 0.8 mmsec⁻¹ to 0.4 mmsec⁻¹. Thus the spectra of a range of possible degradation products could be combined to account for the observed spectra. Another factor which must be taken into consideration is that the recoil-free fractions of organotin(IV) compounds are considerably smaller than those of inorganic tin(IV) compounds, and thus the presence of the latter could dominate the spectrum.

In view of the uncertainty about the precise nature of the tin species present, and the above implication of severe degradation of the toxicant during the compounding/curing processes, ancillary techniques have been applied to the problem of identification. Prolonged Soxhlet extraction of the elastomers with dichloromethane gave extracts in which the presence of tin compounds was not detectable by ¹¹⁹Sn n.m.r. spectroscopy, indicating their possible migration to the polymer matrix. Accordingly, two elastomer samples derived from triphenyltin chloride and bis(triphenyltin) oxide were heated under reflux with an excess of *n*-propylmagnesium chloride in an attempt to convert all chlorotin species into tetraorganotins which could then be amenable to extraction and subsequent gas-chromatographic analysis. This technique has previously been used in studies of tin speciation in gamma-irradiated VC.⁴ The final extracts from these reactions revealed the presence of phenyltripropyltin (as the major component) with smaller amounts of tetrapropyltin and still smaller amounts of the diphenyl and triphenyltin derivatives. This result supports the authors' initial suggestion of drastic degradation of the triphenyltin compounds in a series of rotodestannylation steps resulting, ultimately, in the formation of stannic chloride (probably as an adduct with hydrogen chloride). All stages of dephenylation are apparent on the chromatograms, clearly indicating the extensive degradation that has taken place. This is in

marked contrast to the behaviour of the related tributyltin toxicants in which the tributyltin moiety survives the compounding/curing processes to a great extent, only traces of dibutyltin compounds being detectable by ¹¹⁹Sn n.m.r. spectroscopy and by application of the above Grignard alkylation procedure to the elastomers containing these materials.⁵

In view of the rather drastic nature of the degradation process undergone by the triphenyltin toxicants resulting, ultimately, in the formation of inorganic tin compounds, there would seem to be little point in promoting the use of triphenyltin-based toxicants in neoprene elastomer coatings. The related tributyltin compounds would appear to be the better choice based on the above studies.

Received 17 October 1986

References

- 1 Allen, D.W., Bailey, S., Brooks, J.S., & Taylor, B.F., *Chem. Ind. (London)*, 1985, 826-7
- 2 See eg Blunden, S.J., Cusack, P.A., & Hill, R., 'The industrial uses of tin chemicals', 1985, Chapters 3 and 4, and references therein, *London: Royal Society of Chemistry*
- 3 Ruddick, J.N.R., in 'Rev. on Si, Ge, Sn and Pb compounds', Ed. Gielen, M., 1976, **2**, 115-222
- 4 Allen, D.W., Brooks, J.S., & Unwin, J., *Chem. Ind. (London)*, 1985, 524-5
- 5 Allen, D.W., Bailey, S., & Brooks, J.S., to be published